Fall 1-31-2011

Pattern formation in oscillatory systems

Hui Wu
New Jersey Institute of Technology

ABSTRACT

PATTERN FORMATION IN OSCILLATORY SYSTEMS

by
Hui Wu

Synchronization is a kind of ordinary phenomenon in nature, the study of it includes many mathematical branches. Phase space is one of the most powerful inventions of modern mathematical science. There are two variables, the position and velocity, that can describe the 2-dimensional phase space system. For example, the state of pendulum may be specified by its position and its velocity, so its phase space is 2-dimensional. The state of the system at a given time has a unique corresponding point in the phase space. In order to describe the motion of an oscillator, we can talk about its motion in phase space. Self-sustained oscillators exhibit regular rhythms- they revisit the same points time after time. So the stable oscillation state of a self sustained oscillator can be expressed as some closed curve in phase space, and this closed curve is defined as a limit cycle.

There are two topics in this dissertation: Kuramoto model and FitzHugh-Nagumo (FHN) model. Kuramoto's original analysis of his model gives the critical synchronization value for K (K is the coupling constant). He also gives an estimate for the value of order parameter r when K is close to critical point K_c. However when we give different initial values for the oscillators, the order parameters are different after a long time. The objective of the first topic is to give the distribution of the value of order parameter r under different initial conditions. We divide the oscillators to synchronized part and unsynchronized part, and find that the order parameter satisfies a Gaussian distribution.

For the second topic, we start with an introduction for oscillatory clusters in the Belousov-Zhabotinsky reaction. The main idea of this topic is to find the phase property of oscillators in the Oregonator and FHN type models with global inhibitory feedback. Numerical simulations suggest that, in many cases, the cubic system has the same phase value as the piecewise linear system. To simplify this model, we reduce the cubic FHN system to piecewise linear system.

In a network of two mutually-coupled neural oscillators, a spike time response curve (STRC) describes the period change of an oscillator given by a perturbation of another oscillator. The STRC is used to predict the phase relations of the two-cell network. We also create a spike time difference map that describes the evolution of the neuron's network based on the STRC.

PATTERN FORMATION IN OSCILLATORY SYSTEMS

by
Hui Wu

A Dissertation
Submitted to the Faculty of
New Jersey Institute of Technology and
Rutgers, The State University of New Jersey – Newark
in Partial Fulfillment of the Requirements for the Degree of
Doctor of Philosophy in Mathematical Sciences

Department of Mathematical Sciences, NJIT
Department of Mathematics and Computer Science, Rutgers-Newark

January 2011

APPROVAL PAGE

PATTERN FORMATION IN OSCILLATORY SYSTEMS

Hui Wu

Horacio G Rotstein, Dissertation Co-Advisor — Date
Assistant Professor, Department of Mathematical Sciences, NJIT

Louis Tao, Dissertation Co-Advisor — Date
Professor, Center for Bioinformatics School of Life Sciences, Peking University

---

Amitabha Bose, Committee Member — Date
Professor, Department of Mathematical Sciences, NJIT

Victor V. Matveev, Committee Member — Date
Associate Professor, Department of Mathematical Sciences, NJIT

Denis Blackmore, Committee Member — Date
Professor, Department of of Mathematical Sciences, NJIT

BIOGRAPHICAL SKETCH

Author: Hui Wu

Degree: Doctor of Philosophy

Date: January 2011

Undergraduate and Graduate Education:

- Doctor of Philosophy in Mathematical Sciences,
  New Jersey Institute of Technology, Newark, NJ, 2011
- Master of Science in Computational Mathematics,
  University of Sciences and Technology of China, Hefei, Anhui, 2005
- Bachelor of Arts in Mathematics,
  Anhui University, Hefei, Anhui, 2002

Major: Mathematical Sciences

Presentations and Publications:

Hui Wu, Jiansong Deng, "Degree reduction of ball control point Bezier surfaces," *Journal of University of Science and Technology of China, Vol 6, 2006* .

Hui Wu, "An Introduction for FitzHugh-Nagumo model," *Applied Mathematics Seminar*, Department of Mathematical Sciences, NJIT, July 11, 2006.

Hui Wu, Yueqiang Chen, "Degree reduction of ball-control-point Bezier surfaces over triangular domain," *Journal of University of Science and Technology of China, Vol 37, 2007.*

Hui Wu, "Oscillatory patterns in piece-wise linear relaxation oscillators of FitzHugh-Nagumo type with inhibitory global feedback," *the Seventh Annual Conference on Frontiers in Applied and Computational Mathematics (FACM '10)*, Department of Mathematical Sciences, NJIT, May 21-23, 2010.

Hui Wu, "Kuramoto model and Belousov-Zhabotinsky(BZ) reaction," *Applied Mathematics Seminar*, Department of Mathematical Sciences, NJIT, June 8, 2010.

Only those who have the patience to do simple things perfectly ever acquire the skill to do difficult things easily.

—Friedrich Schiller

ACKNOWLEDGMENT

First of all, I wish to thank my Co-advisors, Professor Horacio G. Rotstein and Professor Louis Tao for their tremendous assistance with this dissertation. From beginning to end, they have been a steadfast source of information, ideas, support, and energy. I am deeply grateful for their guidance, patience, and encouragement in NJIT through the last few years and I will be forever grateful for their trust and support that this dissertation could be completed.

I also would like to extend my gratitude to the other members of my committee for their encouragement and support throughout my years in graduate school as well as through the process of researching and writing this dissertation: Professor Victor V. Matveev, Professor Amitabha Bose, Professor Gregor Kovacic, and Professor Denis Blackmore.

I would also like to thank all of the graduate students in the Department of Mathematical Sciences whom I have got to know in the last five years.

Finally, I would like to thank my family for their support and encouragement: my parents and my parents in law. Mom and Dad, I owe them everything. While all have been encouraging, I would quite simply not have completed this project without the support and encouragement of my husband, Yun Zhou.

TABLE OF CONTENTS

TABLE OF CONTENTS
(Continued)

Chapter **Page**

LIST OF TABLES

Table **Page**

LIST OF FIGURES

LIST OF FIGURES
(Continued)

Figure **Page**

LIST OF FIGURES
(Continued)

Figure **Page**

LIST OF FIGURES
(Continued)

Figure **Page**

CHAPTER 1

INTRODUCTION

1.1 General Overview

The focus of this thesis is to investigate the effects of global coupling in oscillatory system [14],[8].

An 'oscillator' is a circuit that behaves periodically - i.e. which repeats its behaviour at regular intervals. A differential equation may have a solution which behaves periodically, in which case we can say that it describes an oscillator. Oscillators are useful for describing real-world objects which periodically repeat their actions - e.g neurons (sometimes), certain electrical circuits, waves, cells, etc. They can also be used as crude models of more complicated real-world objects.

Oscillators are 'coupled' if they are allowed to interact with each other in some way. For example one neuron might send a signal to another at regular intervals. Mathematically speaking, the differential equations have coupling terms which represent how one oscillator interacts with all the others.

A set of oscillators are globally coupled if every oscillator is coupled to every other oscillator in a symmetric way. In other words the 'force' an oscillator experiences from all the other oscillators is not dependent on the identity of that oscillator. In the simplest case, all the oscillators are identical, but this is not necessarily so [14] [15].

Systems of globally coupled oscillators can exhibit complicated behavior that cannot be deduced by analyzing the dynamics of individual elements but emerges from the interactions between the oscillators.

One of the major challenges in neuroscience today is to understand how coherent activity emerges in neural networks from the interactions between their neurons, as well as its role in normal and pathological brain function. There are two most relevant examples of coherent activity in the brain: Synchronization and Phase-locking. The phase oscillator

approximation used in physics and the mathematical models provide a powerful tool to investigate the biophysical mechanisms underlying these phenomena. In particular, the experimental or numerical determination of the spike time response curve, which derives from the intrinsic properties of a real or a simulated neuron, allows one to greatly simplify the analytical treatment of their dynamics, as well as their computational modeling. In this way, it is possible to predict the existence and stability of phase-locked states and of synchronized assemblies in real and simulated neural networks with electrical or chemical synapses. The spike time response curve also determines the stability of repetitive neuronal firing thereby affecting spike time reliability and noise-induced synchronization. Moreover, for neurons that fire repetitively, the spike time response curve is directly related to the waveform of the input that most likely precedes an action potential.

Our research on globally coupled oscillators include two parts: the Kuramoto model and the models of Belousov-Zhabotinsky (BZ) reaction.

In the Kuramoto model, each oscillator has the same amplitude, so we only need to consider the phases. In contrast, in the BZ model, we consider both phases and amplitudes. To investigate the effects of globally coupling in the BZ reaction, I will use a 'toy' model- the FitzHugh-Nagumo (FHN) model- with global inhibitory feedback. The FHN model has an explicit phase via a given set of parameters ϵ, γ, α, λ, and α_1. To further simplify this model, I used the piecewise-linear (PWL) model for analysis. In most cases, specifically, when ϵ is less than 0.1, we get the same pattern in both of piecewise linear and cubic cases. However when ϵ is not less than 0.1, sometimes we get large amplitude oscillations and mixed-mode oscillations in piecewise-linear case but the amplitude shrinks to zero in smooth systems.

In order to investigate the mechanism of synchronization of our results we used spike-time response curves and spike-time difference maps. These techniques have been borrowed from the neurosciences. We use spike-time difference maps to predict the oscillatory pattern in FHN model.

1.2 The Kuramoto Model

The Kuramoto model describes the synchronization behavior of a large population of coupled limit-cycle oscillators whose natural frequencies satisfy some certain distribution [19]. The Kuramoto model predicts that, if the oscillators have strong coupling, they will become phase-locked. The model gives a condition for synchronization to happen. It is possible to solve the critical coupling value needed for synchronization to happen. There is an order parameter to measure the extent these oscillators coupling, Kuramoto gave a mathematical formula of order parameter. But the real result of order parameter always have a little difference from Kuramoto's estimation. My research involved studying the basics of Kuramoto's analysis and then investigating how the order parameter is distributed by given different initial conditions. There are some examples of numerical simulation of the distribution and these simulations are consistent with my analytical result. In the deduction process, to use the central limit theory, I showed that these variables are independent.

1.3 The Belousov-Zhabotinsky Reaction

The field of nonlinear dynamics studies the time evolution of systems whose behavior depends on a nonlinear fashion on the value of some key variables [41, 36, 25, 20]. Examples of these variables are concentrations in a chemical reaction, and voltage and gating variables in neural systems [26].

Nonlinear chemical dynamics studies chemical systems far from equilibrium[10]. A major focus area of nonlinear chemical dynamics is the study of how complex structures arise, both in time and space. Important examples of these spatio-temporal patterns are chemical oscillations where the concentrations of one or more species vary periodically, or nearly periodically, in time.

The Belousov-Zhabotinsky (BZ) reaction, is one of a class of reactions of non-equilibrium thermodynamics. It generates oscillations and propagating pulses (chemical waves). It is the prototypical oscillatory system in nonlinear chemistry [2, 3, 50, 51], and has been utilized primarily to understand the dynamics of patterns and spiral waves. The BZ reaction consists

on the oxidation of malonic acid, in an acid medium, by bromate ions, and catalized by Cerium. Cerium has has 2 ionization states: Ce^{3+} and Ce^{4+}. Sustained periodic relaxation oscillations are observed in the concentration of these cerium ions. These oscillations are reflected in the periodic change of color of the solution from yellow (Ce^{4+}) to colorless (Ce^{3+}). When ferroin ($[Fe(phen)_3^{2+}]$) is used as catalyst, instead of Ce, the concentration color changes from red to blue. Using this catalyst, spatial patterns consisting of spirals or concentric rings (target patterns) can be observed [48]. In these patterns blue spirals or rings are spontaneously generated in an initially homogeneous red dish.

1.4 Oscillatory Clusters in the BZ reaction with Global Inhibitory Feedback

Oscillatory cluster patterns have been recently discovered in the BZ reaction with photochemical global feedback (coupling) [43, 44] and the periodically illuminated BZ reaction [45]. Photochemical global feedback is imposed through illumination using the photosensitive catalyst Rubipy ($Ru(bipy)_3^{2+}$). The average spatial concentration of Rubipy, $< w >$, is employed to control the intensity of the so called actinic light according to a function of $< w > -\bar{w}$ where $\bar{w}$ is set close to the equilibrium value in such a way that $< w > -\bar{w}$ is positive.

Oscillatory clusters are sets of oscillators, or spatial domains, where all elements in each domain oscillate with nearly the same amplitude and phase. Cluster patterns resemble standing waves, except that they lack a characteristic wavelength [43]. Three important cluster patterns observed in the BZ reaction with global inhibitory feedback are two-phase, three-phase and localized clusters[15]. The former two consist of two or three clusters oscillating synchronously out of phase. This is the focus of this project. The latter consists of a two-phase clusters in one region of the reactor while the reminder appears uniform or oscillate with very small amplitude. Note that each cluster can occupy multiple fixed spatial domains.

1.5 The Oregonator Model for the BZ reaction

The most widely accepted kinetic scheme for the BZ reaction is the Fields-Koros-Noyes (FKN) mechanism [11]. It involves many chemical species and reactions (equations), but it can be simplified by applying quasi-steady-state and rate-limiting-step approximations [11]. The Oregonator, is the simplest realistic model of oscillatory chemical dynamics in the oscillatory BZ reaction. This network is obtained by reduction of the complex chemical mechanism of the BZ reaction suggested by Field, Koros and Noyes (1974) and referred to as the FKN mechanism.

The Oregonator model consists of the following reaction steps and associated rate equations:

$$BrO_3^- + Br^- \rightarrow HBrO_2 + HOBr, \quad Rate = k_1[BrO_3^-][Br^-]$$

$$HBrO_2 + Br^- \rightarrow 2HOBr, \quad Rate = k_2[HBrO_2][Br^-]$$

$$BrO_3^- + HBrO_2 \rightarrow 2HBrO_2 + 2Ce^{4+}, \quad Rate = k_3[BrO_3^-][HBrO_2]$$

$$2HBrO_2 \rightarrow BrO_3^- + HOBr, \quad Rate = k_4[HBrO_2]$$

$$2B + Ce^{4+} \rightarrow 1/2fBr^-, \quad Rate = kc[Z][Ce^{4+}]$$

Here B represents all oxidizable organic species present and f is stoichiometric factor that encapsulates the organic chemistry involved.

Let the various chemical entities be given by:

$$A : [BrO_3^-]$$

$$B : [All \ \ oxidizable \ \ organic \ \ species]$$

$$P : [HOBr]$$

$$X : [HBrO_2]$$

$$Y : [Br^-]$$

$$Z : [Ce^{4+}]$$

If we treat the concentrations of the reactants A and B as constant and rescale the time t to τ: $\tau = \varepsilon t$, the rate equations for X, Y, and Z become [26]:

$$\begin{cases} \dfrac{dX}{d\tau} &= k_1AY - k_2XY + k_3AX - 2k_4X^2 \\ \dfrac{dY}{d\tau} &= -k_1AY - k_2XY + \frac{1}{2}fk_cBZ \\ \dfrac{dZ}{d\tau} &= 2k_3AX - k_cBZ \end{cases} \tag{1.1}$$

We follow [26] and nondimensionalize the model (1.1). So let the dimensionless parameters ε, σ', and q be given by:

$$\begin{cases} \varepsilon = \dfrac{k_cB}{k_3A} \\ \sigma' = \dfrac{2k_ck_4B}{k_2k_3A} \\ q = \dfrac{2k_1k_4B}{k_2k_3A} \end{cases} \tag{1.2}$$

Let us define variables x, y, z, and t as follows:

$$\begin{cases} x = \dfrac{2k_4 x}{k_3 A}, \\ \\ y = \dfrac{k_4 Y}{k_3 A} \\ \\ z = \dfrac{k_c k_4 B Z}{(k_3 A)^2} \\ \\ t = k_c B \tau \end{cases} \tag{1.3}$$

The dimensionless kinetic equations are given by 1.4.

By substituting (1.2) and (1.3) into system (1.1) and rearranging terms we obtain

$$\begin{cases} \epsilon \, \dfrac{dx}{dt} = q\, y - x\, y + x\,(1 - x), \\ \\ \sigma \, \dfrac{dy}{dt} = -q\, y - x\, y + f\, z, \\ \\ \dfrac{dz}{dt} = x - z. \end{cases} \tag{1.4}$$

Note that the three dimensionless variables x, y and z are normalized concentrations of $HBrO_2$, Br^- and the oxidized form of the catalyst respectively. The constants used in the dimensionless procedure include the rate equations of the five irreversible steps of the reduced mechanism and the concentrations of malonic acid. The three dimensionless parameters have typical values of $\epsilon \sim 10^{-2}$, $\sigma \sim 10^{-5}$ and $q \sim 10^{-4}$. The parameter f is a stoichiometric factor that serves as an adjustable parameter. By noting that $\sigma \ll q \ll \epsilon \ll 0$, (1.4) yields

$$-qy - xy + fz = \sigma \; dy/dt \approx 0$$

So

$$y \approx \frac{f\,z}{q+x}. \tag{1.5}$$

Plugging this into (1.4) yields

$$\begin{cases} \epsilon\,\dfrac{dx}{dt} = x\,(1-x) + f\ (q-x)/(q+x)\ z, \\ \\ \dfrac{dz}{dt} = x - z \end{cases} \tag{1.6}$$

In the literature, x is usually referred to as the activator variable and z as the inhibitor variable. System (1.6) is fast-slow($\epsilon = 10^{-2}$). The corresponding nullclines are given by

$$N_x(x) = -\frac{x\ (1-x)\ (q+x)}{f\ (q-x)} \qquad \text{and} \qquad N_z(x) = x. \tag{1.7}$$

Examples of phase-planes and traces (x and z vs. t) are shown in Fig. 1.1.

A change of variables $\hat{z} = f\,z$, $\hat{z} \to z$ allows for changes in the parameter f to be reflected in changes in the z-nullcline ($N_z(x)$). The resulting equations are

$$\begin{cases} \epsilon\,\dfrac{dx}{dt} &= x\,(1-x) + (q-x)/(q+x)\ z, \\ \\ \dfrac{dz}{dt} &= f\ x - z, \end{cases} \tag{1.8}$$

with nullclines given by

$$N_x(x) = -\frac{x\ (1-x)\ (q+x)}{q-x} \qquad \text{and} \qquad N_z(x) = f\,x. \tag{1.9}$$

A

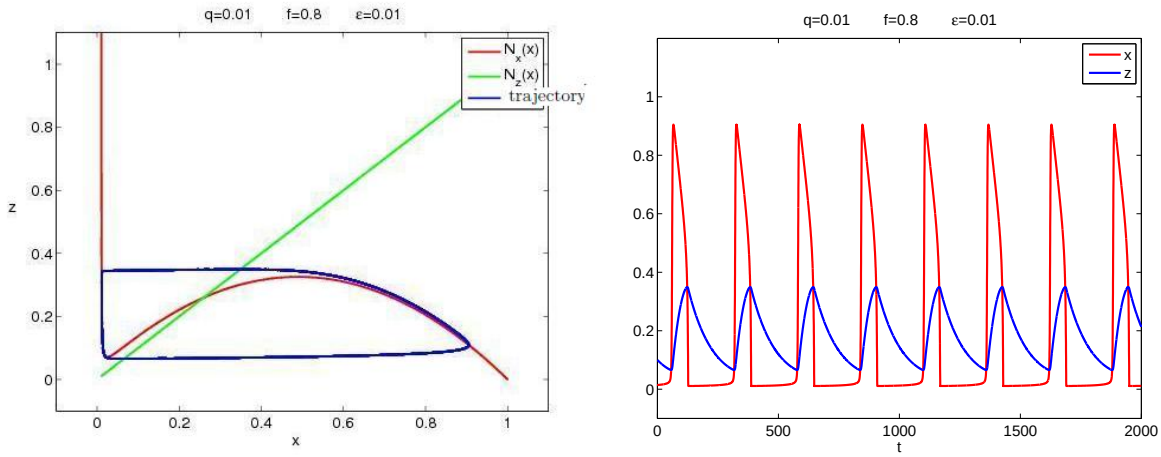

B

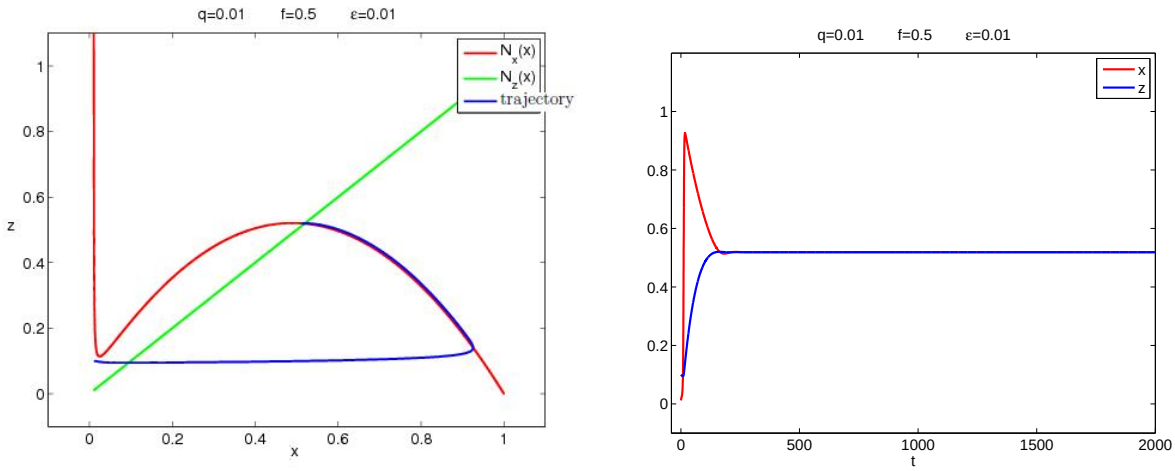

C

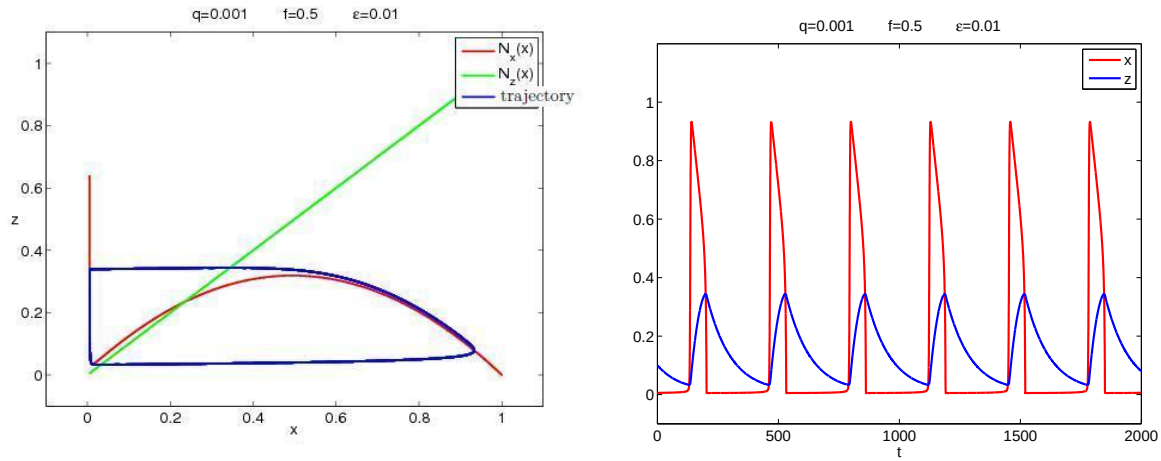

Figure 1.1 Phase-plane (left) and activator (x) inhibitor (z) traces (right) for the Oregonator model (1.6) for various representative parameter values. The nullclines are given by (1.7).

1.6 A Modified Oregonator Model

A modified version of the Oregonator model was introduced by Zhabotinsky et al [52]. The dimensionless version of the modified Oregonator model is given by

$$\begin{cases} \epsilon \dfrac{dv}{d\tau} = f(v,v), \\ \\ \dfrac{dw}{d\tau} = g(v,w), \end{cases} \tag{1.10}$$

where

$$f(v,w) = \bar{f}(v,w,u) = -v^2 - \alpha\, v + \delta\, u^2 + \eta\, u\,(1-w) - \eta\, v\, w - (q\, w + \beta)\,\psi(v), \tag{1.11}$$

$$u = \frac{2\, v\,(\eta\, w + 2\,\alpha)}{\eta\,(1-w) + \sqrt{\eta^2\,(1-w)^2 + 8\,\delta\, v\,(\eta\, w + 2\,\alpha)}}, \tag{1.12}$$

$$\psi(v) = \frac{v-\mu}{v+\mu}, \tag{1.13}$$

and

$$g(v,w) = \bar{g}(v,w,u) = u\,(1-w) - v\, w - w. \tag{1.14}$$

This modified Oregonator model can be reduced to the Oregonator model (1.6) in a neighborhood of the fixed-point (intersection between the nullclines [35]).

1.7 FitzHugh-Nagumo Type Models

The FitzHugh-Nagumo (FHN) model was proposed independently by FitzHugh [12, 13] and Nagumo [27] to qualitatively describe the events occurring in an excitable neuron. The

FHN model is a generic model for excitable media and has been used as a caricature model in a variety of systems, most notably chemistry biology and neuroscience [9]. The precise mathematical mechanism involves appearance and disappearance of a limit cycle attractor, and it is reviewed in detail by Izhikevich [17]. Its fast-slow system version is able to describe relaxation oscillations in some parameter regimes. These oscillations and the nullclines are qualitatively similar to the ones displayed by the Oregonator model. For this reason the FHN model can been used as a toy model for the BZ reaction (1.16). The general form of the FHN model is

$$\begin{cases} v' = f(v) - w, \\ w' = \epsilon \, [\, g(v;\lambda) - w \,] \end{cases} \tag{1.15}$$

where

$$f(v) = -h \; v^3 + a \; v^2 - b \; v + c, \tag{1.16}$$

and

$$g(v;\lambda) = \alpha \; v - \lambda. \tag{1.17}$$

with h, a, b, c and α non-negative constants, and $0 < \epsilon \ll 1$. In the classical FHN model, $h = 1/3$, $a = 1$, $b = c = 0$, so the cubic v-nullcline has a minimum at $(0, 0)$, and intersects the w-nullcline at this point.

A modified version of the FHN model where $g(v;\lambda)$ is sigmoid rather than linear has been used in [34] as a toy model for the modified Oregonator model. More specifically, the w-nullcline for the modified FitzHugh-Nagumo (MFHN) model is given by

$$g(v;\lambda) = \beta\left(\tanh\frac{v-\lambda}{\eta}\right) + \frac{1}{2}. \tag{1.18}$$

where η, λ and β are non-negative constants.

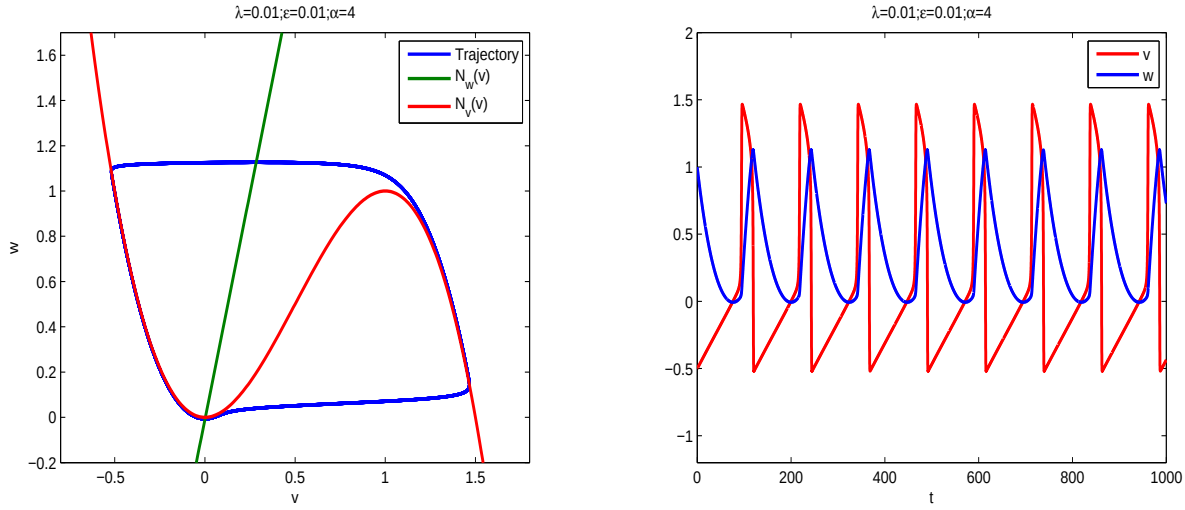

Figure 1.2 Phase-plane (left) and traces (right) for the FHN (1.15) for representative parameter values.

CHAPTER 2

THE KURAMOTO MODEL

In the past decades, the synchronization in complex networks has been a research topic in many fields [22]. Among many models that have been proposed to address synchronization phenomena, one of the most successful models is the Kuramoto model [19]. This model can be used to understand the emergence of synchronization in networks of oscillators. In particular, this model presents a second-order phase transition from incoherence to synchronization.

Kuramoto found that there is a certain value of the coupling constant, K_C, above which synchronization can occur, and below which it cannot. For any distribution of the natural frequencies of the oscillators, he was able to calculate K_C. For example, for a Lorentzian distribution of natural frequencies, K_C is just equal to the full width at half-max of the Lorentzian curve. For other distributions, the formula for K_C is more complex, but we can still calculate it.

In this section we first describe the history of Kuramoto model. Kuramoto also gave an initial estimate for the value of order parameter for a given value of coupling constant. i.e. He gave a initial estimate for the value of the order parameter by giving the value of the coupling constant. But the numerical results for the value of the order parameter are a little bit different from Kuramoto's estimation. I gave an estimate for the distribution of order parameter for different values of initial conditions.

In the 1960s, scientists began to build mathematical models for synchronization in many natural systems. Particularly, Arthur Winfree's model become very popular. He gave a model in which each oscillator's phase is determined by combining the state of all of the oscillators. In his model, the rate of change of the phase of an oscillator is determined by its own natural frequency ω_i and the state of all of the other oscillators combined. Each oscillator's sensitivity to the combination is represented as a function Y, and its own contribution to the combination is given by a function X. Then each oscillator has an equation to describe how its phase changes [39, 40]:

$$\theta_i' = \omega_i + \sum_{j=1}^{N} X(\theta_j)Y(\theta_i) \tag{2.1}$$

Here θ_i is the phase of oscillator, $\dot{\theta}_i$ is the rate of change of phase of oscillator, ω_i is the natural frequency of oscillator i, and N is the total number of oscillators.

Winfree made numerical simulations and analytical approximations for this model and found that if the coupling is large enough, the oscillators could synchronize.

In 1975, Japanese scientist Yoshiki Kuramoto was inspired by Winfree's works, and he began exploring the behavior of collective synchronization. He used the following assumptions:

1. The oscillators are almost identical.

2. The coupling among oscillators is small.

After some complicated mathematical averaging, he proved that long term dynamics of any system of almost identical, weakly coupled limit cycle oscillators system have the following govern equation [41, 40, 22]:

$$\dot{\theta}_i = \omega_i + \sum_{j=1}^{N} \Gamma_{ij}(\theta_j - \theta_i) \tag{2.2}$$

Here the interaction function Γ_{ij} determines the form of coupling between oscillator i and oscillator j.

Kuramoto assumed that each oscillator take part in the affecting other oscillators. He called the interaction "global coupling".

He further assumed that the coupling were equally weighted can be expressed by a sin function of the difference of phases.

$$\Gamma_{ij}(\theta_j - \theta_i) = \frac{K}{N}\sin(\theta_j - \theta_i) \tag{2.3}$$

This derives the govern equations for Kuramoto model:

$$\theta_i' = \omega_i + \frac{K}{N}\sum_{j=1}^{N}\sin(\theta_j - \theta_i) \tag{2.4}$$

Here K is the coupling constant, and N is the total number of oscillators. The model assumed that N is very large, i.e large number of oscillators. The natural frequencies ω_i distributed by a probability density function $g(\omega)$, and it is symmetric about some value Π: $g(\Pi + \omega) = g(\Pi - \omega)$.

To simplify the governing equation of Kuramoto model, we need to define the order parameter, the order parameter describes the "mean field of the system".

Let us write the governing equations of Kuramoto model in terms of order parameter:

$$re^{i\psi} = \frac{1}{N}\Sigma_{j=1}^{N}e^{i\theta_j} \tag{2.5}$$

Here ψ is the average phase of all the oscillators.

2.1 The Relations between the Order Parameter r and the Critical Point K_c

The modulus of r, is a measure of the coherence of the oscillator system, it describes how close the oscillators are together. If we increase the order parameter, the phases of the oscillators will get closer together. The graphs in Fig. 2.1 show the order parameter being an arrow pointing from the center of the circle.

Let us consider (2.5): Multiplying both sides by $e^{-i\theta_i}$ we get:

$$re^{i(\psi-\theta_i)} = \frac{1}{N}\Sigma_{j=1}^{N}e^{i(\theta_j-\theta_i)} \tag{2.6}$$

$$r\sin(\psi - \theta_i) = \frac{1}{N}\Sigma_{j=1}^{N}\sin(\theta_j - \theta_i) \tag{2.7}$$

Therefore, Equation (2.4) may be rewritten as

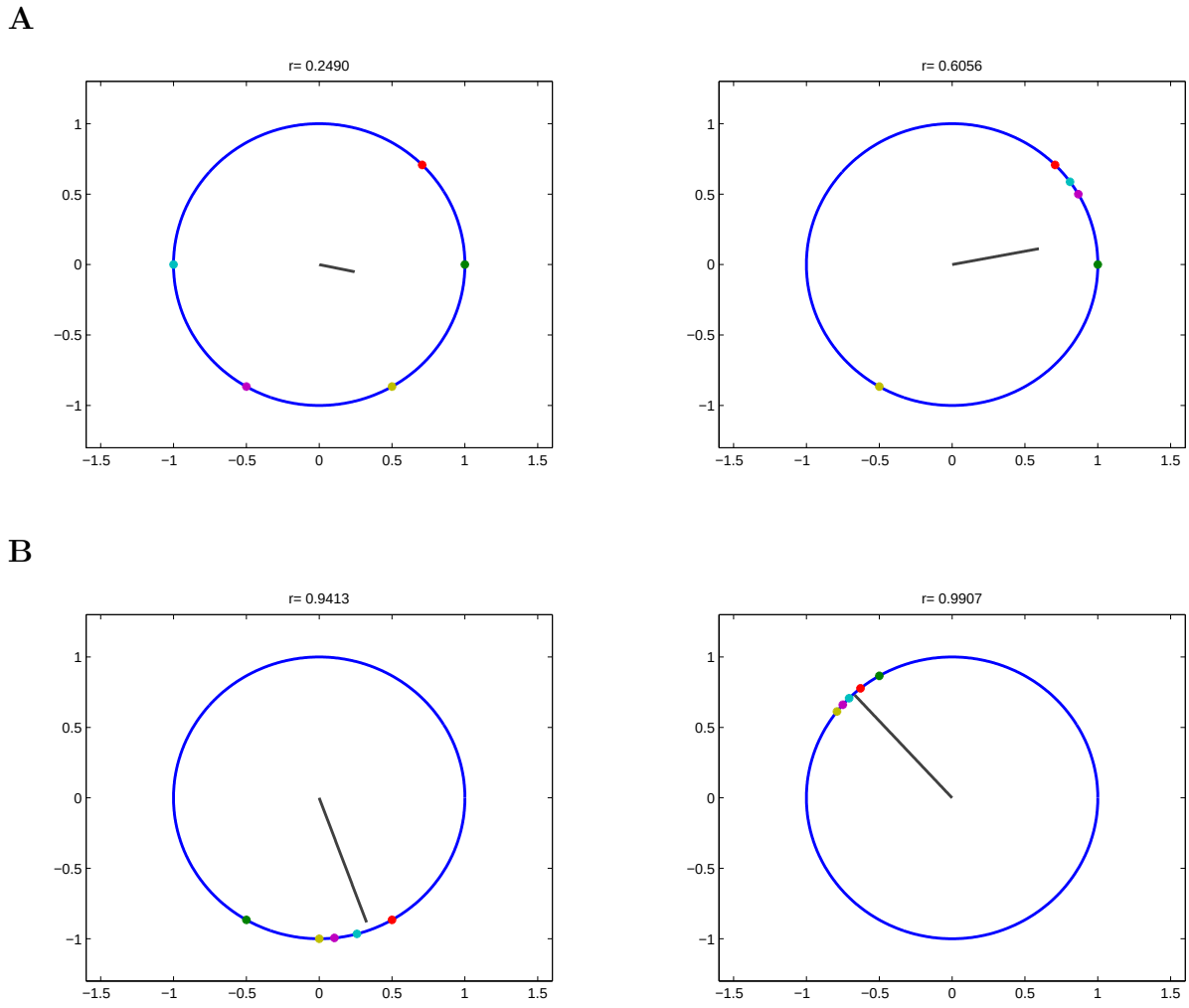

Figure 2.1 The order parameter is represented by the vector pointing from the center of the unit circle.

$$\dot{\theta}_i = \omega_i + Kr\sin(\psi - \theta_i) \quad for \quad i = 1, 2, ...N. \tag{2.8}$$

The corresponding stationary density:

$$\rho = \begin{cases} \delta[\theta - \psi - \sin^{-1}(\frac{w}{Kr})]\ H(\cos\theta)\ \ when\ |\omega| < Kr \\ \dfrac{C}{|\omega - Kr\sin(\theta - \psi)|} \quad when\ |\omega| \geq Kr \end{cases} \tag{2.9}$$

Here $H(x)$ is the Heaviside unit step function.

We take the natural frequency density function to be the Lorentzian density, defined as

$$g(\omega) = \frac{\gamma}{\pi(\gamma^2 + \omega^2)} \tag{2.10}$$

Actually $r(t)$ does not depend on time or $\psi(t)$ and $\psi(t)$ rotates uniformly at an angular frequency ϕ. We can set up a frame of reference that is rotating at the same frequency. Hence r(t) is stationary. So we can set $\psi(t)$ to any constant value. Without loss of generality, set $\psi(t) \equiv 0$ in the rotating frame. So we get

$$\dot{\theta}_i = \omega_i - Kr\sin\theta_i \tag{2.11}$$

and correspondingly, the stationary density function is

$$\rho = \begin{cases} \delta[\theta - \sin^{-1}(\frac{w}{Kr})]\ H(\cos\theta), \quad when\ |\omega| < Kr \\ \dfrac{C}{|\omega - Kr\sin\theta|} \quad , when\ |\omega| \geq Kr \end{cases} \tag{2.12}$$

then

$$\begin{aligned} re^{i\psi} &= re^{i0} = r \\ &= \frac{1}{N}\Sigma_{j=1}^{N} e^{i\theta_j} =< e^{i\theta} > \\ &=< e^{i\theta} >_{lock} + < e^{i\theta} >_{unlock} \end{aligned}$$

According to (2.12)

$$\rho(\theta + \pi, -\omega) = \rho(\theta, \omega)$$

Compute the contribution of unlocked oscillators:

$$\begin{aligned} < e^{i\theta} >_{unlock} &= \int_{-\pi}^{\pi}\int_{-\infty}^{-Kr} e^{i\theta}\rho(\theta,\omega)g(\omega)\ d\omega\ d\theta \\ &\quad + \int_{-\pi}^{\pi}\int_{Kr}^{\infty} e^{i\theta}\rho(\theta,\omega)g(\omega)\ d\omega\ d\theta \\ &= I_1 + I_2 \end{aligned} \tag{2.13}$$

where

$$\begin{aligned} I_1 &= \int_{-\pi}^{\pi}\int_{-\infty}^{-Kr} e^{i\theta}\rho(\theta,\omega)g(\omega)\ d\omega\ d\theta \\ &= -\int_{-\pi}^{\pi}\int_{\infty}^{Kr} e^{i\theta}\rho(\theta,-\omega)g(-\omega)\ d\omega\ d\theta \end{aligned}$$

Let $\theta' = \theta - \pi$, then

$$I_1 = -\int_{-2\pi}^{0}\int_{\infty}^{Kr} e^{i\theta'}e^{i\pi}\rho(\theta'+\pi,-\omega)g(-\omega)\ d\omega\ d\theta'$$

Since $\rho(\theta'+\pi,-\omega) = \rho(\theta',\omega)$, $\ g(-w) = g(w)$, $\ e^{i\pi} = -1$, we hence have

$$I_1 = -\int_{-2\pi}^{0}\int_{Kr}^{\infty} e^{i\theta'}e^{i\pi}\rho(\theta',\omega)g(\omega)\ d\omega\ d\theta'$$

Because the periodic boundary condition, we can shift θ' interval with any constant. So we can shift the integral interval to right with π.

So

$$I_1 = -\int_{-\pi}^{\pi}\int_{Kr}^{\infty} e^{i\theta'}e^{i\pi}\rho(\theta',\omega)g(\omega)\ d\omega\ d\theta' = -I_2 \tag{2.14}$$

According to (2.13),

$$< e^{i\theta} >_{unlock} = I_1 + I_2 = 0$$

So the unlocked oscillators have no contributions.

The locked oscillators are centered symmetrically on 0, therefore $< \sin\theta >_{lock} = 0$ and

$$\begin{aligned} r = \ & < e^{i\theta} >_{lock} \ = \ < \cos\theta >_{lock} \\ & = \int_{-Kr}^{Kr} cos(\theta(\omega))g(\omega)d\omega \end{aligned}$$

Consider (2.11) and (2.12)

$$\begin{aligned} r &= \int_{-\frac{\pi}{2}}^{\frac{\pi}{2}} \cos\theta g(Kr\sin\theta)Kr\cos\theta\ d\theta \\ &= Kr\int_{-\frac{\pi}{2}}^{\frac{\pi}{2}} \cos^2\theta g(Kr\sin\theta)\ d\theta \end{aligned} \tag{2.15}$$

This implies

$$1 = K\int_{-\frac{\pi}{2}}^{\frac{\pi}{2}} \cos^2\theta g(Kr\sin\theta)\ d\theta$$

When make $r \to 0^+$ in the above equation, we can find the critical point K_c at which the order parameter rises from zero.

$$\begin{aligned} 1 &= K_c \int_{-\pi/2}^{\pi/2} \cos^2\theta g(0)\ d\theta \\ &= K_c g(0) \int_{\pi/2}^{\pi/2} \cos^2\theta\ d\theta\ =\ K_c g(0)\frac{\pi}{2} \end{aligned}$$

Hence

$$K_c = \frac{2}{\pi g(0)} \tag{2.16}$$

Plug in (2.10): the function of $g(w)$

$$\begin{aligned} 1 &= K \int_{-\frac{\pi}{2}}^{\frac{\pi}{2}} \cos^2\theta \frac{\gamma}{\pi(\gamma^2 + K^2r^2\sin^2\theta)}\ d\theta \\ &= \frac{K\gamma}{\pi} \int_{-\frac{\pi}{2}}^{\frac{\pi}{2}} \frac{1-\sin^2\theta}{\gamma^2 + K^2r^2\sin^2\theta}\ d\theta \\ &= -\frac{\gamma}{Kr^2} + \frac{Kr}{\pi}(1+\frac{\gamma^2}{K^2r^2}) \int_{-\frac{\pi}{2}}^{\frac{\pi}{2}} \frac{d\theta}{\gamma^2 + K^2r^2\sin^2\theta} \\ &= -\frac{\gamma}{Kr^2} + 2\frac{Kr}{\pi}(1+\frac{\gamma^2}{K^2r^2}) \int_0^{\infty} \frac{d(\tan\theta)}{\gamma^2\sec^2\theta + K^2r^2\tan^2\theta} \\ &= -\frac{\gamma}{Kr^2} + 2\frac{Kr}{\pi}(1+\frac{\gamma^2}{K^2r^2}) \int_0^{\infty} \frac{du}{\gamma^2(1+u^2) + K^2r^2u^2} \\ &= -\frac{\gamma}{Kr^2} + \frac{\sqrt{K^2r^2+\gamma^2}}{Kr^2} \end{aligned}$$

Therefore we have

$$Kr^2 = -\gamma + \sqrt{K^2r^2+\gamma^2}$$

and hence

$$r = \sqrt{1 - \frac{2\gamma}{K}}. \tag{2.17}$$

To make the process of synchronization clear, the graphs Fig. 2.2 shows how the order parameter r rises as the coupling K between oscillators is increased. Numerical curves are taken from 500 oscillators with natural frequencies distributed with Lorentzian distribution:

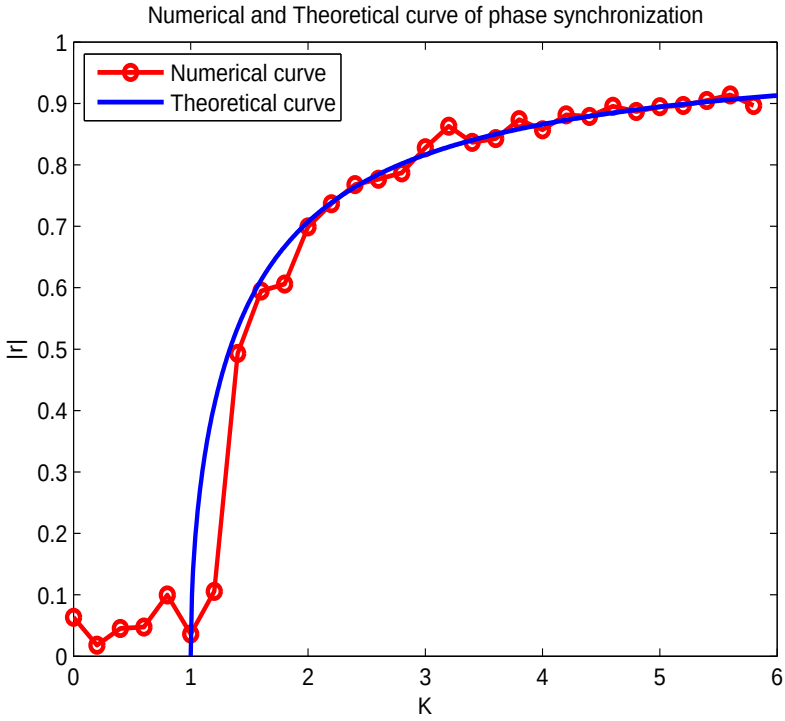

Figure 2.2 Numerical curve and analytical curve for order parameter by changing K

$$g(\omega) = \frac{\gamma}{\pi(\gamma^2 + \omega^2)}$$

with $\gamma = 0.5$. Analytical curve is given by (2.17), according to (2.16), $K_c = 1$.

There is another way to visualize the synchronization: There are three graphs in Figure 2.3. The oscillators are numbered from the lowest to highest natural frequency, natural frequencies also distributed by Lorentzian distribution.

$$g(\omega) = \frac{\gamma}{\pi(\gamma^2 + \omega^2)}$$

with $\gamma = 0.5$.

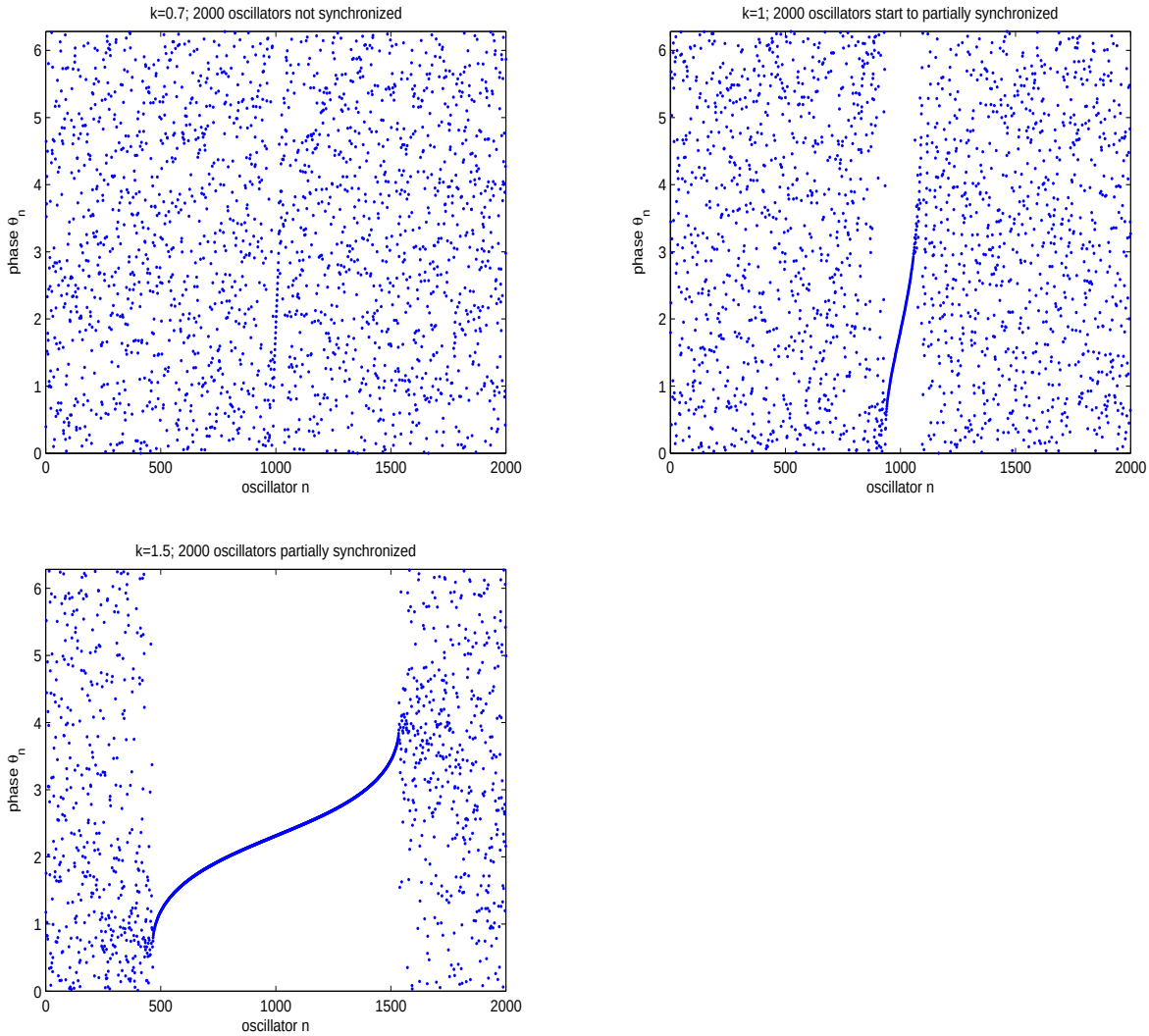

Figure 2.3 The synchronize phase θ_n of 2000 oscillators, take K=0.7, 1, 1.5

So

$$K_c = \frac{2}{\pi g(0)} = 1$$

, We can see obvious partial synchronization at or above K_c.

2.2 The Density Functions of Locked Terms and Unlocked Terms

To prove that the locked terms and unlocked terms are independent, we first try to get the probability density function of locked terms and unlocked terms separately.

Suppose the probability density function of locked terms is $f(y)$, then it satisfies the following equation:

$$P(y \leq \cos\theta \leq y + dy |\ \theta\ locked) = f(y)\ dy$$

$$\frac{P(\arccos(y + dy) \leq \theta \leq \arccos y)}{P(\theta\ locked)} = f(y)\ dy$$

For $y > 0$,

$$LHS = \frac{2P(\sin(\arccos(y + dy)) \leq \frac{\omega}{kr} \leq \sin(\arccos y))}{P(\theta\ locked)}$$

This derives

$$P(\theta\ locked) = \int_{-kr}^{kr} \frac{\gamma}{\pi(\gamma^2 + \omega^2)} d\omega = \frac{2}{\pi} \arctan(\frac{kr}{\gamma})$$

$$P(\sin(\arccos(y+dy)) \le \frac{\omega}{kr} \le \sin(\arccos y)))$$
$$= P(kr\sin(\arccos(y+dy)) \le \omega \le kr\sin(\arccos y))$$
$$= P(kr\sqrt{1-(y+dy)^2} \le \omega \le kr\sqrt{1-y^2})$$
$$= \int_{kr\sqrt{1-(y+dy)^2}}^{kr\sqrt{1-y^2}} \frac{\gamma}{\pi(\gamma^2+\omega^2)} d\omega$$
$$= \frac{1}{\pi}\int_{\frac{kr}{\gamma}\sqrt{1-(y+dy)^2}}^{\frac{kr}{\gamma}\sqrt{1-y^2}} \frac{du}{1+u^2}$$
$$= \frac{1}{\pi}(\arctan(\frac{kr}{\gamma}\sqrt{1-y^2}) - \arctan(\frac{kr}{\gamma}\sqrt{1-(y+dy)^2}))$$

Let $\alpha = \arctan(\frac{kr}{\gamma}\sqrt{1-y^2}) - \arctan(\frac{kr}{\gamma}\sqrt{1-(y+dy)^2})$

As $dy \to 0$, $\alpha \to 0$, $\alpha \to \tan\alpha$

So

$$\alpha \to \tan\alpha = \frac{\frac{kr}{\gamma}(\sqrt{1-y^2} - \sqrt{1-(y+dy)^2})}{1+(\frac{kr}{\gamma})^2\sqrt{(1-y^2)(1-(y+dy)^2)}}$$

As $dy \to 0$,

$$\frac{k\ r\ y\ dy}{\gamma\sqrt{1-y^2}} \frac{1}{1+(kr/\gamma)^2(1-y^2)} \to \frac{k\ ry\ \gamma\ \sqrt{1-y^2}\ dy}{\gamma^2(1-y)^2+(kr(1-y^2))^2}$$

This derives the density function: for $0 \le y \le 1$,

$$f(y) = \frac{k\ r\ \gamma\ y\sqrt{1-y^2}}{arctan(\frac{kr}{\gamma})(\gamma^2(1-y^2)+(kr(1-y^2))^2)}$$

The density function of unlocked term satisfies:

$$P(y \le \cos\theta \le y+dy|\ \theta\ unlocked) = \bar{f}(y)\ dy$$

For $0 \le y \le 1$, $y \le \cos\theta \le y+dy$.

So $\sqrt{1-(y+dy)^2} \le \sin\theta \le \sqrt{1-y^2}$, $d\theta = \frac{dy}{\sqrt{1-y^2}}$

or $-\sqrt{1-y^2} \leq \sin\theta \leq -\sqrt{1-(y+dy)^2}$, $d\theta = \frac{dy}{\sqrt{1-y^2}}$

$$\rho(\theta,\omega) = \frac{C}{|\theta'|} = \frac{C}{|\omega - kr\sin\theta|}$$

So

$$1 = \int_{-\pi}^{\pi} \rho(\theta,\omega)d\theta = C\int_{-\pi}^{\pi} \frac{d\theta}{|\omega - kr\sin\theta|}$$

Which derives

$$C = \frac{\sqrt{\omega^2-(kr)^2}}{2\pi}$$

So

$$P(y \leq \cos\theta \leq y+dy|\theta\ unlocked) = \frac{P(y \leq \cos\theta \leq y+dy, |\omega| > kr)}{P(|\omega| > kr)}$$

$$= \frac{P(-\sqrt{1-(y+dy)^2} \leq \sin\theta \leq -\sqrt{1-y^2}, |\omega| > kr)}{P(|\omega| > kr)}$$

$$+\frac{P(-\sqrt{1-y^2} \leq \sin\theta \leq -\sqrt{1-(y+dy)^2}, |\omega| > kr)}{P(|\omega| > kr)}$$

$$= \frac{\int_I g(\omega)\int_{I_1}\rho(\theta,\omega)d\theta d\omega + \int_I g(\omega)\int_{I_2}\rho(\theta,\omega)d\theta d\omega}{2\int_{kr}^{\infty}\frac{\gamma}{\pi(\gamma^2+\omega^2)}d\omega}$$

$$\begin{aligned} A_1 &= \int_I g(\omega)\int_{I_1}\rho(\theta,\omega)d\theta d\omega \\ &= \frac{1}{2\pi}\int_I \frac{\gamma}{\pi(\gamma^2+\omega^2)}\int_{I_1}\frac{\sqrt{\omega^2-(kr)^2}}{|\omega - kr\sqrt{1-y^2}|}d\theta d\omega \\ &= \frac{1}{2\pi^2}\int_I \frac{\gamma}{\gamma^2+\omega^2}\int_{I_1}\frac{\sqrt{\omega^2-(kr)^2}}{|\omega - kr\sqrt{1-y^2}|}\frac{dy}{\sqrt{1-y^2}}d\omega \end{aligned}$$

As $dy \to 0$, $d\theta \to 0$, $I_1 \to 0$, $I_2 \to 0$

$$\begin{aligned} A_1 &\to \frac{1}{2\pi^2}(\int_I \frac{\gamma}{\gamma^2+\omega^2}\frac{\sqrt{\omega^2-(kr)^2}}{\omega-kr\sqrt{1-y^2}}\frac{1}{\sqrt{1-y^2}}d\omega)dy \\ &= \frac{1}{2\pi^2\sqrt{1-y^2}}\int_I \frac{\gamma}{\gamma^2+\omega^2}\frac{\sqrt{\omega^2-(kr)^2}}{|\omega-kr\sqrt{1-y^2}|}d\omega dy \end{aligned}$$

$$\begin{aligned} A_2 &= \int_I\int_{I_2} g(\omega)\rho(\theta,\omega)d\theta d\omega \\ &= \frac{1}{2\pi^2}\int_I\int_{I_2}\frac{1}{\sqrt{1-y^2}}\frac{\gamma}{\gamma^2+\omega^2}\frac{\sqrt{\omega^2-(kr)^2}}{|\omega+kr\sqrt{1-y^2}|}dyd\omega \\ &= (\frac{1}{2\pi^2\sqrt{1-y^2}}\int_I \frac{\gamma}{\gamma^2+\omega^2}\frac{\sqrt{\omega^2-(kr)^2}}{|\omega+kr\sqrt{1-y^2}|}d\omega)dy \end{aligned}$$

This derives

$$A_1+A_2 = \frac{1}{2\pi^2\sqrt{1-y^2}}(\int_I \frac{\gamma\sqrt{\omega^2-(kr)^2}}{\gamma^2+\omega^2}(\frac{1}{|\omega+kr\sqrt{1-y^2}|}+\frac{1}{|\omega-kr\sqrt{1-y^2}|}))d\omega dy$$

Similarly, for $-1 \le y < 0$,

$$\begin{aligned} A_1+A_2 &= \frac{1}{2\pi^2\sqrt{1-y^2}}\int_I \frac{\gamma\sqrt{\omega^2-(kr)^2}}{\gamma^2+\omega^2}(\frac{1}{|\omega+kr\sqrt{1-y^2}|}+\frac{1}{|\omega-kr\sqrt{1-y^2}|})d\omega dy \\ &= \frac{\gamma}{2\pi^2\sqrt{1-y^2}}\int_I \frac{\sqrt{\omega^2-(kr)^2}}{\gamma^2+\omega^2}\frac{2|\omega|}{\omega^2-(kr)^2(1-y^2)}d\omega dy \\ &= \frac{2\gamma}{\pi^2\sqrt{1-y^2}}\int_{kr}^{\infty}\frac{\omega\sqrt{\omega^2-(kr)^2}}{(\gamma^2+\omega^2)(\omega^2-(kr)^2(1-y^2))}d\omega dy \\ &= \frac{\gamma}{\pi^2\sqrt{1-y^2}}\int_{\alpha}^{\infty}\frac{\sqrt{t-\alpha}}{(t+\gamma^2)(t-\alpha(1-y^2))}dtdy \\ &= \frac{\gamma}{\pi^2\sqrt{1-y^2}}\int_0^{\infty}\frac{\sqrt{t}}{(t+\alpha+\gamma^2)(t+\alpha y^2)}dtdy \end{aligned}$$

$\Rightarrow$

$$\frac{P(y \le \cos\theta \le y+dy, |\omega| > kr)}{P(|\omega| > kr)} = \bar{f}(y)dy$$
$$= \frac{\gamma}{\pi^2\sqrt{1-y^2}} \frac{1}{1-\frac{2}{\pi}arctan(\frac{kr}{\gamma})} \int_0^\infty \frac{\sqrt{t}dtdy}{(t+\alpha+\gamma^2)(t+\alpha y^2)}$$
$$= \frac{\gamma}{\pi\sqrt{1-y^2}} \frac{1}{\pi-2arctan(\frac{kr}{\gamma})} \int_0^\infty \frac{\sqrt{t}dtdy}{(t+\alpha+\gamma^2)(t+\alpha y^2)}$$

$\Rightarrow$

$$\bar{f}(y) = \frac{\gamma}{\pi\sqrt{1-y^2}(\pi-2\arctan(kr/\gamma))} \int_0^\infty \frac{\sqrt{t}dt}{(t+\alpha+\gamma^2)(t+\alpha y^2)}$$
$$= \frac{\gamma}{\sqrt{1-y^2}(\pi-2arctan(kr/\gamma))} \frac{1}{\sqrt{\alpha+\gamma^2}+\sqrt{\alpha y^2}}$$
$$= \frac{\gamma}{\sqrt{1-y^2}(\pi-2arctan(kr/\gamma))} \frac{1}{\sqrt{(kr)^2+\gamma^2}+kr|y|}$$

So we have the density function f for locked part and $\bar{f}$ for unlocked part:

$$f(y) = \frac{k\ r\ \gamma\ y\sqrt{1-y^2}}{arctan(\frac{kr}{\gamma})(\gamma^2(1-y^2)+(kr(1-y^2))^2)} \quad (2.18)$$
$$\bar{f}(y) = \frac{\gamma}{\sqrt{1-y^2}(\pi-2arctan(kr/\gamma))(\sqrt{(kr)^2+\gamma^2}+kr|y|)} \quad (2.19)$$

To prove the locked terms are independent, we want to show that the sum of any two locked terms satisfies the analytical probability density function derived by convolution law:

If X and Y are two locked terms, Z is the sum of X and Y:

$$Z = X + Y$$

$$
\begin{aligned}
E(e^{tZ}) &= \int_{-\infty}^{\infty} e^{tu} f_z(u) du && (2.20)\\
&= \int_{-\infty}^{\infty}\int_{-\infty}^{\infty} e^{tx} e^{ty} f_x(x) f_y(y) dx du && (2.21)\\
&= \int_{-\infty}^{\infty} e^{tu} \int_{-\infty}^{\infty} f_x(x) f_y(u-x) dx du && (2.22)
\end{aligned}
$$

$\Rightarrow$

$$f_z(u) = \int_{-\infty}^{\infty} f_x(x) f_y(u-x) dx$$

Similarly, to prove the unlocked terms are independent, we can also get the analytical probability density function of two unlocked terms by the convolution law:

If $\bar{X}$ and $\bar{Y}$ are two unlocked terms, $\bar{Z}$ is the sum of $\bar{X}$ and $\bar{Y}$:

$$\bar{Z} = \bar{X} + \bar{Y}$$

$$
\begin{aligned}
E(e^{t\bar{z}}) &= \int_{-\infty}^{\infty} e^{tu} f_{\bar{z}}(u) du && (2.23)\\
&= \int_{-\infty}^{\infty}\int_{-\infty}^{\infty} e^{t\bar{x}} e^{t\bar{y}} f_{\bar{x}}(\bar{x}) f_{\bar{y}}(\bar{y}) d\bar{x} du && (2.24)\\
&= \int_{-\infty}^{\infty} e^{tu} \int_{-\infty}^{\infty} f_{\bar{x}}(\bar{x}) f_{\bar{y}}(u-\bar{x}) d\bar{x} du && (2.25)
\end{aligned}
$$

$\Rightarrow$

$$f_{\bar{z}}(u) = \int_{-\infty}^{\infty} f_{\bar{x}}(\bar{x}) f_{\bar{y}}(u-\bar{x}) d\bar{x}$$

In the following figures, we compare the numerical and analytical result for the density functions, the numerical result of density function for one oscillator satisfies the analytical result very well. The analytical density function of the sum of two locked oscillators and

two unlocked oscillators are given by convolution law separately, and we also compare the results, the numerical curve also approximate the analytical curve very well. This shows the locked oscillators are independent and unlocked terms are also independent.

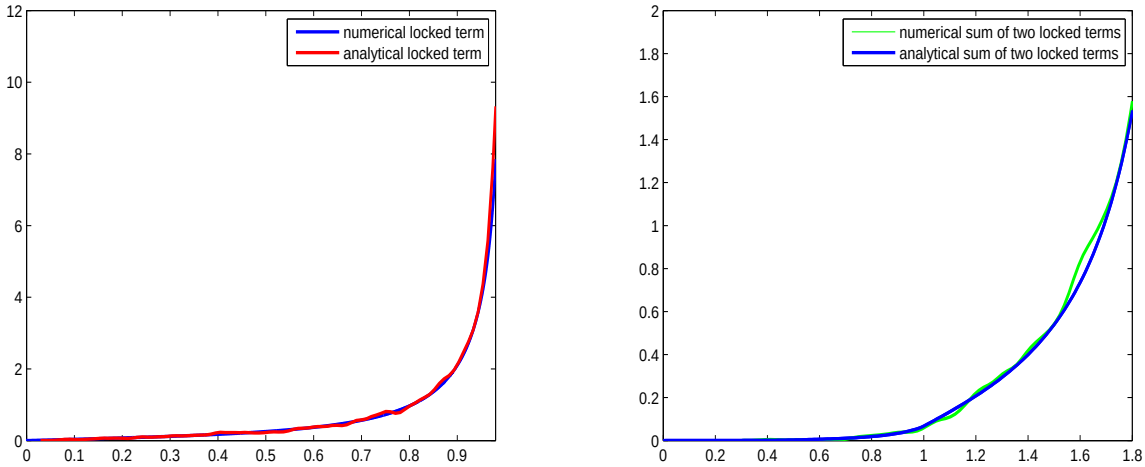

Figure 2.4 Comparison of the numerical and analytical density function for the locked oscillators and the sum of two locked oscillators

2.3 The Distribution of Order Parameter r

If we set $\psi \equiv 0$ (in a rotating frame), then $\sum_{j=1}^{N} \sin\theta_j = 0$.

The order parameter satisfies the following equation:

$$r = \frac{1}{N}\sum_{j=1}^{N} e^{i\theta_j} = \frac{1}{N}\sum_{j=1}^{N} \cos\theta_j. \tag{2.26}$$

According to the analysis on the drift term, we know that the contribution of the drift term is 0. Namely

$$r = < \cos\theta >_{lock} + < \cos\theta >_{unlock}$$

$$\approx < \cos\theta >_{lock}$$

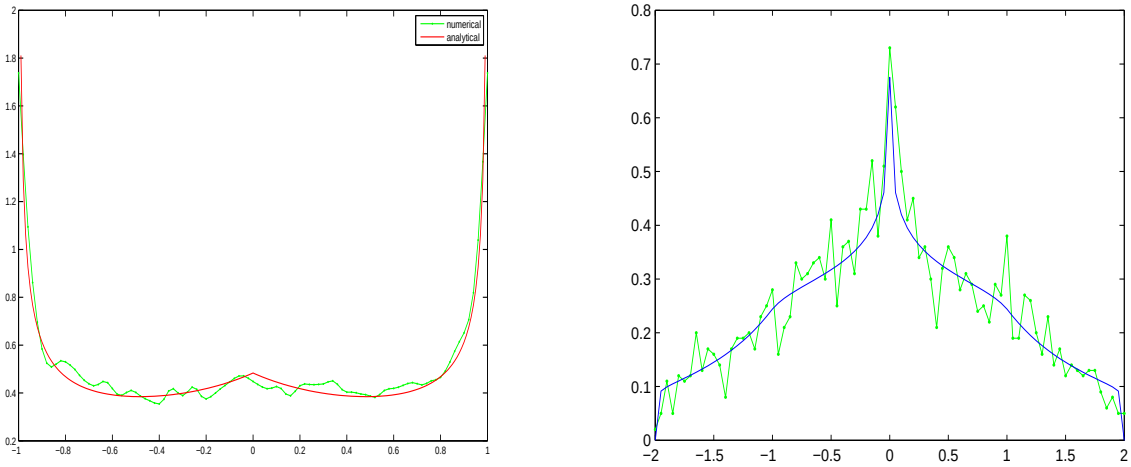

Figure 2.5 Comparison of the numerical and analytical density function for the unlocked oscillators and the sum of two unlocked oscillators

There are totally N terms $\theta_1, \theta_2, ...\theta_N$. Without loss of generality, we suppose the first n terms $\theta_1, \theta_2, ...\theta_n$ are synchronized, and the last $N-n$ terms $\theta_{n+1}, \theta_{n+2}, ...\theta_N$ are not synchronized. Here $0 < n < N$.

From equation (2.26), we get

$$\begin{aligned} r = & \frac{1}{N}\sum_{j=1}^{N} e^{i\theta_j} = \frac{1}{N}\sum_{j=1}^{N}\cos\theta_j \\ = & \frac{1}{N}\sum_{j=1}^{n}\cos\theta_j + \frac{1}{N}\sum_{j=n+1}^{N}\cos\theta_j \end{aligned} \tag{2.27}$$

Suppose $S_1 = \sum_{j=1}^{n}\cos\theta_j$, $S_2 = \sum_{j=n+1}^{N}\cos\theta_j$, $S = \sum_{j=1}^{N}\cos\theta_j$,

then

$$S_1 + S_2 = S = Nr$$

and

$$S_2 \approx 0,\ S_1 \approx S = Nr$$

.

For a fixed number N, if we also fix a series of natural frequency $\omega_1, \omega_2, ...\omega_N$, and these series of natural frequency satisfies the Lorentzian distribution very well-proportionally, the density function is

$$g(\omega) = \frac{\nu}{\pi(\nu^2 + \omega^2)}$$

.

Take different series of initial values of $\theta_j,\ j = 1, 2, ...N$.

These series of θ_j are taken randomly which satisfy uniformly distribution. We will get different values of order parameter r for each series of $\theta_j,\ j = 1, 2, ...N$.

Question: When the value of N is very large, what is the distribution of the value of order parameter r?

When N is large, n and N-n are large. According to central limit theorem,

$$\frac{S_1 - n\mu_1}{\sigma_1\sqrt{n}} \sim N(0, 1)$$

. Here μ_1 and σ_1 are the mean and variance of locked terms $\cos\theta_j,\ j = 1, 2, ...n$.

$$\frac{S_2 - (N-n)\mu_2}{\sigma_2\sqrt{N-n}} \sim N(0, 1)$$

Here μ_2 and σ_2 are the mean and variance of unlocked terms $\cos\theta_j,\ j = n+1, n+2, ...N$

We know that S_1 and S_2 both satisfy Gaussian distribution. From equation (2.27) the order parameter

$$r = \frac{1}{N}(S_1 + S_2)$$

is the linear combination of Gaussian distributed functions. So r also satisfies Gaussian distribution. The variance of S_1 is $\sigma_1^2 n$ and the variance of S_2 is $\sigma_2^2(N-n)$,

σ satisfies the following equation:

$$\sigma = \frac{1}{N^2}(\sigma_1^2 n + \sigma_2^2(N-n))$$

.

So the question is reduced to calculate the value of σ_1 and σ_2.

σ_1 is the variance of locked terms $\cos\theta_1, \cos\theta_2, ..., \cos\theta_n$.

$\sigma_1 = Var(\theta)_{locked} = E(\cos^2\theta)_{locked} - (E(\cos\theta)_{locked})^2$

$$E(\cos^2\theta)_{locked} = \frac{\int_{-\frac{\pi}{2}}^{\frac{\pi}{2}} \cos^2\theta g(Kr\sin\theta)Kr\cos\theta \ d\theta}{\int_{-\frac{\pi}{2}}^{\frac{\pi}{2}} g(Kr\sin\theta)Kr\cos\theta \ d\theta} \tag{2.28}$$

Here

$$\begin{aligned}\int_{-\frac{\pi}{2}}^{\frac{\pi}{2}} \cos^2\theta g(Kr\sin\theta)Kr\cos\theta \ d\theta &= \frac{Kr\nu}{\pi}\int_{-\frac{\pi}{2}}^{\frac{\pi}{2}} \frac{\cos^3\theta}{\nu^2 + K^2r^2\sin^2\theta} \ d\theta \\ &= \frac{2\nu}{\pi Kr}(\frac{\nu^2 + K^2r^2}{Kr\nu}\arctan(\frac{Kr}{\nu}) - 1)\end{aligned}$$

$$\begin{aligned}\int_{-\frac{\pi}{2}}^{\frac{\pi}{2}} g(Kr\sin\theta)Kr\cos\theta \ d\theta &= \frac{Kr\nu}{\pi}\int_{-\frac{\pi}{2}}^{\frac{\pi}{2}} \frac{\cos\theta}{\nu^2 + K^2r^2\sin^2\theta} \ d\theta \\ &= \frac{2}{\pi}\arctan(\frac{Kr}{\nu})\end{aligned}$$

Plug these results into the equation (2.28), we can get

$$E(\cos^2\theta)_{locked} = \frac{\nu}{Kr}(\frac{\nu^2 + K^2r^2}{Kr\nu} - \frac{1}{\arctan(\frac{Kr}{\nu})}) \tag{2.29}$$

The variance of unlocked terms is

$$\sigma_2 = Var(\theta)_{unlocked} = E(\cos^2\theta)_{unlocked} - (E(\cos\theta)_{unlocked})^2$$

$$E(\cos^2\theta)_{unlocked} = \int_{-\pi/2}^{\pi/2}\int_{|\omega|>Kr} \cos^2\theta \frac{Cg(\omega)}{|\omega - Kr\sin\theta|}\, d\theta\, d\omega$$
$$= 2\int_{-\pi/2}^{\pi/2}\int_{\omega>Kr} \cos^2\theta \frac{Cg(\omega)}{|\omega - Kr\sin\theta|}\, d\theta\, d\omega$$

and

$$E(\cos\theta)_{unlocked} = \int_{-\pi/2}^{\pi/2}\int_{|\omega|>Kr} \cos\theta \frac{Cg(\omega)}{|\omega - Kr\sin\theta|}\, d\theta\, d\omega$$
$$= 2\int_{-\pi/2}^{\pi/2}\int_{\omega>Kr} \cos\theta \frac{Cg(\omega)}{|\omega - Kr\sin\theta|}\, d\theta\, d\omega$$

Here $g(\omega) = \frac{\nu}{\pi(\nu^2+\omega^2)}$, $C = \frac{\sqrt{\omega^2 - K^2r^2}}{2\pi}$.

These integrals are relatively hard to simplify, but we can use numerical methods to get the variance of the unlocked terms.

The variance of order parameter r is $\sigma = \frac{1}{N^2}(\sigma_1^2 n + \sigma_2^2(N-n))$.

i.e

$$\frac{r - mean(r)}{\frac{1}{N}\sqrt{\sigma_1^2 n + \sigma_2^2(N-n)}} \sim N(0,1) \tag{2.30}$$

Taking 1000 series of uniformly distributed initial values θ_1, θ_2, ... θ_N, we can get 1000 values of order parameter r. The order parameter r approximately satisfies Gaussian distribution, the equation for this distribution is (2.30).

The graphs in Figure 2.6 compare the LHS of (2.30) with $N(0,1)$ (standard normal distribution). The blue line is the density function of standard normal distribution, the red line is the density function of the distribution of LHS function.

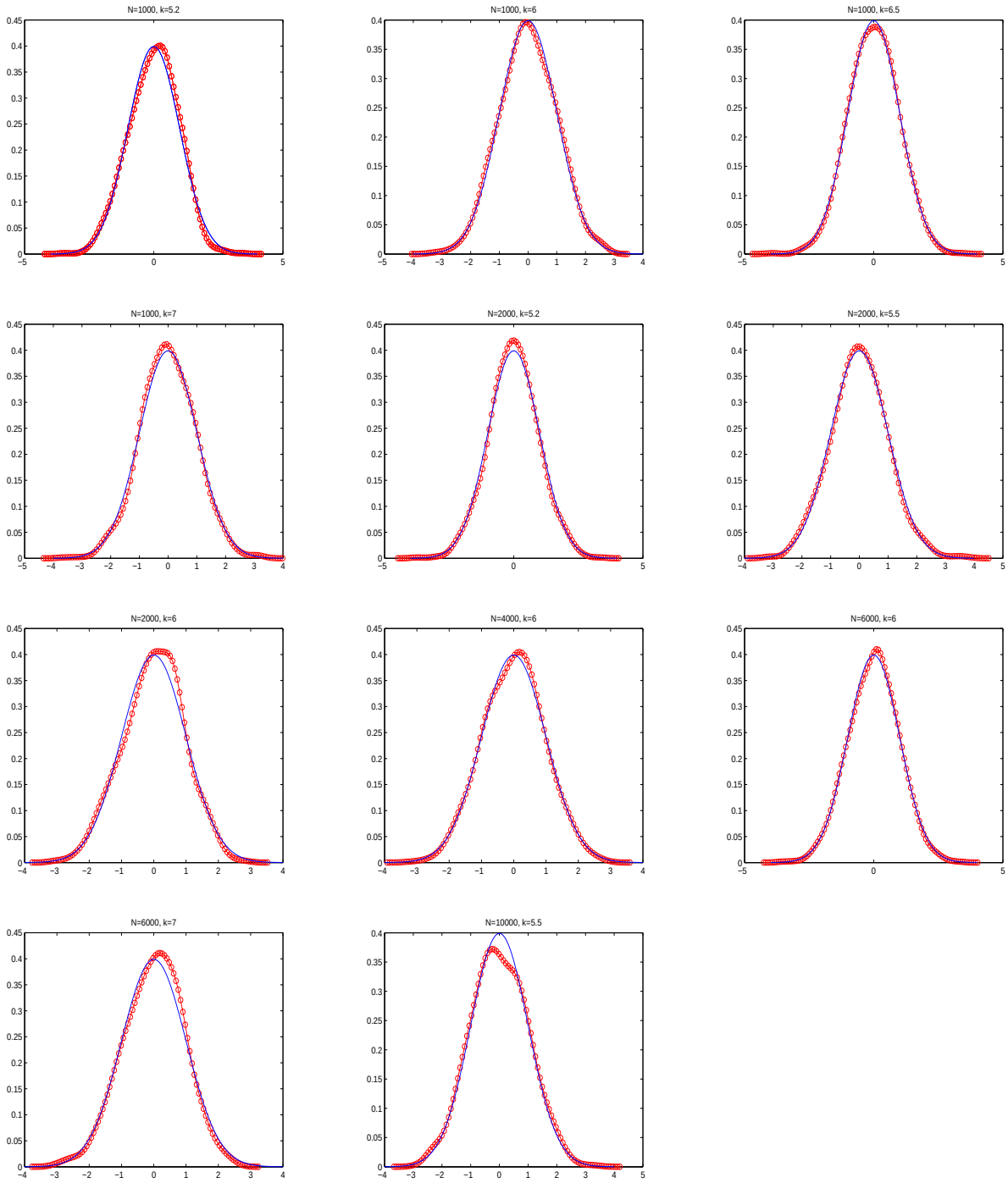

Figure 2.6 Comparison of distribution of order parameter and normal distribution

CHAPTER 3

OSCILLATORY CLUSTERS IN THE BZ REACTION

Physicochemical systems with coupled processes on different length scales often exhibit stationary spatially periodic structures [35]. The photosensitive BZ reaction has proven to be an ideal model system for studies of perturbed excitable media. Numerical simulations of chaotic states in some low dimensional models are carried out and novel structures of the first return maps representitive of BZ chaos in a three-variable model are discovered [44].

The FitzHugh-Nagumo model [42],[23] is a generic model for excitable media and can be applied to a variety of systems. FitzHugh called this simplified model the Bon Hoeffer-van der Pol model and derived it in the 1960's as a simplification of the Hodgkin-Huxley equations.

In this chapter, first I will introduce the Oregonator and FHN type models. The classic FHN model has a cubic shaped function in the inhibitory term, but I used the piecewise linear function to approximate the cubic term. The piecewise linear system has the same shape as the cubic oscillators system for most of the parameters. It's a good method to use piecewise linear model to approximate the cubic FHN model.

3.1 Oscillatory Clusters in the Oregonator and FHN type Models with Global Inhibitory Feedback

The modified Oregonator model (1.10) introduced in [52] with diffusion terms added to both the activator and the inhibitor equations has been extended by Yang et al. to include global feedback. This model reproduces the experimentally observed stable localized, two-phase and three-phase clusters referred to above. The following global feedback term

$$\gamma(< w > -\bar{w})\psi(v) \tag{3.1}$$

Here $\psi(v)$ is defined in 1.13.

was added to the activator (v) equation. In (1.7), $< w >$ represents the instantaneous spatial average of the activator variable w, and $\bar{w}$ represents the target value of the oxidized form of the catalyst, which was set equal to the unstable steady state concentration (unstable fixed-point). The parameter γ is the global feedback coefficient, which depends on the maximum actinic light intensity and on the quantum yield of the photochemical reaction. Note that the global feedback represents the global effect of the inhibitor on the activator rather than the global effect of the activator onto itself as is commonly encountered.[49]

The modified Oregonator model with global inhibitory feedback in the absence of diffusion reads

$$\begin{cases} \epsilon_1 \, dv_k d\tau = f(v_k, w_k) - \gamma \, (< w > -\bar{w}) \, \psi(v_k), \\ \quad dw_k/d\tau = g(v_k, w_k), \end{cases} \tag{3.2}$$

for $k = 1, \ldots, N$, where $f(v, w)$ and $g(v, w)$ are given by (1.11) and (1.14) respectively, γ is the global feedback parameter, $\psi(v_k)$ is defined in 1.13.

In a subsequent study, Rotstein et al. [35, 34] studied a mechanism of localized cluster formation in the modified Oregonator model and in a model of FitzHugh-Nagumo type [34] with global inhibitory feedback and no diffusion. If the system has N oscillators, the global feedback term reads

$$< w > \; = \; \frac{1}{N} \sum_{k=1}^{N} w_k. \tag{3.3}$$

The parameter $\bar{w}$ is the w-coordinate of the intersection point between the nullclines when $\gamma = 0$. Note that the intersection point between nullsurfaces does not change with γ.

In these studies a "cluster simplification" was made. By assuming that all oscillators in a cluster have the same amplitude and frequency, all the oscillators belonging to the same cluster are indistinguishable from the dynamic point of view, and can be described by the

same equations. Thus, a system of N globally coupled oscillators having M clusters can be described by the following globally coupled system of M-oscillators

$$\begin{cases} v_k' = f(v_k) - w_k - \gamma\,[\,< w > -\bar{w}\,], \\ w_k' = \epsilon\,[\,g(v_k;\lambda) - w_k\,], \end{cases} \tag{3.4}$$

for $k = 1, \ldots, M$ with

$$< w > \;\; = \;\; \sum_{k=1}^{M} \alpha_k\, w_k \tag{3.5}$$

where α_k, $k = 1, \ldots, M$ is the fraction of oscillators belonging to each cluster, note that $\sum_{k=1}^{n} \alpha_k = 1$.

If $M = 1$, single oscillator system reads:

$$\begin{cases} v' = f(v) - (1+\gamma)w - \bar{w}\,], \\ w' = \epsilon\,[\alpha v - \lambda - w\,] \end{cases} \tag{3.6}$$

If $M = 2$ (two clusters) sytem (3.4) reads

$$\begin{cases} v_k' = f(v_k) - w_k - \gamma\,[\,\alpha_1\, w_1 + \alpha_2\, w_2 - \bar{w}\,], \\ w_k' = \epsilon\,[\alpha v_k - \lambda - w_k\,] \end{cases} \tag{3.7}$$

for $k = 1, 2$. This is a system of two oscillators globally coupled through the inhibitor variables w_1 and w_2. Where the function f is given by (1.16). Here we have chosen $h = 2$ and $a = 3$, the result of making $v_1' = v_2' = w_1' = w_2' = 0$ are not one-dimensional curves but higher dimensional objects. In particular, by making $v_k' = 0$ for $k = 1, 2$ one gets

$$w_k = \frac{f(v_k) + \gamma\,\bar{w}}{1 + \alpha_k\gamma} - \frac{\gamma\,\alpha_j w_j}{1 + \alpha_k\gamma} \tag{3.8}$$

for $k, j = 1, 2$ and $j \neq k$. Eq. (3.8) describes a two-dimensional surface $w_k = N_{v,k}(v_k, w_j)$ having the shape of the first term in eq. (3.8), which can be thought as curves moving up and down due to the effect of the second term.

3.2 Piecewise Linear Approximation of Single Oscillator

(i) The exact solution of single oscillator

In order to simplify the analysis, first, we just consider the system without global feedback term, i.e. $\gamma = 0$. The McKean model [23, 42] is the simplest PWL model with a cubic-like v-nullcline. It has three linear pieces, one for each branch. This model has been used to study several aspects of neural dynamics, and preserves many basic dynamic features of the FHN model such as the existence of (large amplitude) relaxation oscillations (spikes) and a non-smooth version of the Hopf-bifurcation [8, 33, 37, 46, 7].

We substitute the cubic function $f(v)$ with three piecewise linear function as explained below, and check whether this piecewise linear system still captures the cluster dynamics observed in the smooth system.

The general form of each linear component is

$$\begin{cases} \dot{v_j} = \eta_j(v - \hat{v}_{j-1}) + \hat{\omega}_{j-1} - \omega_j, \\ \dot{\omega_j} = \varepsilon[\alpha v_j - \lambda - \omega_j], \qquad j = 0, 1, 2. \end{cases} \tag{3.9}$$

Here $\eta_0 = -1$, $\eta_1 = 1$, and $\eta_2 = -1$.

The corresponding fixed point is given by $(\bar{v}, \bar{\omega})$, where

$$\bar{v} = \frac{\lambda - \eta_j \hat{v}_{j-1} + \hat{\omega}_{j-1}}{\alpha - \eta_j} \quad \bar{\omega} = \frac{\lambda\eta_j - \alpha\eta_j\hat{v}_{j-1} + \alpha\hat{\omega}_{j-1}}{\alpha - \eta_j}.$$

For simplicity, we make change of variables with the goal of shifting the fixed point to the origin to study the dynamics in each linear regime.

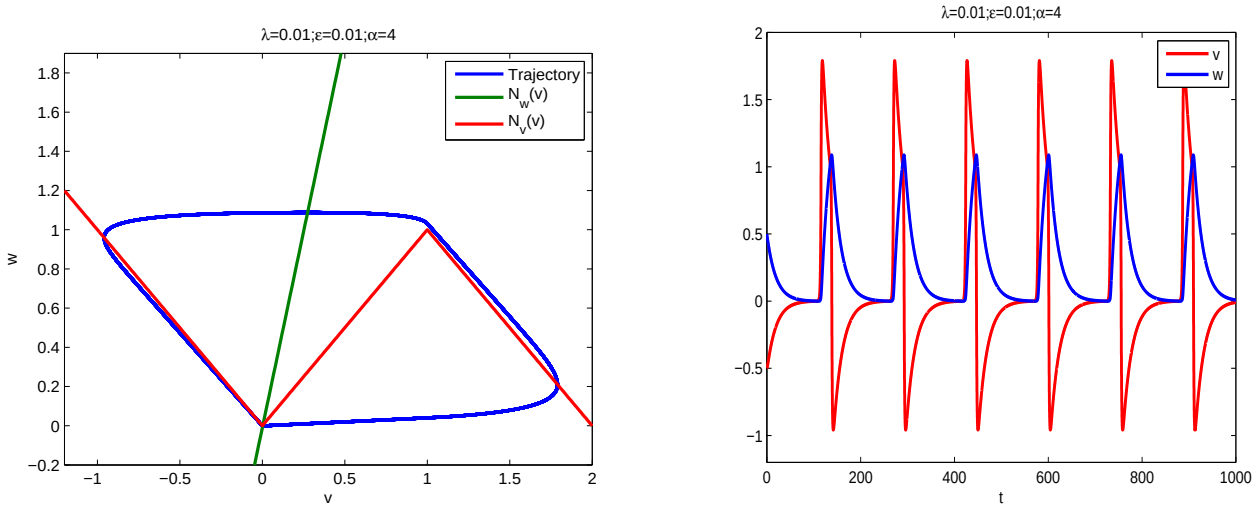

Figure 3.1 Phase-plane (left) and traces (right) for the piecewise-linear approximation of FHN (3.9) for representative parameter values.

Let us consider $V := v - \bar{v}$ and $W := \omega - \bar{\omega}$ with the following equation

$$\begin{cases} V' &= \eta V - W, \qquad V(0) = v_0 - \bar{v} \\ W' &= \varepsilon[\alpha V - W], \qquad W(0) = \omega_0 - \bar{\omega} \end{cases}$$

The Jacobian matrix of the above piecewise linear equation is

$$J = \begin{pmatrix} \eta & -1 \\ \varepsilon\alpha & -\varepsilon \end{pmatrix}$$

whose eigenvalues are:

$$r_{1,2} = \frac{\eta - \varepsilon \pm \sqrt{(\eta - \varepsilon)^2 - 4\varepsilon(\alpha - \eta)}}{2}$$

The fixed point is stable (unstable) if $\eta < (>)\ \varepsilon$. The eigenvalues are complex if $\eta \in (-\varepsilon - 2\sqrt{\varepsilon\alpha}, -\varepsilon + 2\sqrt{\varepsilon\alpha})$.

(a) **When** $(\eta+\varepsilon)^2-4\varepsilon\alpha>0$**, we have** $r_1-r_2=\sqrt{(\eta+\varepsilon)^2-4\alpha\varepsilon}$**.**

The solution is

$$\begin{pmatrix} v \\ \omega \end{pmatrix} = c_1 \begin{pmatrix} 1 \\ r_2+\varepsilon \end{pmatrix} e^{r_1 t} + c_2 \begin{pmatrix} 1 \\ r_1+\varepsilon \end{pmatrix} e^{r_2 t} + \begin{pmatrix} \bar{v} \\ \bar{\omega} \end{pmatrix}$$

where $c_1 = \dfrac{(v_0-\bar{v})(r_1+\varepsilon)-(\omega_0-\bar{\omega})}{r_1-r_2}$, $c_2 = \dfrac{-(v_0-\bar{v})(r_2+\varepsilon)+(\omega_0-\bar{\omega})}{r_1-r_2}$

(b) **When** $(\eta+\varepsilon)^2-4\varepsilon\alpha<0$ **we have** $\mu = \dfrac{\sqrt{4\alpha\varepsilon-(\eta+\varepsilon)^2}}{2}$.

The solution is

$$\begin{pmatrix} v \\ \omega \end{pmatrix} = c_1 \left[\begin{pmatrix} 1 \\ (\eta+\varepsilon)/2 \end{pmatrix} \cos\mu t + \begin{pmatrix} 0 \\ \mu \end{pmatrix} \sin\mu t \right] e^{(\eta-\varepsilon)t/2}$$

$$+c_2 \left[\begin{pmatrix} 1 \\ (\eta+\varepsilon)/2 \end{pmatrix} \sin\mu t + \begin{pmatrix} 0 \\ \mu \end{pmatrix} \cos\mu t \right] e^{(\eta-\varepsilon)t/2} + \begin{pmatrix} \bar{v} \\ \bar{\omega} \end{pmatrix}$$

where

$$c_1 = v_0-\bar{v}, \quad c_2 = \frac{(v_0-v)(\eta+\varepsilon)-2(\omega_0-\omega)}{2\mu}$$

.

(ii) Comparison of Numerical Solution and Analytical Solution of Single Oscillator

In equation (3.9), we take $\lambda=0.2, \varepsilon=0.01, \alpha=2, \eta_0=\eta_2=-1$ and $\eta_1=1$. The initial conditions are $V(0)=-1$ and $\omega(0)=0.5$

The numerical and analytical solutions are shown in the Fig. 3.2, from which we can tell that they are very close to each other.

A

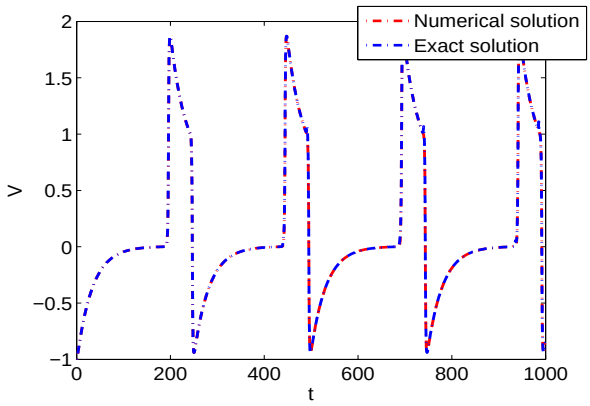
Numerical solution
Exact solution
V
t

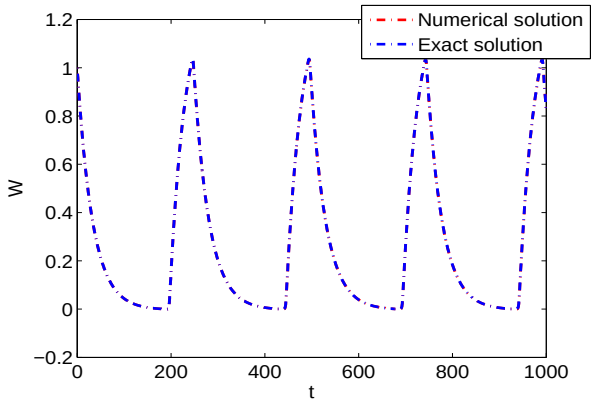
Numerical solution
Exact solution
W
t

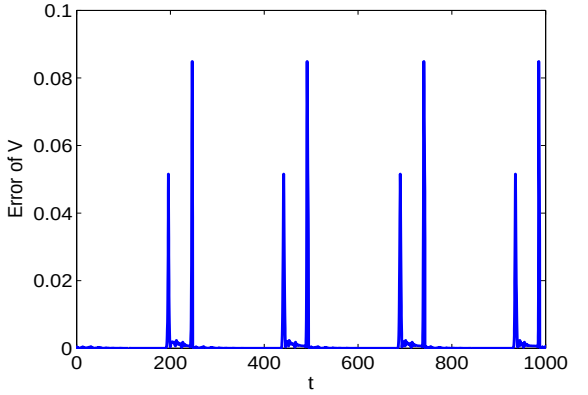
Error of V
t

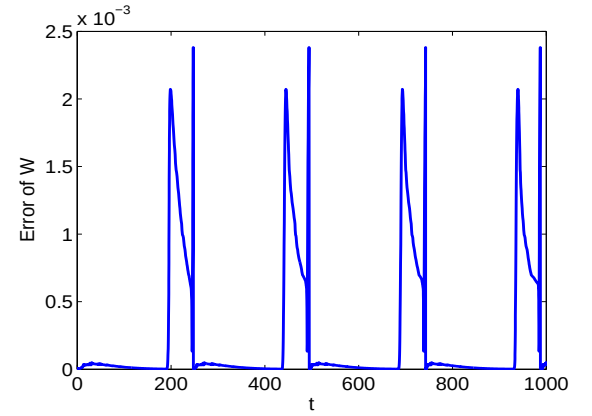
x 10^-3
Error of W
t

B

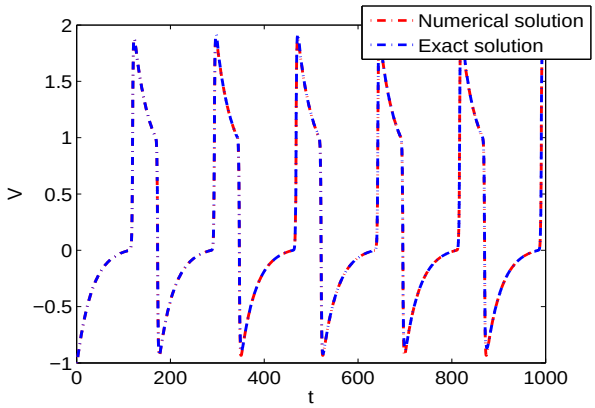
Numerical solution
Exact solution
V
t

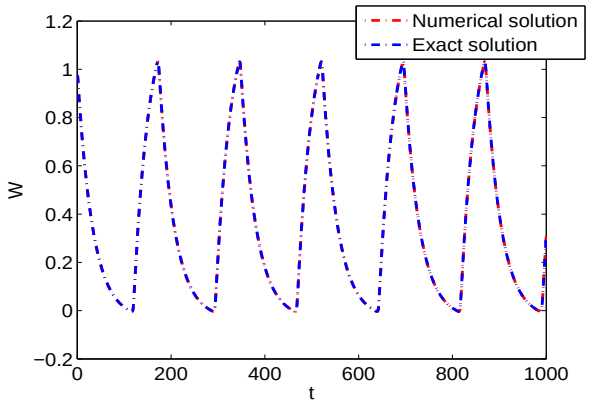
Numerical solution
Exact solution
W
t

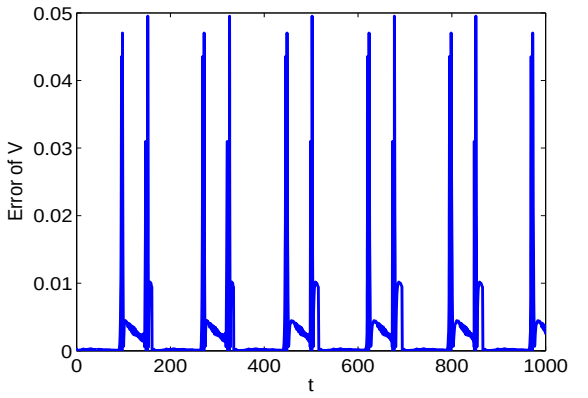
Error of V
t

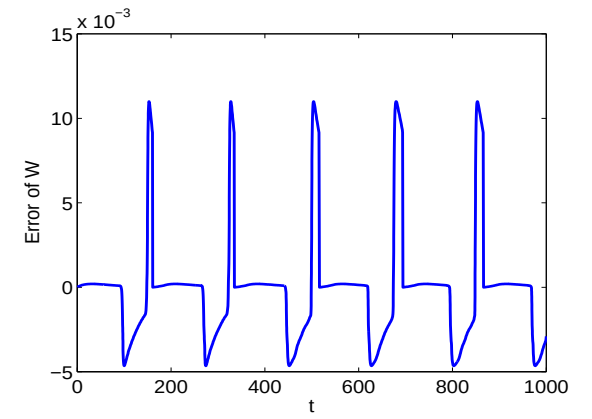
x 10^-3
Error of W
t

C

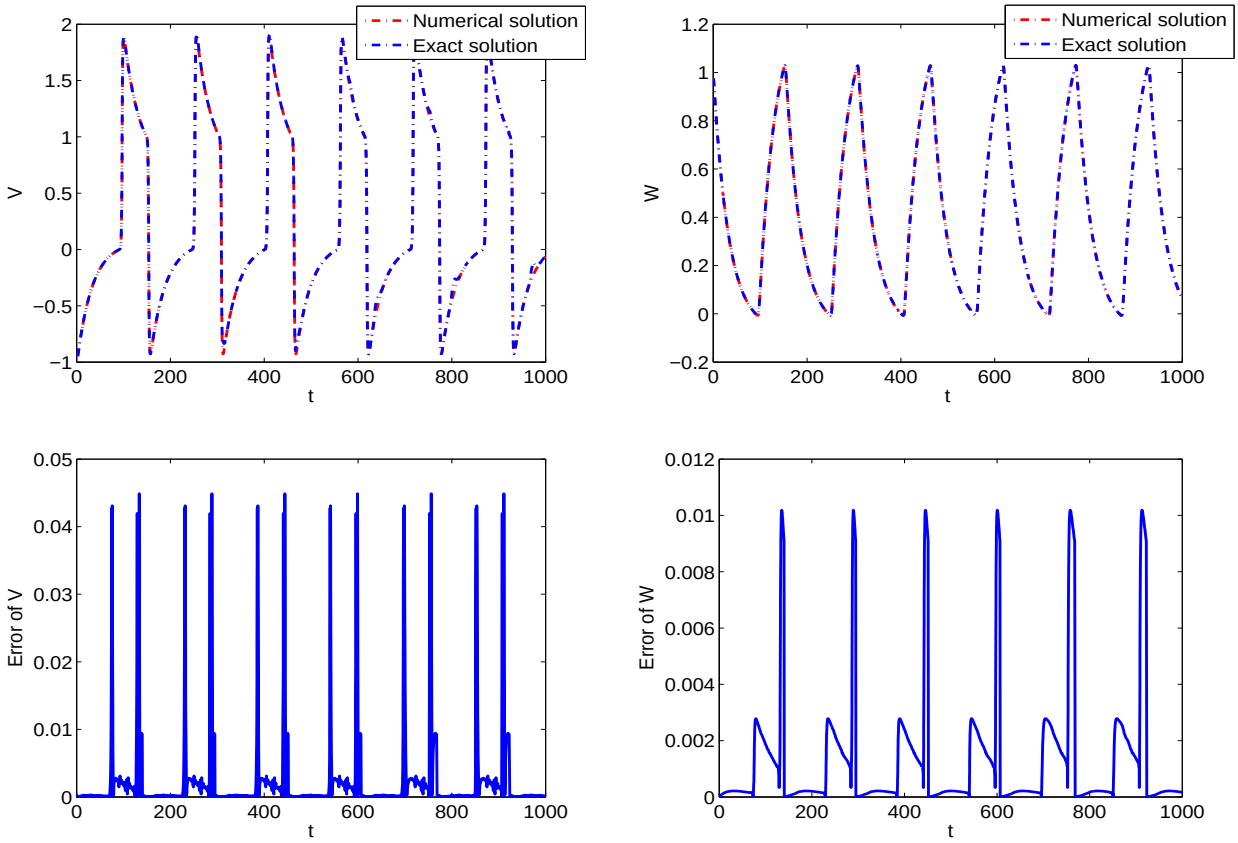

Figure 3.2 Comparison between the analytical and numerical solutions for a single PWL oscillator evolving according to eq. (3.8) with $\alpha = 2$, $\epsilon = 0.01$ and **A** $\lambda = 0.01$, **B:** $\lambda = 0.1$, and **C:** $\lambda = 0.2$. The cubic-like PWL function $f(v)$ is given by (3.10) with $\beta_1 = \beta_2 = 1$. For each value of λ, the numerical ($\tilde{V}$,dashed-red) and analytical (V, dashed-blue) solutions are presented in the top panels. The corresponding absolute errors, defined as $|V(t) - \tilde{V}(t)|$ and $|W(t) - \tilde{W}(t)|$ presented in the bottom panels. The numerical and analytical solutions are in good agreement.

A

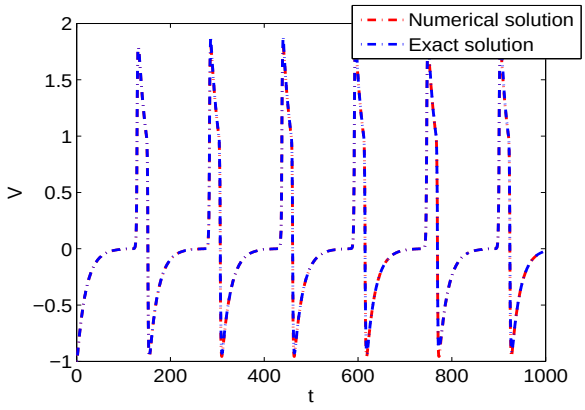
Numerical solution
Exact solution
V
t

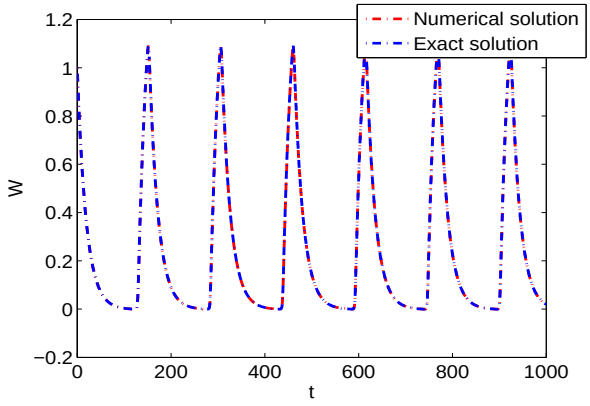
Numerical solution
Exact solution
W
t

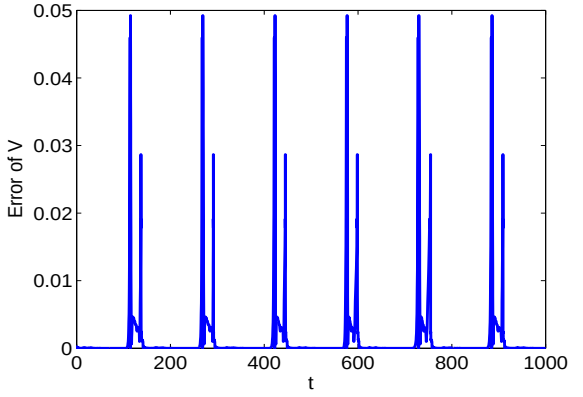
Error of V
t

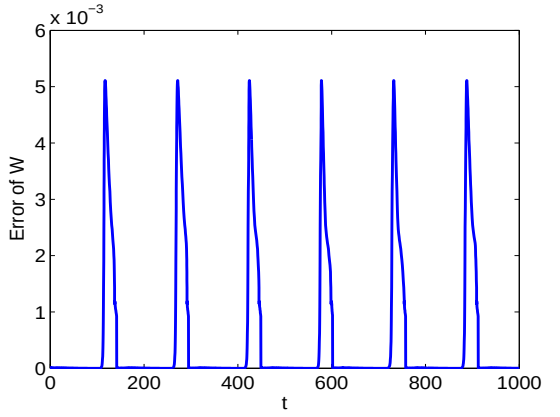
x 10^-3
Error of W
t

B

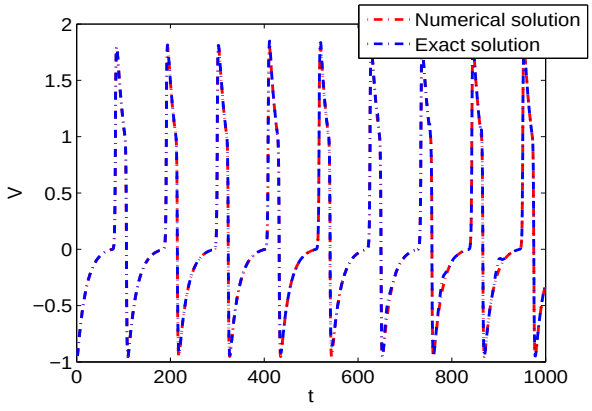
Numerical solution
Exact solution
V
t

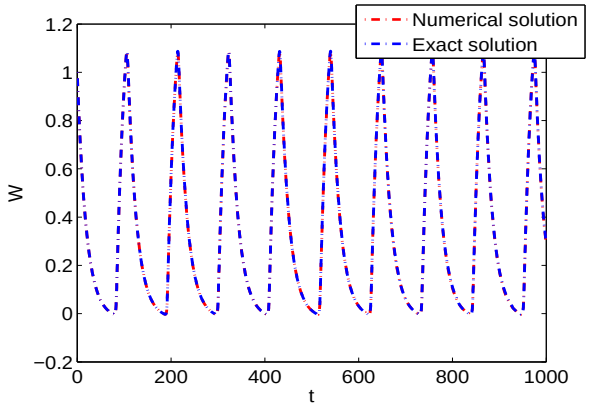
Numerical solution
Exact solution
W
t

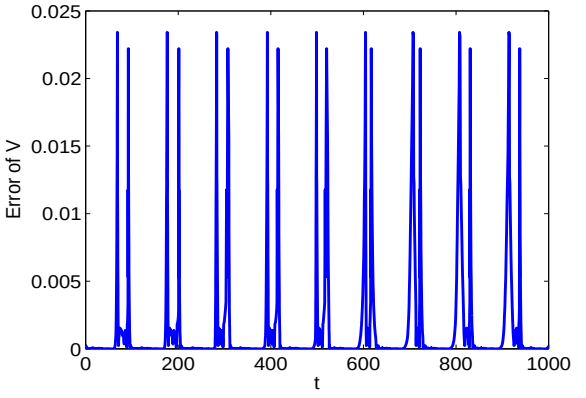
Error of V
t

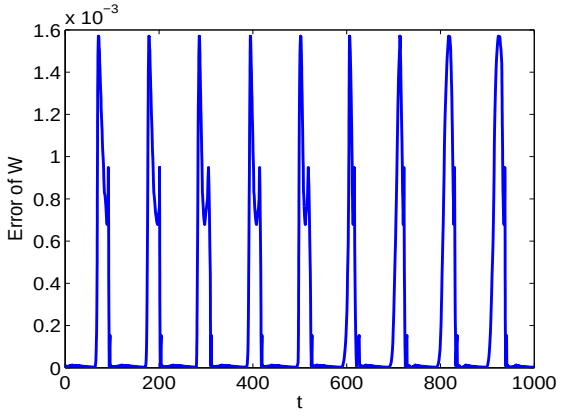
x 10^-3
Error of W
t

C

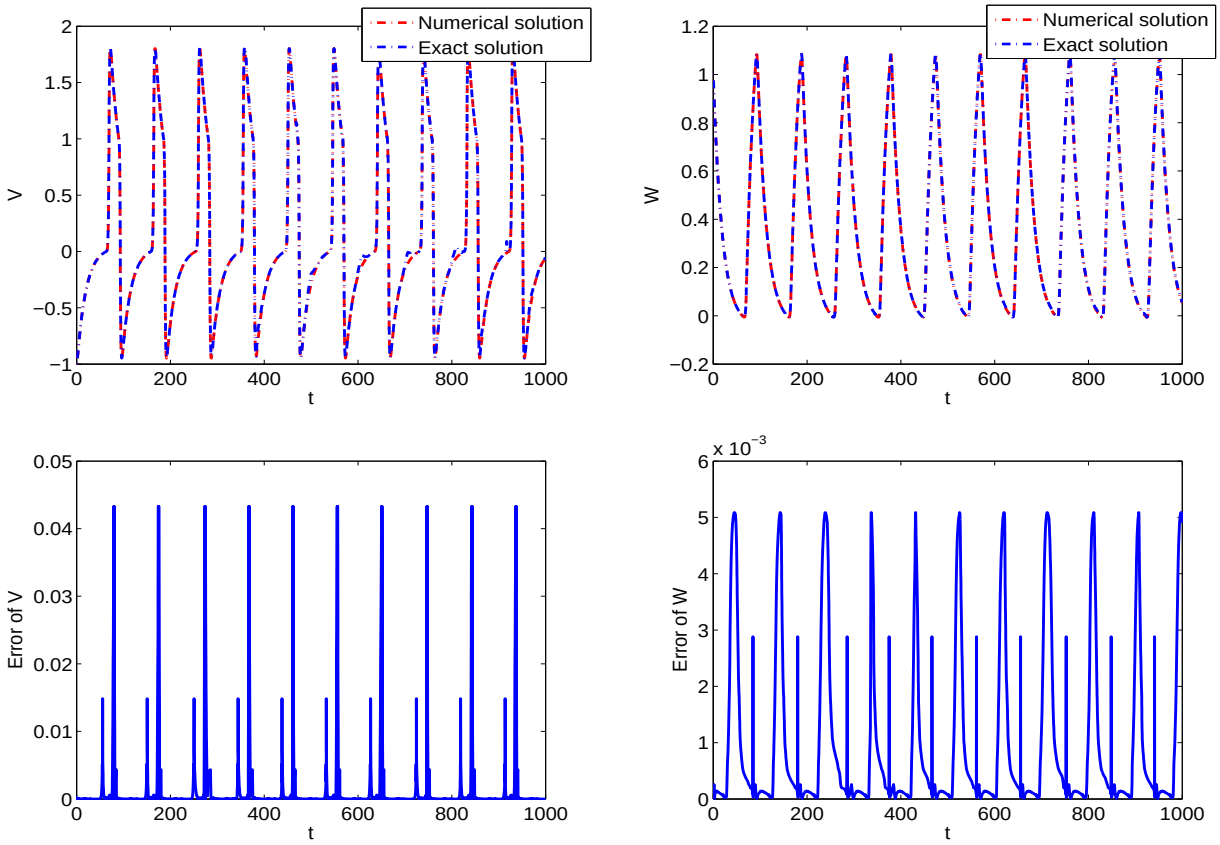

Figure 3.3 Comparison between the analytical and numerical solutions for a single PWL oscillator evolving according to eq. (3.8) with $\alpha = 4$, $\epsilon = 0.01$ and **A** $\lambda = 0.01$, **B:** $\lambda = 0.1$, and **C:** $\lambda = 0.2$. The cubic-like PWL function $f(v)$ is given by (3.10) with $\beta_1 = \beta_2 = 1$. For each value of λ, the numerical ($\tilde{V}$,dashed-red) and analytical (V, dashed-blue) solutions are presented in the top panels. The corresponding absolute errors, defined as $|V(t) - \tilde{V}(t)|$ and $|W(t) - \tilde{W}(t)|$ presented in the bottom panels. The numerical and analytical solutions are in good agreement.

A

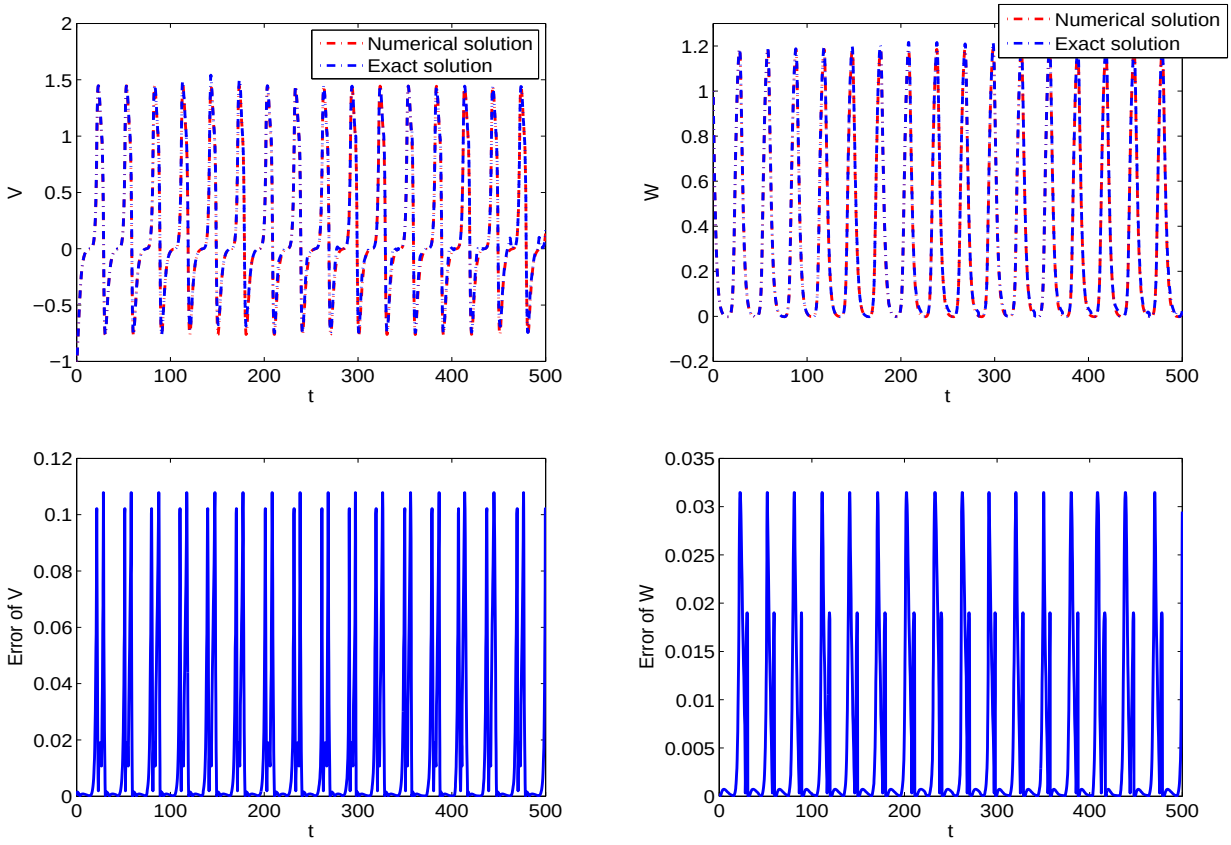
Numerical solution
Exact solution
V
W
Error of V
Error of W
t

B

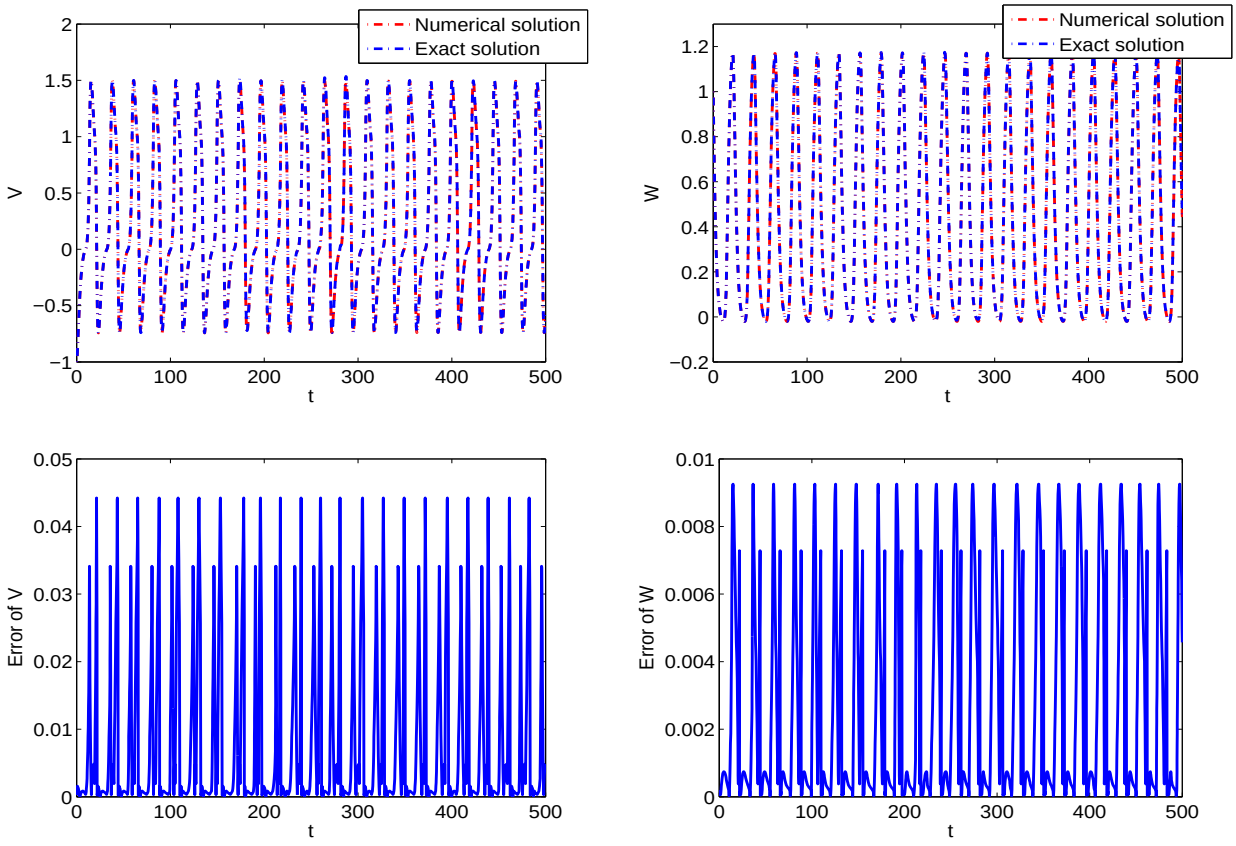
Numerical solution
Exact solution
V
W
Error of V
Error of W
t

C

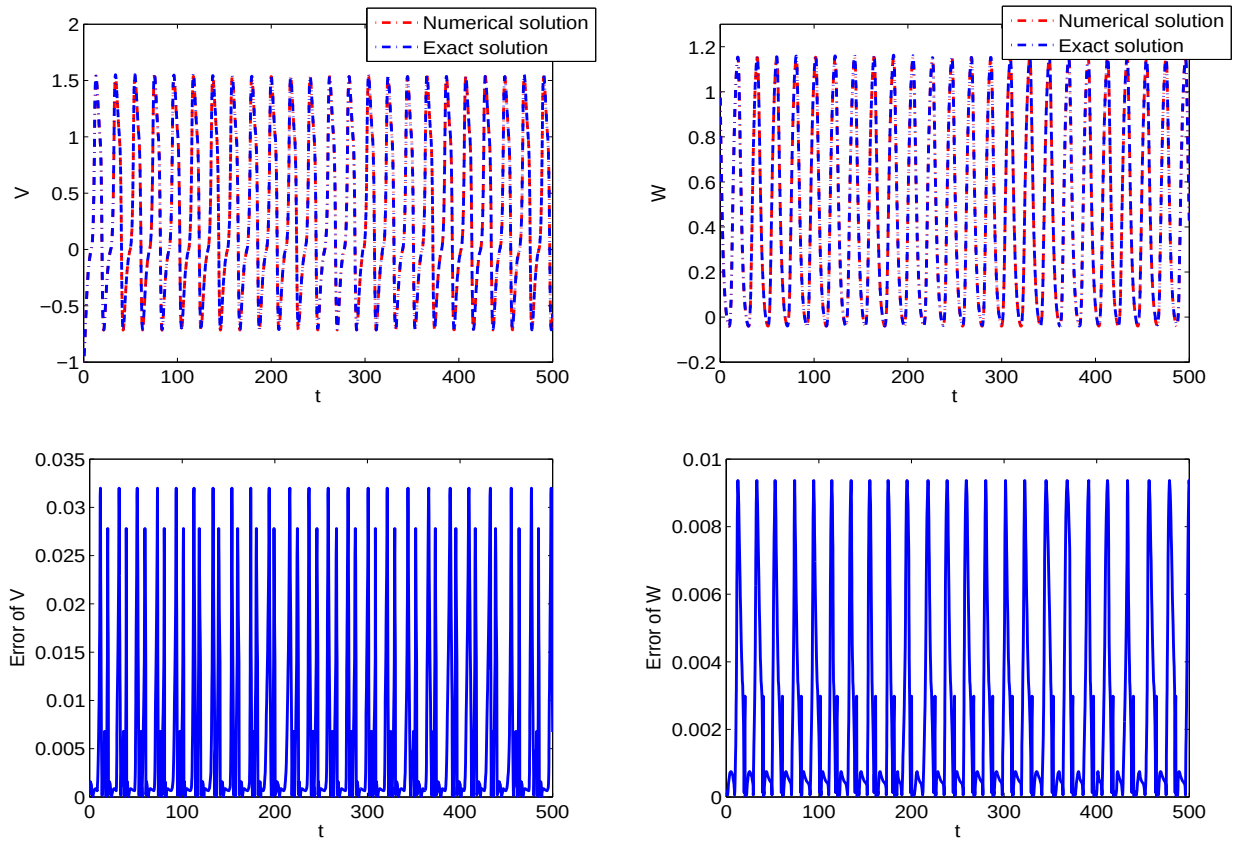

Figure 3.4 Comparison between the analytical and numerical solutions for a single PWL oscillator evolving according to eq. (3.8) with $\alpha = 2$, $\epsilon = 0.1$ and **A** $\lambda = 0.01$, **B:** $\lambda = 0.1$, and **C:** $\lambda = 0.2$. The cubic-like PWL function $f(v)$ is given by (3.10) with $\beta_1 = \beta_2 = 1$. For each value of λ, the numerical ($\tilde{V}$,dashed-red) and analytical (V, dashed-blue) solutions are presented in the top panels. The corresponding absolute errors, defined as $|V(t) - \tilde{V}(t)|$ and $|W(t) - \tilde{W}(t)|$ presented in the bottom panels. The numerical and analytical solutions are in good agreement.

A

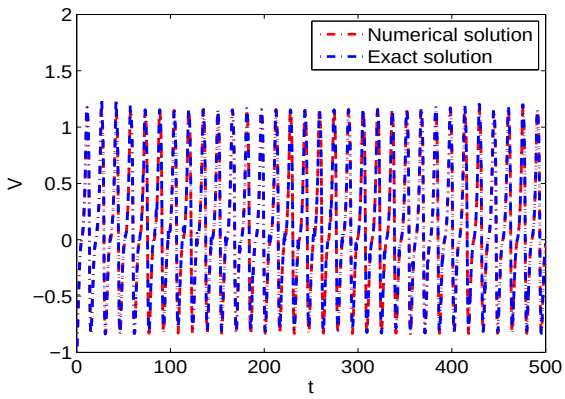
Numerical solution
Exact solution
V
t

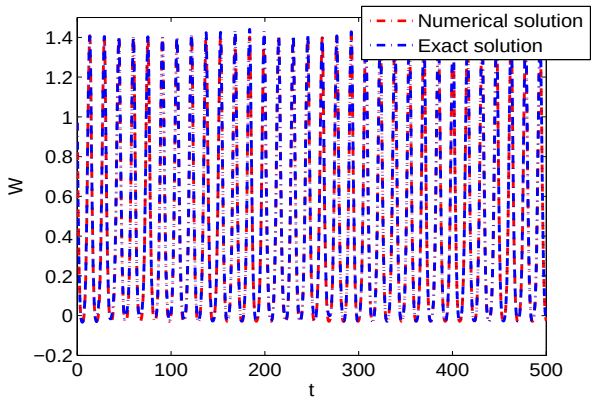
Numerical solution
Exact solution
W
t

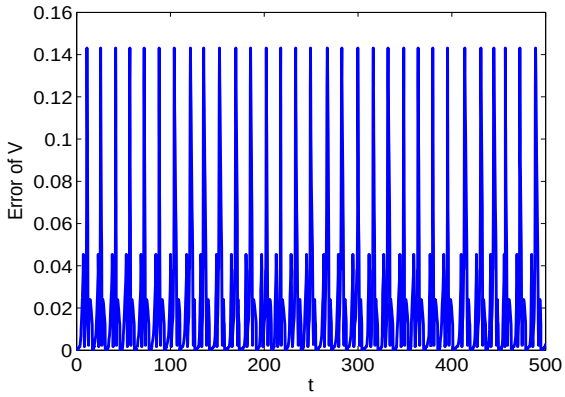
Error of V
t

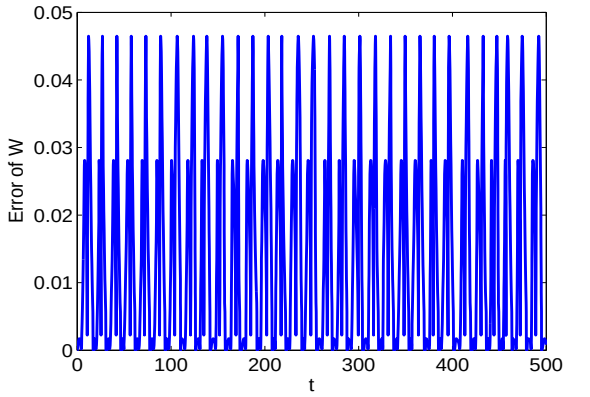
Error of W
t

B

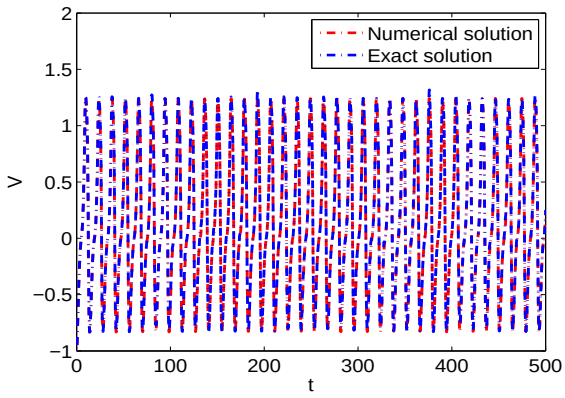
Numerical solution
Exact solution
V
t

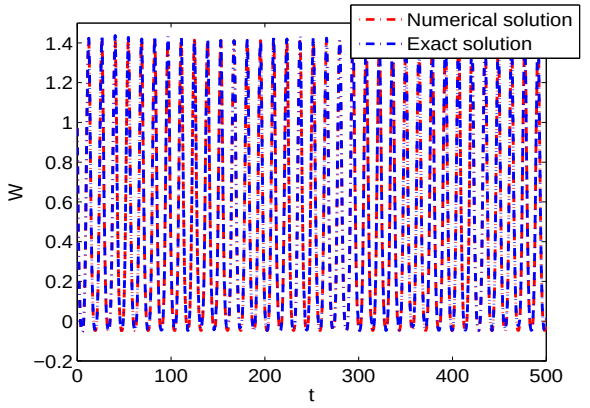
Numerical solution
Exact solution
W
t

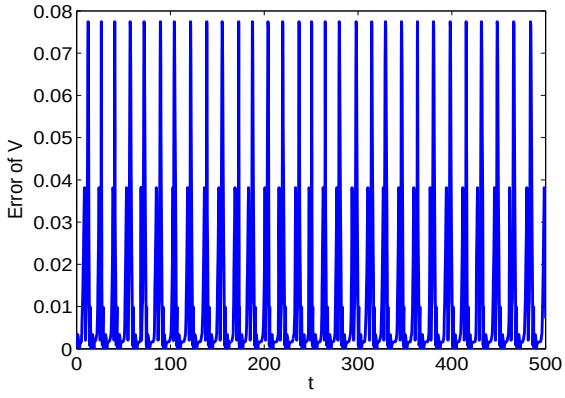
Error of V
t

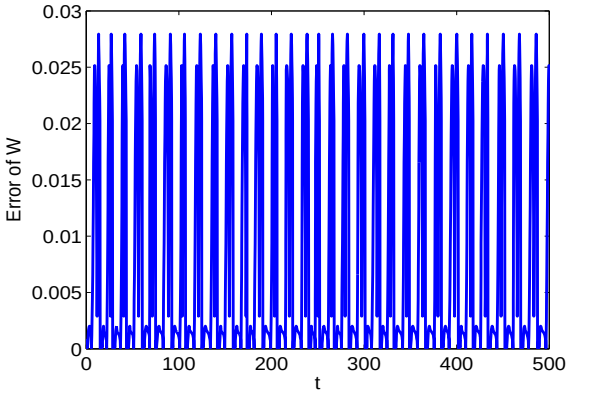
Error of W
t

C

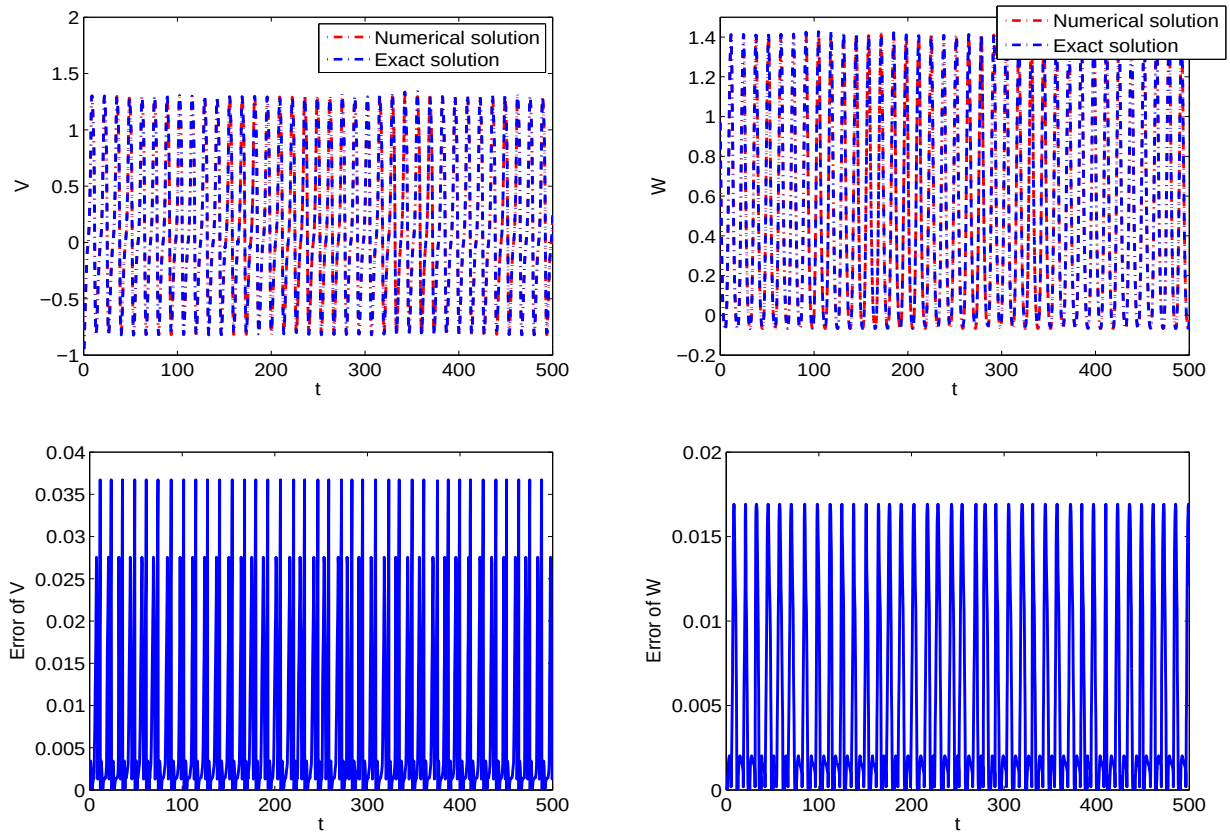

Figure 3.5 Comparison between the analytical and numerical solutions for a single PWL oscillator evolving according to eq. (3.8) with $\alpha = 4$, $\epsilon = 0.1$ and **A** $\lambda = 0.01$, **B:** $\lambda = 0.1$, and **C:** $\lambda = 0.2$. The cubic-like PWL function $f(v)$ is given by (3.10) with $\beta_1 = \beta_2 = 1$. For each value of λ, the numerical ($\tilde{V}$,dashed-red) and analytical (V, dashed-blue) solutions are presented in the top panels. The corresponding absolute errors, defined as $|V(t) - \tilde{V}(t)|$ and $|W(t) - \tilde{W}(t)|$ presented in the bottom panels. The numerical and analytical solutions are in good agreement.

3.3 Comparison of Two Globally Coupled Cubic Oscillators and the Piecewise Linear Approximation

In this section, we study the FHN type model with two coupled oscillators. The globally coupled system functions are given in equations (3.7). Let us also choose a piecewise linear function $\bar{f}(v)$ to approximate the cubic function $f(v) = -hv^3 + av^2 - bv + c$. In particular, when the coefficients $h = 2$, $a = 3$ and $b = c = 0$, we define $\bar{f}(v)$ as

$$\bar{f}(v) = \begin{cases} -\beta_1 v, & \text{when} \quad v < 0 \\ v, & \text{when} \quad 0 \le v \le 1 \\ 1 + \beta_2 - \beta_2 v, & \text{when} \quad v > 1 \end{cases} \tag{3.10}$$

For simplicity we fix $\beta_1 = \beta_2 = 1$. We illustrate the numerical solutions with different values of parameters.

In this case the globally coupling system is

$$\begin{cases} v_k' = \bar{f}(v_k) - w_k - \gamma \, [\, \alpha_1 \, w_1 + \alpha_2 \, w_2 - \bar{w} \,], \\ w_k' = \epsilon \, [\alpha v_k - \lambda - w_k \,], \qquad k = 1, 2 \end{cases} \tag{3.11}$$

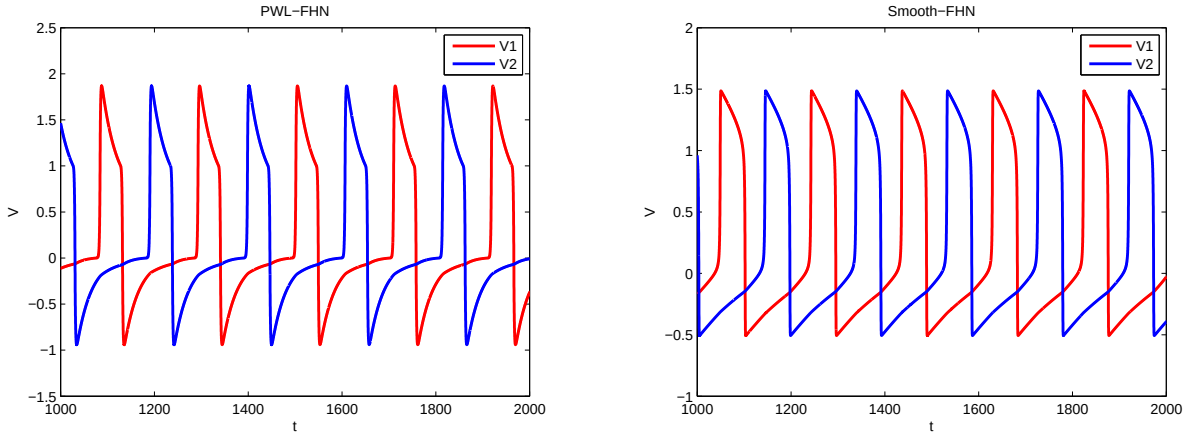

Figure 3.6 Anti-phase oscillations for the globally coupled system (3.9) for a PWL (left panel) and smooth (right panel) cubic-like functions given by (3.11) respectively, in both cases the oscillators go anti-phase for the following parameters $N = 2$, $\alpha = 2$, $\epsilon = 0.01$, $\lambda = 0.01$, $\gamma = 0.1$, and $\alpha_1 = \alpha_2 = 0.5$

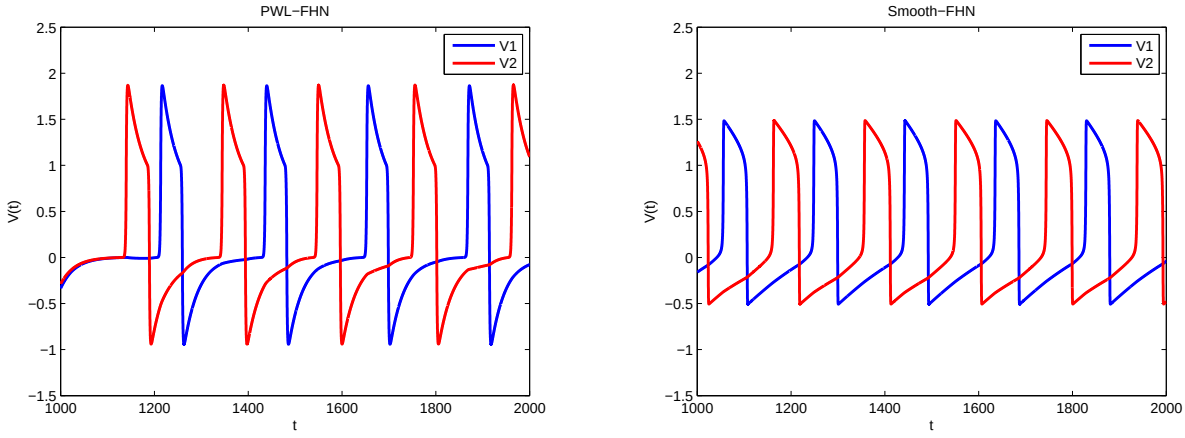

Figure 3.7 Out of phase oscillations for the globally coupled system (3.9) for a PWL (left panel) and smooth (right panel) cubic-like functions given by (3.11) respectively, and for the following parameters $N = 2$, $\alpha = 2$, $\epsilon = 0.01$, $\lambda = 0.01$, $\gamma = 0.1$, and $\alpha_1 = 0.8$, $\alpha_2 = 0.2$

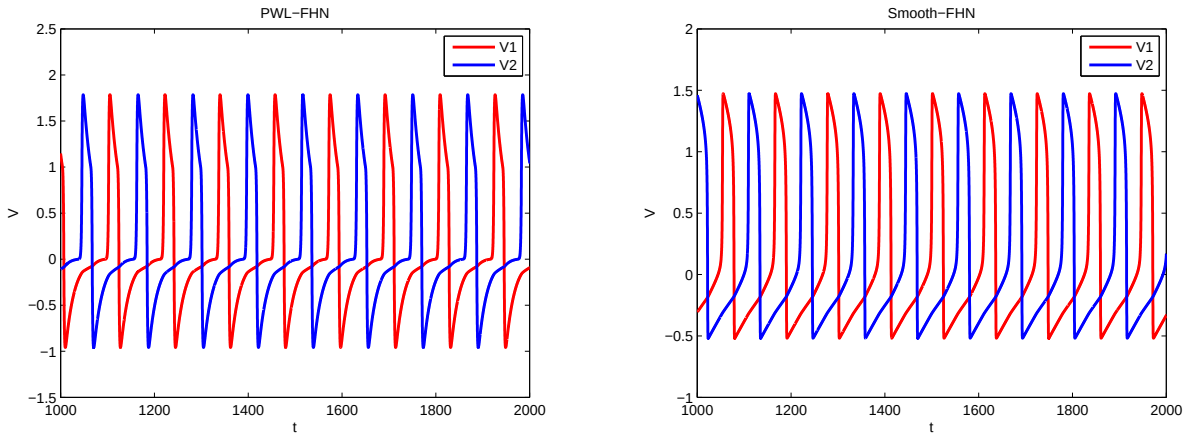

Figure 3.8 Anti-phase oscillations for the globally coupled system (3.9) for a PWL (left panel) and smooth (right panel) cubic-like functions given by (3.11) respectively, and for the following parameters $N = 2$, $\alpha = 4$, $\epsilon = 0.01$, $\lambda = 0.01$, $\gamma = 0.1$, and $\alpha_1 = \alpha_2 = 0.5$

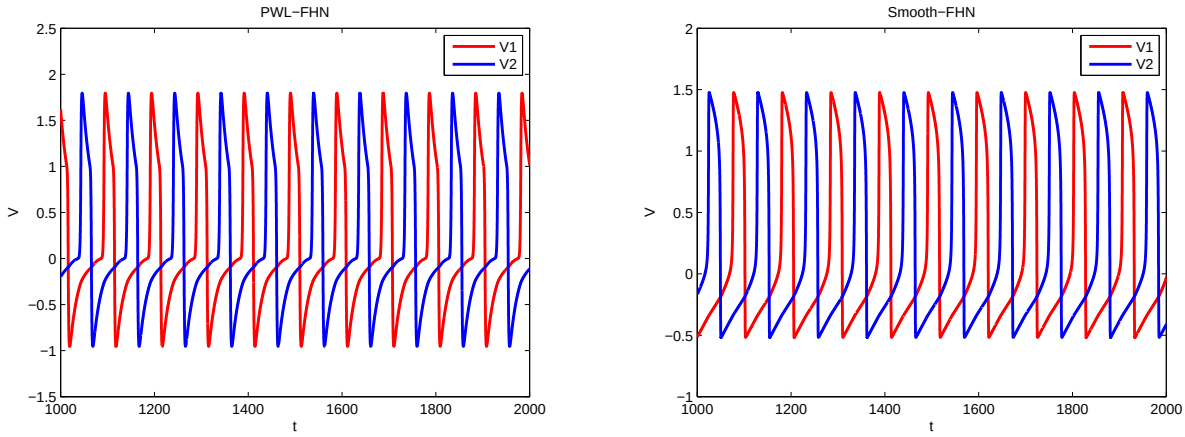

Figure 3.9 Anti-phase oscillations for the globally coupled system (3.9) for a PWL (left panel) and smooth (right panel) cubic-like functions given by (3.11) respectively, and for the following parameters $N = 2$, $\alpha = 4$, $\epsilon = 0.01$, $\lambda = 0.1$, $\gamma = 0.1$, and $\alpha_1 = \alpha_2 = 0.5$

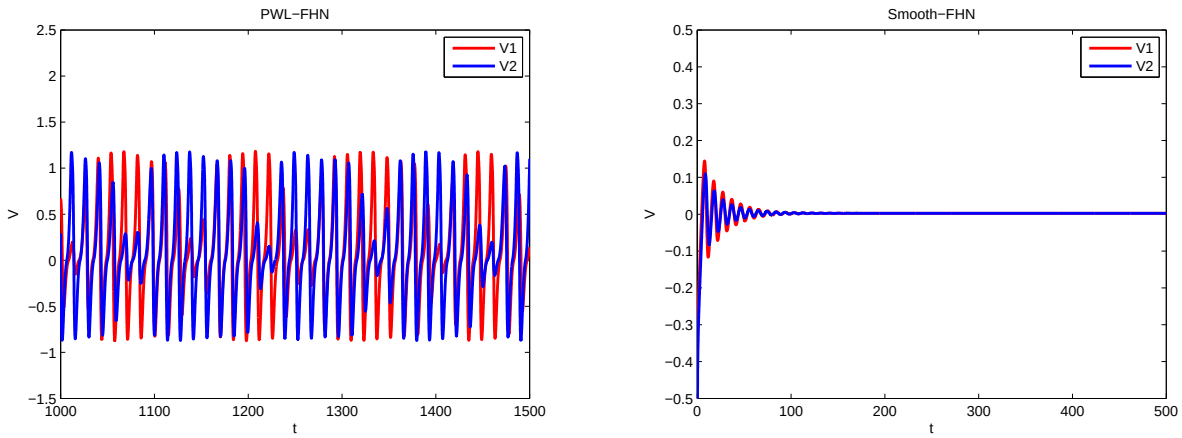

Figure 3.10 Different dynamic behavior between the PWL (left panel) and smooth (right panel) globally coupled system (3.11). The cubic like functions are given by (3.9)respectively, and for the following parameters $N = 2$, $\alpha = 4$, $\epsilon = 0.1$, $\lambda = 0.01$, $\gamma = 0.1$, and $\alpha_1 = \alpha_2 = 0.5$. The smooth system exhibits oscillation death while the PWL system exhibits persistent oscillations. In the PWL system, the "red" oscillator displays only large amplitude oscillations while the "blue" one displays both small amplitude oscillations interspersed with large amplitude oscillations (mixed-mode oscillations).

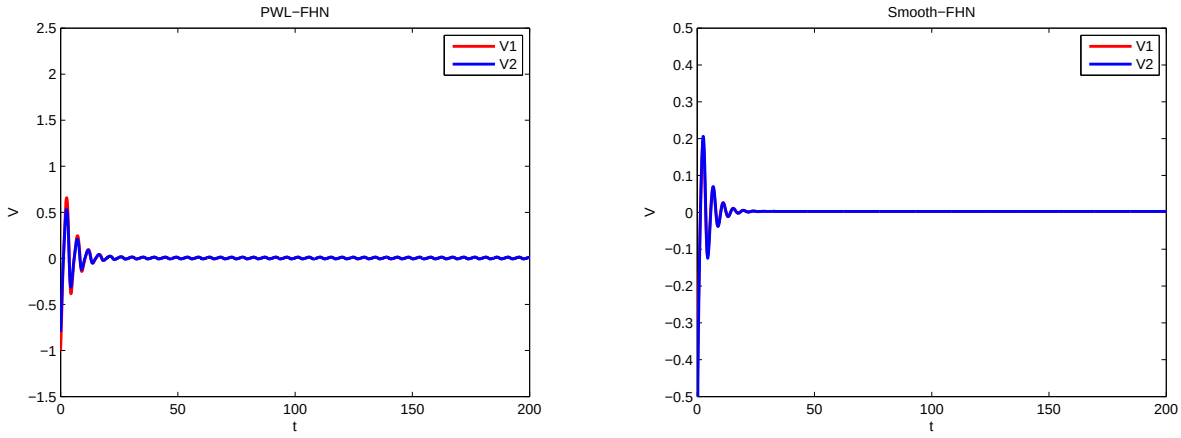

Figure 3.11 Oscillation death for the globally coupled system (3.11) for a PWL (left panel) and smooth (right panel) cubic-like functions given by (3.9) and (number) respectively, and for the following parameters $N = 2$, $\alpha = 4$, $\epsilon = 0.5$, $\lambda = 0.01$, $\gamma = 0.1$, and $\alpha_1 = \alpha_2 = 0.5$.

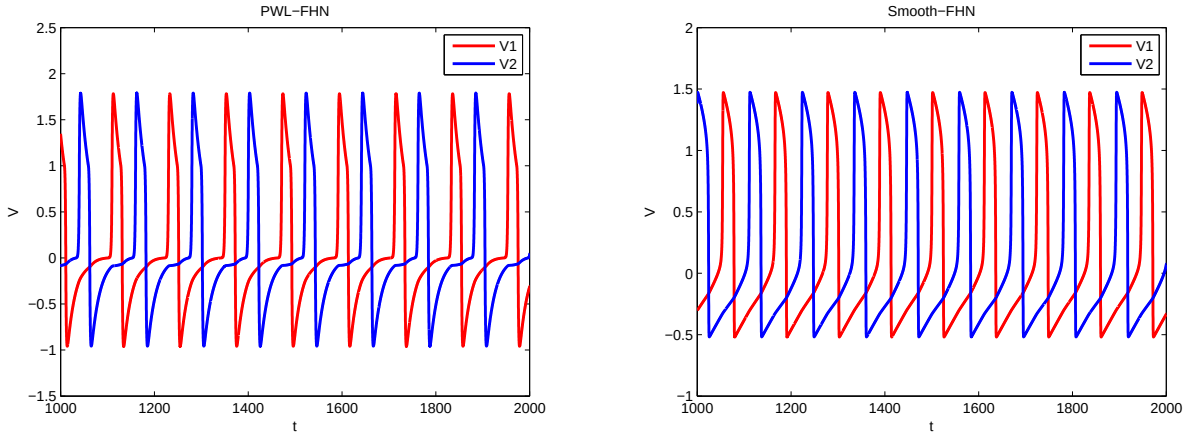

Figure 3.12 Out of phase (phase locked) oscillators for the globally coupled systems (3.11) between the PWL(left panel) and smooth (right panel) : $N = 2, \gamma = 0.1, \lambda = 0.01, \epsilon = 0.01, \alpha = 4, \alpha_1 = 0.6, \alpha_2 = 0.4$. The phase of cubic case is 0.5208, the phase of piecewise-linear is 0.5852.

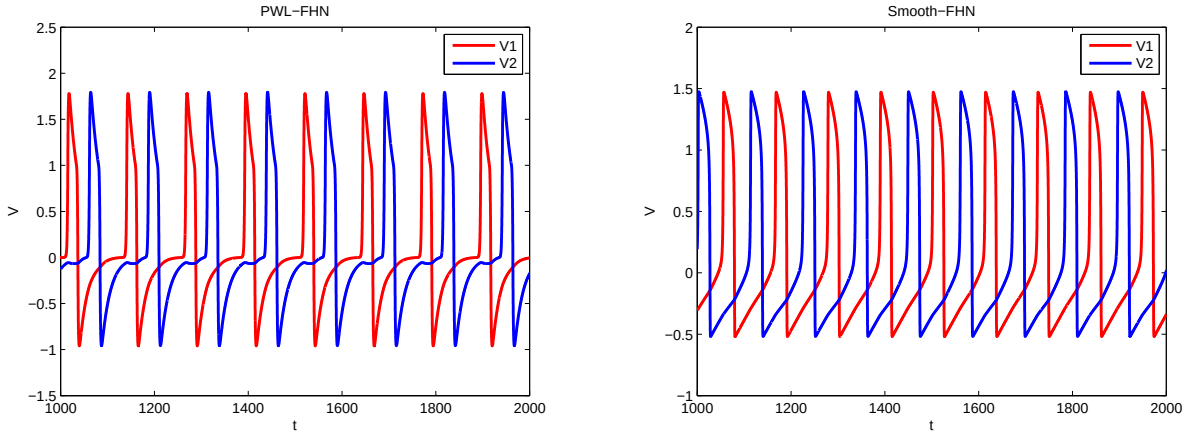

Figure 3.13 Out of phase (phase locked) oscillators for the FHN model (3.11) between the PWL(left panel) and smooth (right panel) : $N = 2, \gamma = 0.1, \lambda = 0.01, \epsilon = 0.01, \alpha = 4, \alpha_1 = 0.7, \alpha_2 = 0.3$. The phase of cubic case is 0.5407, the phase of piecewise-linear is 0.6252.

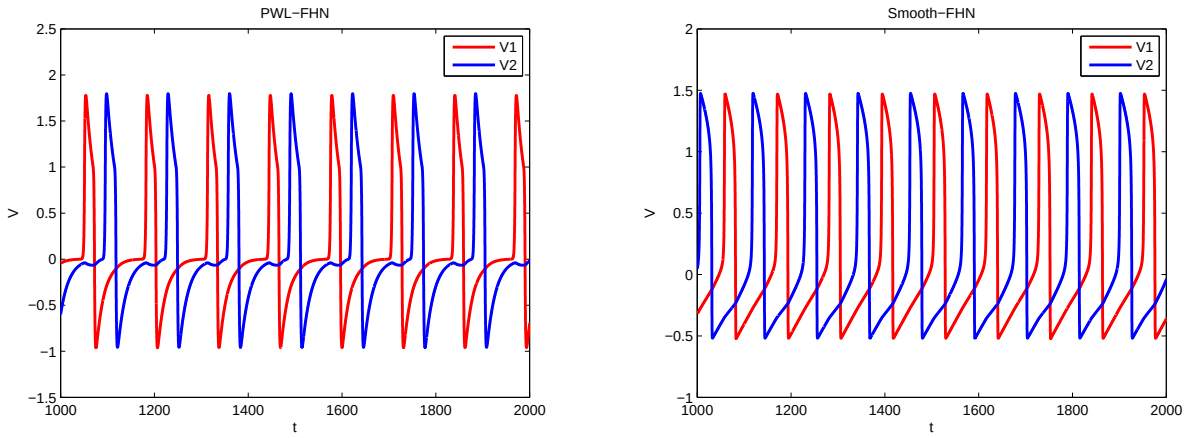

Figure 3.14 Out of phase (phase locked) oscillators for FHN model (3.11) between the PWL(left panel) and smooth (right panel) : $N = 2, \gamma = 0.1, \lambda = 0.01, \epsilon = 0.01, \alpha = 4, \alpha_1 = 0.8, \alpha_2 = 0.2$. The phase of cubic case is 0.5579, the phase of piecewise-linear is 0.6504.

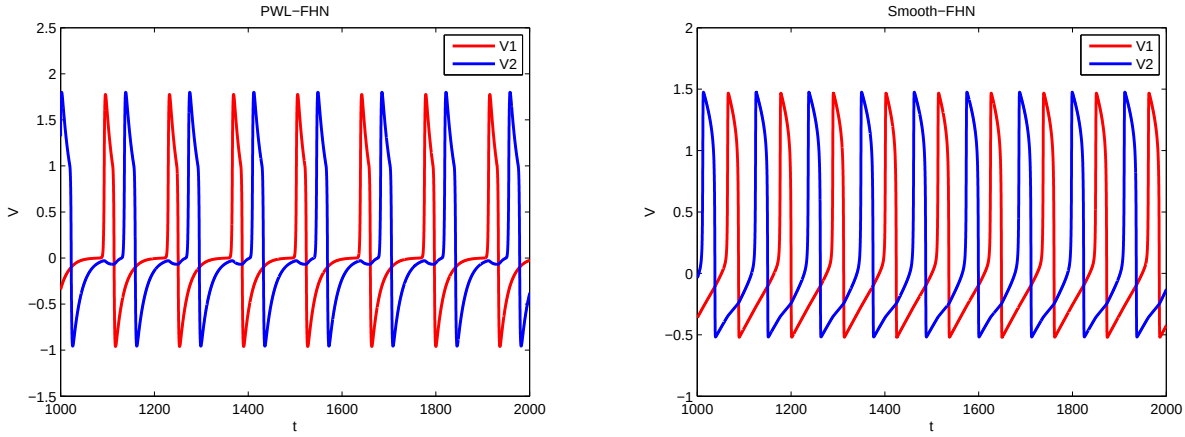

Figure 3.15 Out of phase (phase locked) oscillators for FHN model (3.11) between the PWL(left panel) and smooth (right panel) : $N = 2, \gamma = 0.1, \lambda = 0.01, \epsilon = 0.01, \alpha = 4, \alpha_1 = 0.9, \alpha_2 = 0.1$. The phase of cubic case is 0.5646, the phase of piecewise-linear is 0.6691.

In Fig. 3.6 to Fig. 3.15 we compare the numerical solutions to the Fitzhugh-Nagumo (FHN) model and the piecewise linear approximation described above in (3.10) and (3.11).

In Fig 3.16, in all panels, green lines correspond to the w-nullclines. Red and blue PWL functions correspond to the V-nullclines of the V_1 and V_2 respectively. Red and blue points correspond to the tip of the trajectory at different time. The two oscillators starts on the left branch as shown in panel (A), in panel (B), and panel (C), they move down together close to the point $v = 0$. In panel (D), the first oscillator leaves the w-nullcline and starts to go to the right branch. In panel (E), the second oscillator stays around the point $v = 0$ for a long time when the first oscillator is moving fast to the right branch. In panel (F) and (G), the second oscillator still stays around the point $v = 0$ when the first oscillator crosses the w-nullcline again and moves to the left branch. In panel (H), the second oscillator crosses the w-nullcline when the first oscillator moving down through the left branch. In panel (I) and (J), the first oscillator stays around the point $v = 0$ when the second oscillator reaches the right branch and moves up. In panel (K), the first oscillator still moves along the left branch while the second oscillator crosses the w-nullcline and reaches the left branch, so the two oscillators are moving together on the left branch again.

We explain the mechanism of generation of anti-phase solutions for the globally coupled system Eq.(3.11) in the context of Figure 3.16 which corresponds to $\alpha = 4$, $\gamma = 0.1$ and $\alpha_1 = \alpha_2 = 0.5$. The nullclines N_1 and N_2 corresponding to the two oscillators, O_1 and O_2 respectively, are given by The following nullcline equation; i.e.,

$$N_k(v_k, w_j) = \frac{f(v_k) + \gamma\bar{w}}{1 + \gamma\alpha_k} - \frac{\gamma\alpha_j w_j}{1 + \gamma\alpha_k} \tag{3.12}$$

For $\gamma = 0$ (no global coupling), the two oscillators have the same nullcline. When $\gamma > 0$, the shape of the two nullclines changes and they "move up and down" according to the second term in Eq.(3.12). Since for each oscillator this term contains the w-coordinate of the other oscillator, Eq.(3.12) then each nullcline becomes dynamic; i.e., the motion of each oscillator affects the height of the nullcline of the other one. Note that strictly speaking, Eq.(3.12) describes a surface rather than a curve. We interpret the non-constant height of this surface as curves moving up and down, and we refer to this curves as nullclines.

A

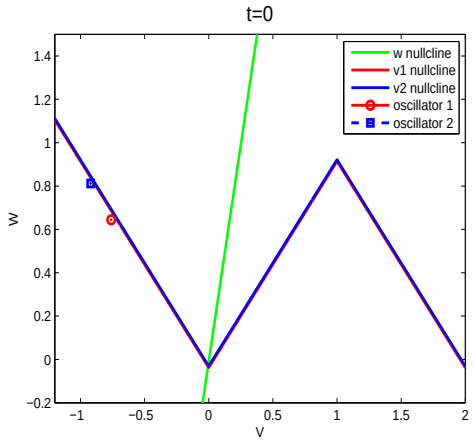
t=0
w nullcline
v1 nullcline
v2 nullcline
oscillator 1
oscillator 2
w
V

B

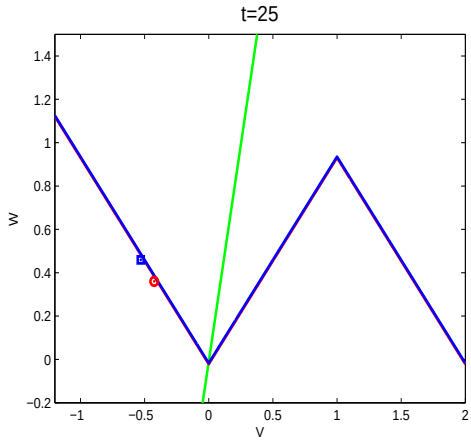
t=25
w
V

C

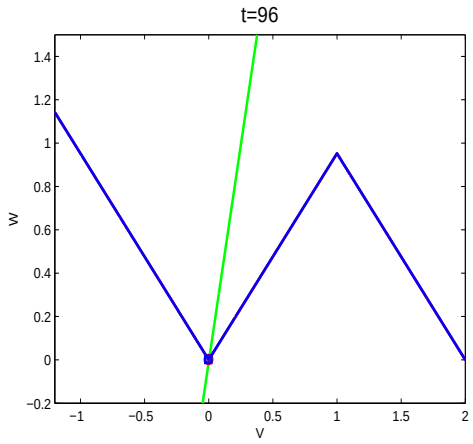
t=96
w
V

Cz

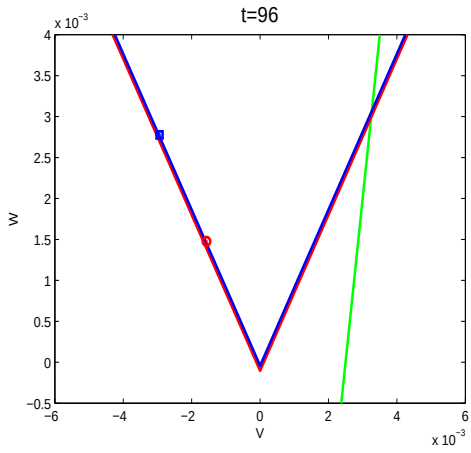
t=96
x 10^-3
w
V
x 10^-3

D

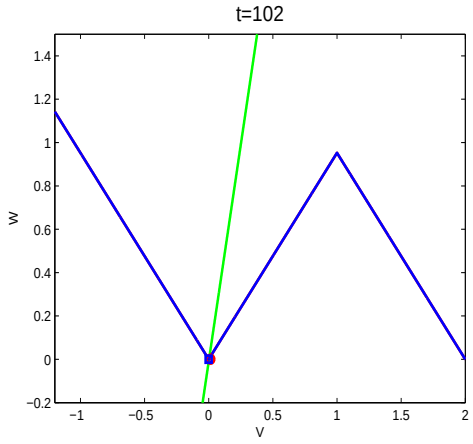
t=102
w
V

Dz

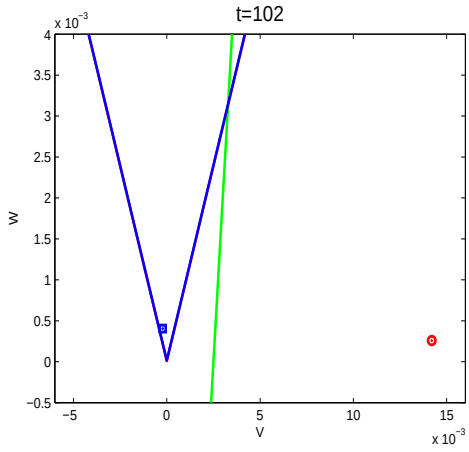
t=102
x 10^-3
w
V
x 10^-3

E

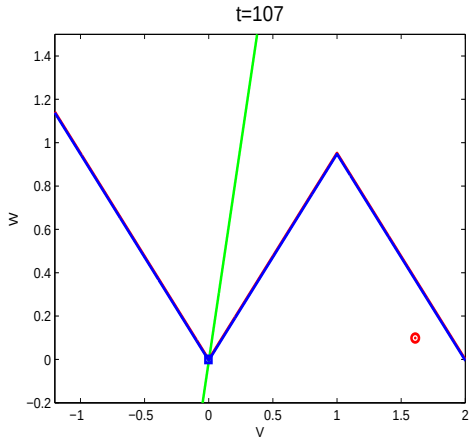

Ez

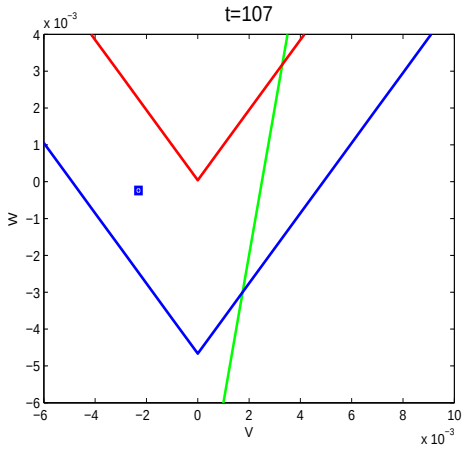

F

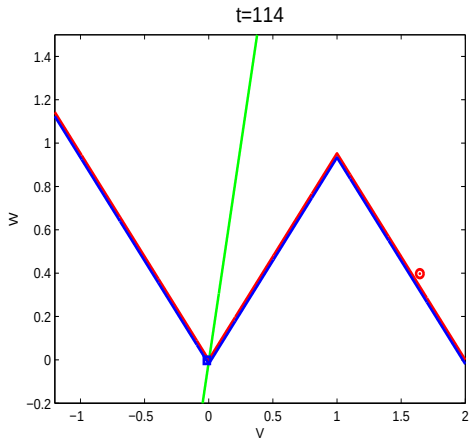

G

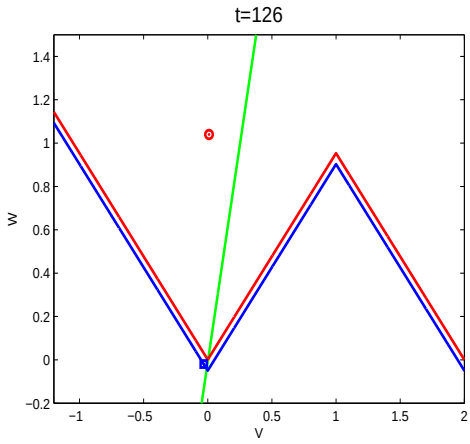

H

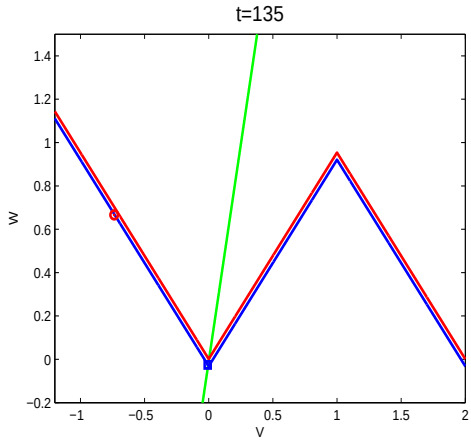

I

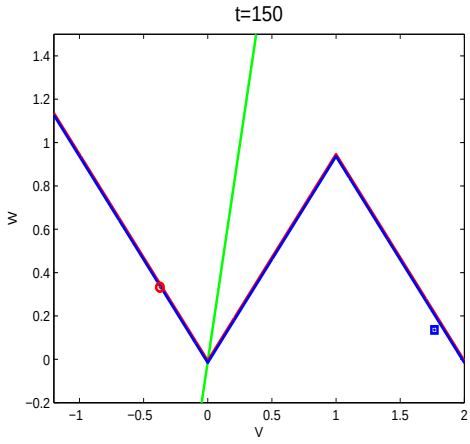

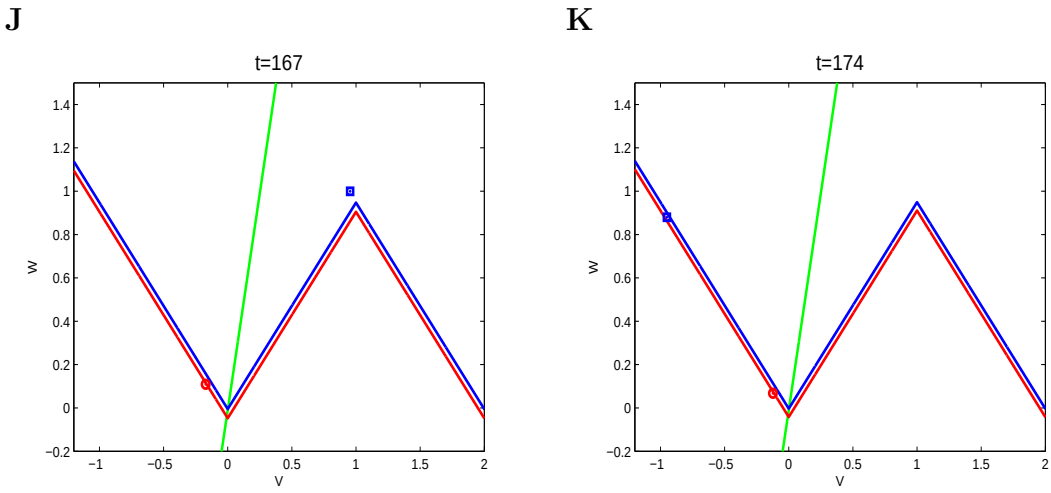

Figure 3.16 Two globally coupled oscillators moving with equation (3.11) in piecewise-linear case, and two anti-phase clusters for the following parameters: $\alpha = 4, \gamma = 0.1, \alpha_1 = 0.5, \alpha_2 = 0.5$

Fig. 3.16-A shows the initial location of the two oscillators. We set the initial conditions lying in a vicinity of the left branch of the corresponding nullclines N_1 and N_2. In Fig. 3.16, oscillator O_1 is marked in red and oscillator O_2 is marked in blue. The full dots correspond to the tip of the trajectory for the time shown in the top of the panel. When appropriate for the geometric description of the dynamics we will refer to the w-coordinates of the red and blue oscillators as w_r and w_b respectively and to the corresponding nullclines as N_r and N_b.

Since $\epsilon << 1$ the trajectories of the two oscillators will evolve in a vicinity of N_r and N_b. As time increases the two oscillators move down along these nullclines and get closer together (the distance between their locations decreases) but the order is preserved; i.e., the red oscillator is ahead of the blue oscillator as long both are moving along the left branch of the v-nullclines (Fig. 3.16-B, Fig. 3.16-C and Fig. 3.16-Cz).

The red oscillator arrives to the minimum of N_r before the blue oscillator arrives to the minimum of N_b. This is due to the fact that $w_r < w_b$. When the red oscillators reaches the minimum of N_r it moves along a fast direction of motion towards the right branch of N_r. This direction is almost horizontal with a small vertical component. This slight increase in the value of w_r causes N_b to move down (Fig. 3.16-E and Fig. 3.16)-Ez thus preventing the

blue oscillator from crossing to the middle branch regime. Once the red oscillator arrives to a vicinity of the right branch of N_r it moves in moves along it in the upward direction (Fig. 3.16)-F which further prevents the blue oscillator from crossing to the left branch of N_b due to the increase in the value of w_r. Only when the red oscillator returns to a vicinity of the left branch of N_r moves down along it decreasing value of w_r (Fig.3.16-G to Fig. 3.16)-I the nullcline N_b moves up and allows the blue oscillator to move to the right branch of N_b (Fig. 3.16)-I and move up along it while the red oscillator moves down along N_r (Fig. 3.16)-J. When the blue oscillator returns to the left branch of N_b the red oscillators is close to the minimum of N_r. The distance between the their location is larger than initially (Compare Fig. 3.16-K and Fig. 3.16)-A so the oscillators will never synchronize in phase.

The similar dynamical process is shown in Fig. 3.17 to Fig. 3.19 in both of piecewise linear case and cubic case.

In the figures Fig. 3.20 to Fig. 3.23, $\alpha_1 \neq 0.5$ and $\alpha_2 \neq 0.5$, so we get out of phase pattern instead of anti-phase pattern.

A

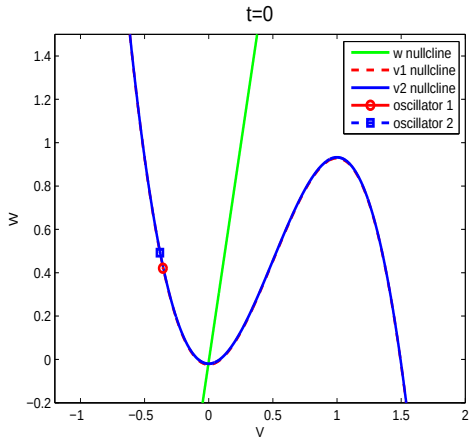
t=0
w nullcline
v1 nullcline
v2 nullcline
oscillator 1
oscillator 2
w
V

B

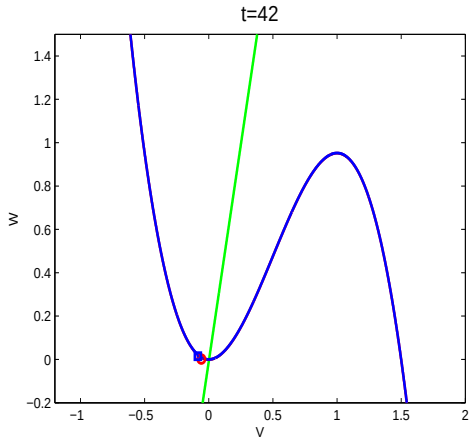
t=42
w
V

Bz

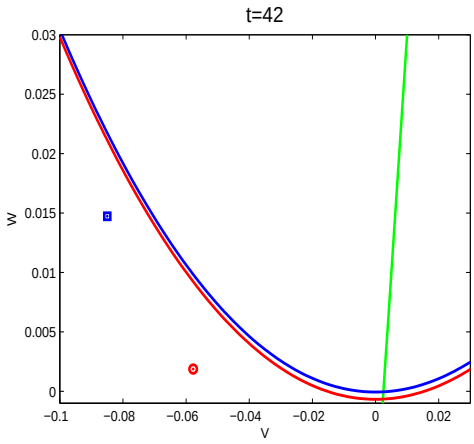
t=42
w
V

C

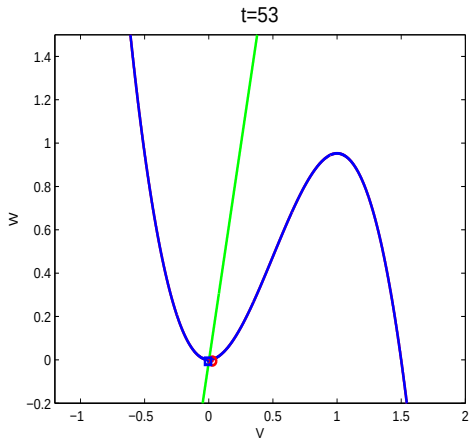
t=53
w
V

Cz

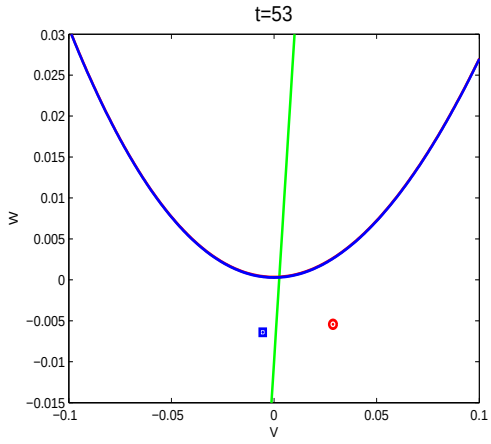
t=53
w
V

D

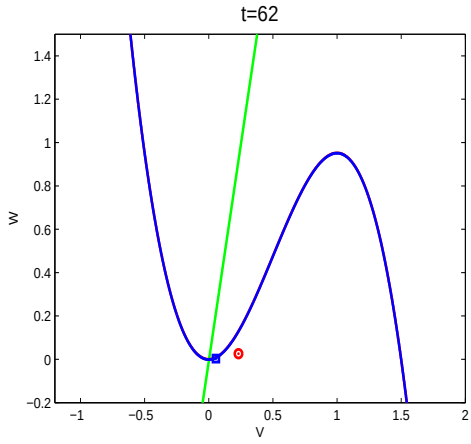
t=62
w
V

Dz

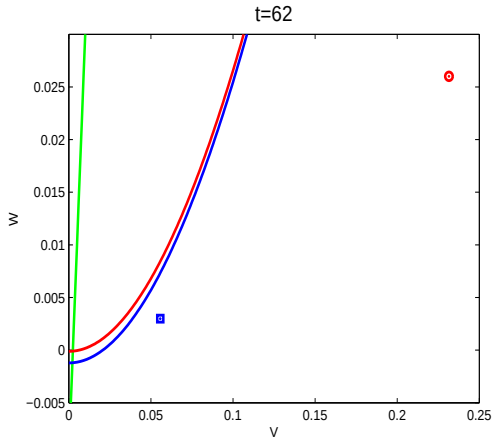

E

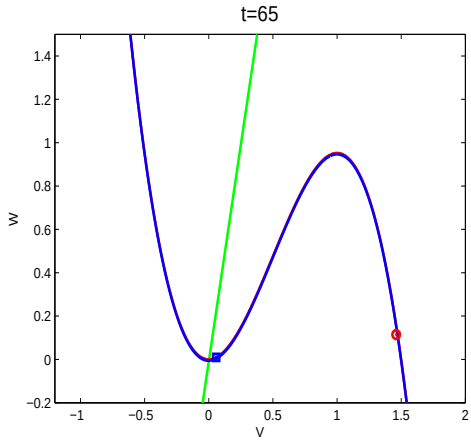

Ez

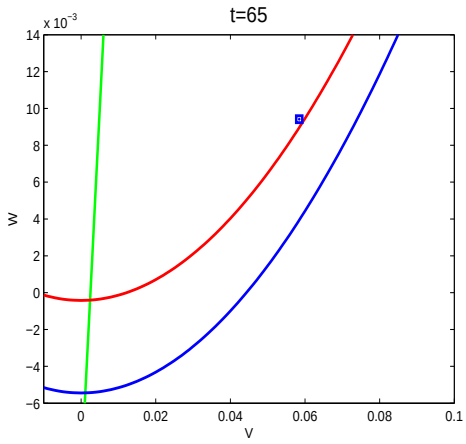

F

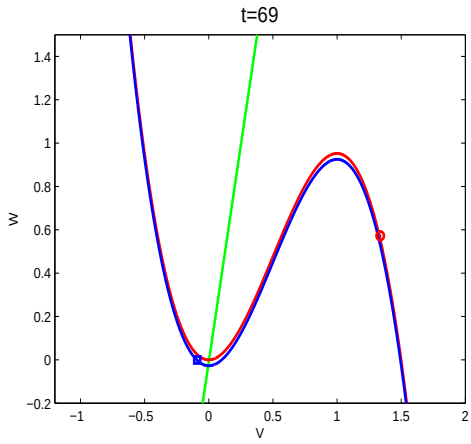

G

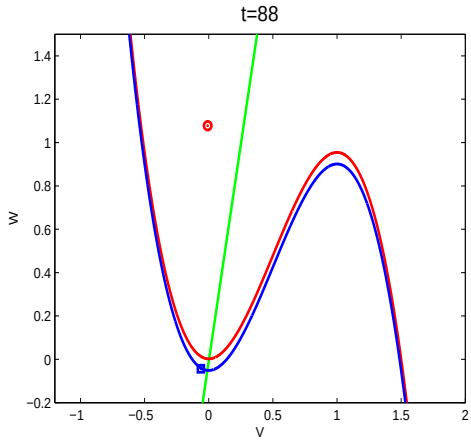

H

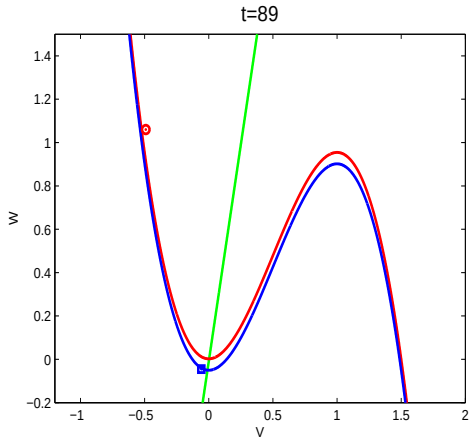

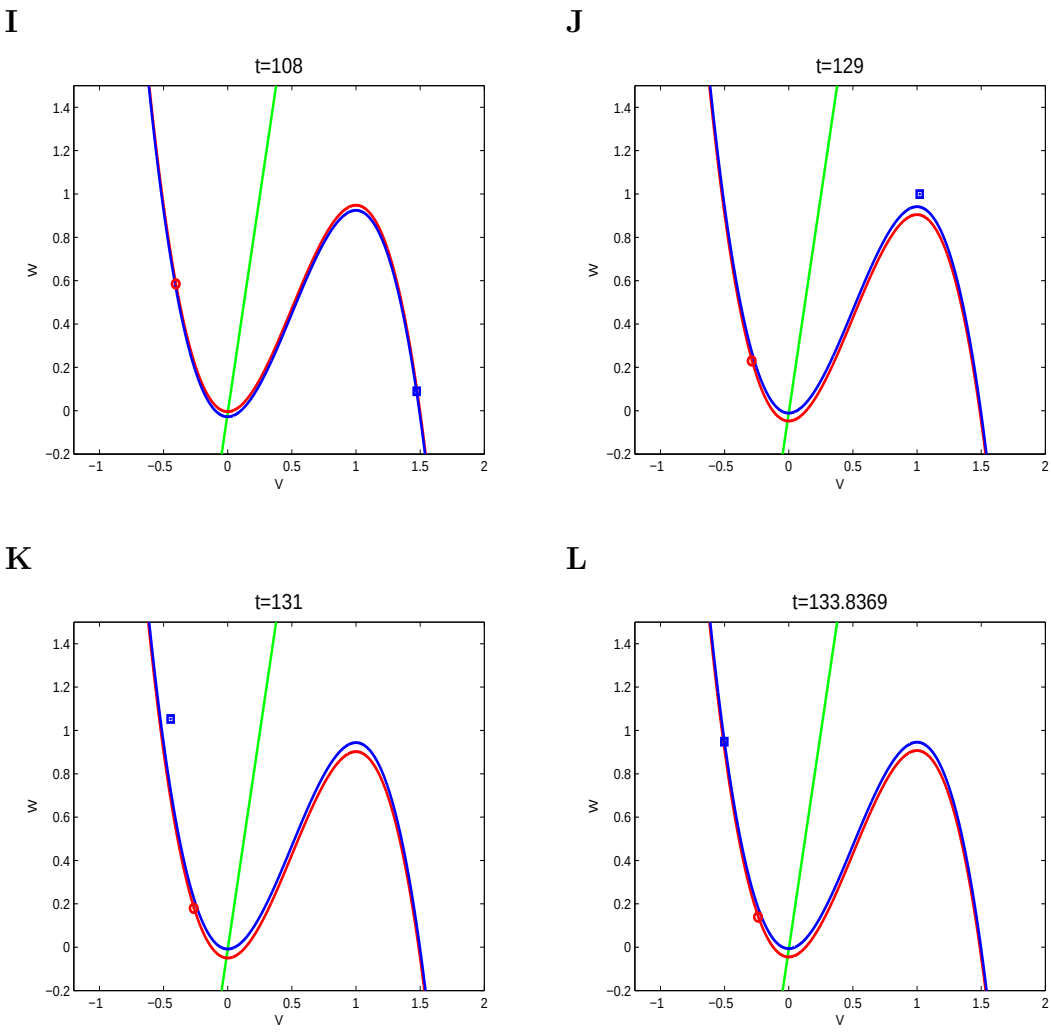

Figure 3.17 Two globally coupled oscillators moving with equation (3.11) in cubic case, and two anti-phase clusters for the following parameters: $\alpha = 4, \gamma = 0.1, \alpha_1 = 0.5, \alpha_2 = 0.5$

A

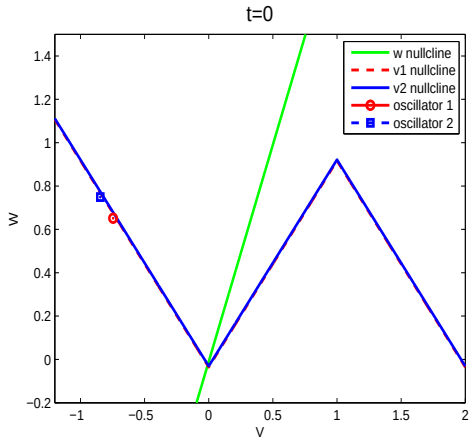
t=0
w nullcline
v1 nullcline
v2 nullcline
oscillator 1
oscillator 2
w
V

B

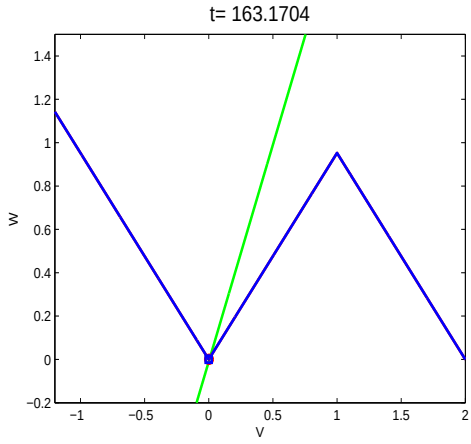
t= 163.1704
w
V

Bz

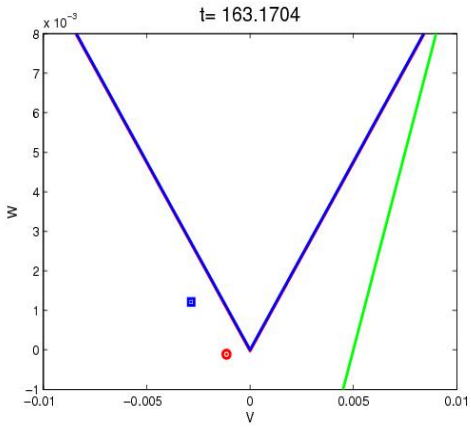
t= 163.1704
x 10^-3
w
V

C

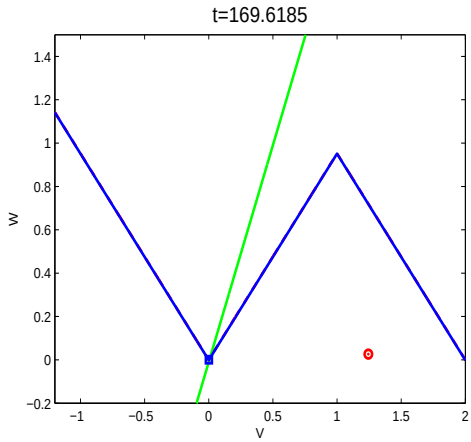
t=169.6185
w
V

Cz

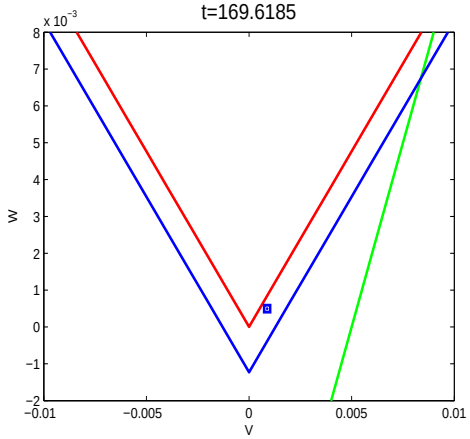
t=169.6185
x 10^-3
w
V

D

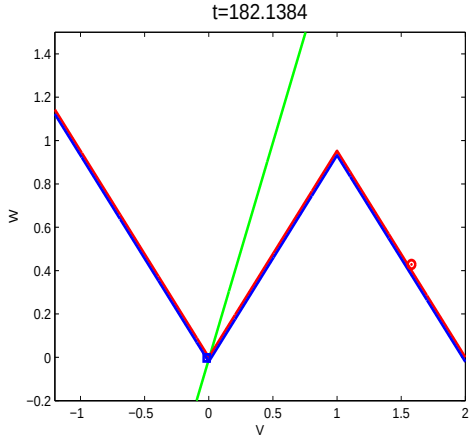
t=182.1384
w
V

Dz

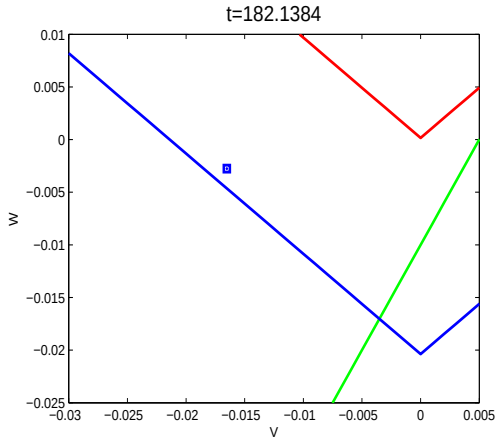
t=182.1384
w
V

E

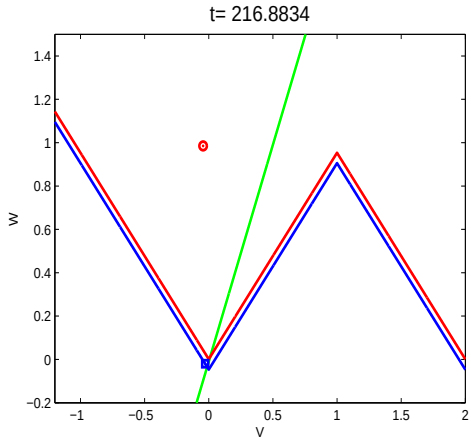
t= 216.8834
w
V

F

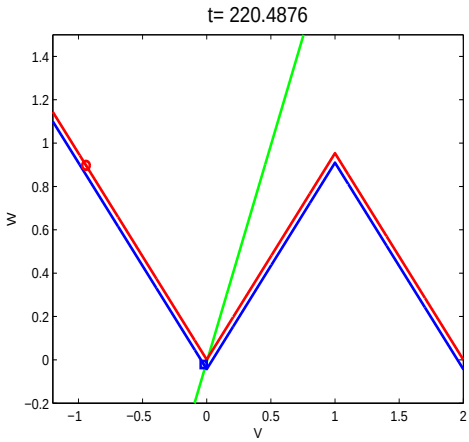
t= 220.4876
w
V

G

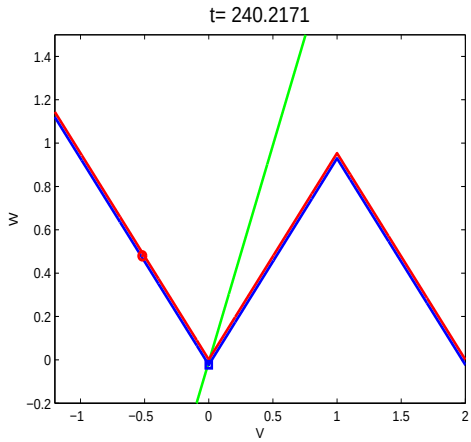
t= 240.2171
w
V

H

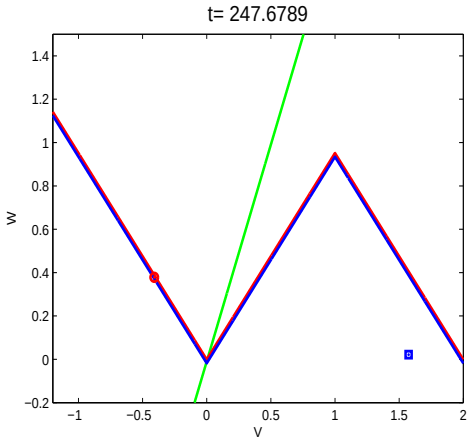
t= 247.6789
w
V

I

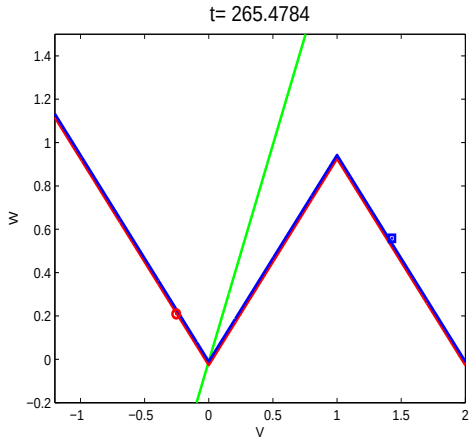
t= 265.4784
w
V

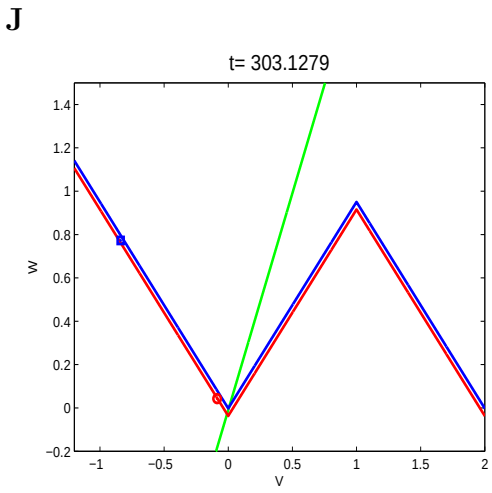

Figure 3.18 Two globally coupled oscillators moving with equation (3.11) in piecewise-linear case, and two anti-phase clusters for the following parameters: $\alpha = 2, \gamma = 0.1, \alpha_1 = 0.5, \alpha_2 = 0.5$

In Fig. 3.20 to Fig. 3.23, the oscillators go out of-phase instead of anti-phase in both of cubic oscillators and the piecewise linear approximated oscillators, but the dynamical process is the same as Fig. 3.16 to Fig. 3.19.

A

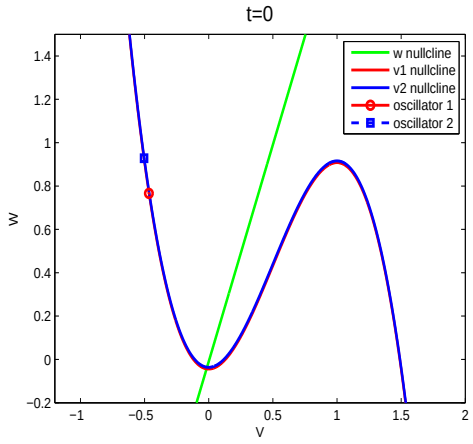
t=0
w nullcline
v1 nullcline
v2 nullcline
oscillator 1
oscillator 2
w
V

B

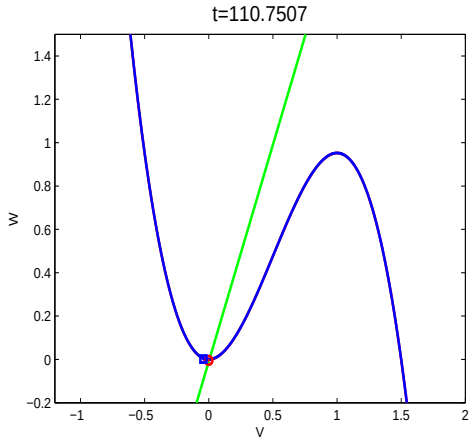
t=110.7507
w
V

Bz

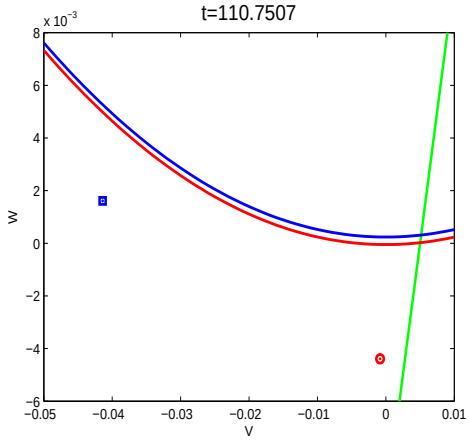
t=110.7507
x 10^-3
w
V

C

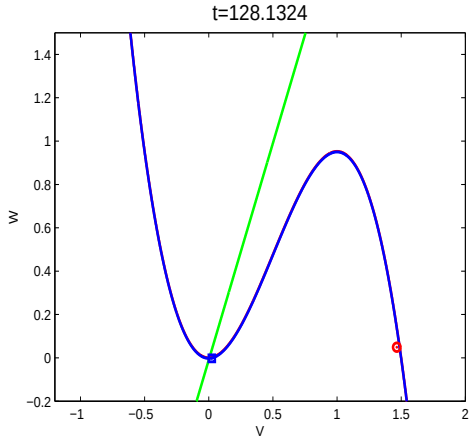
t=128.1324
w
V

Cz

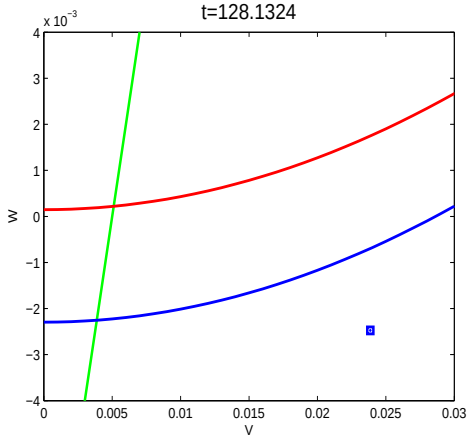
t=128.1324
x 10^-3
w
V

D

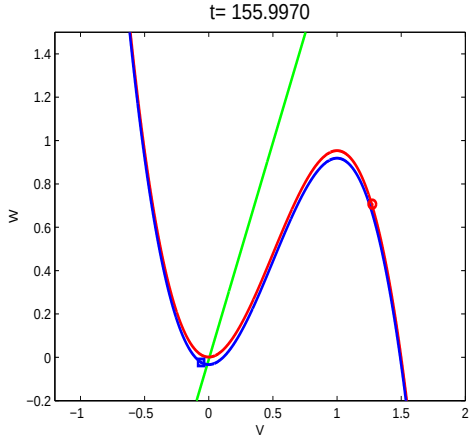
t= 155.9970
w
V

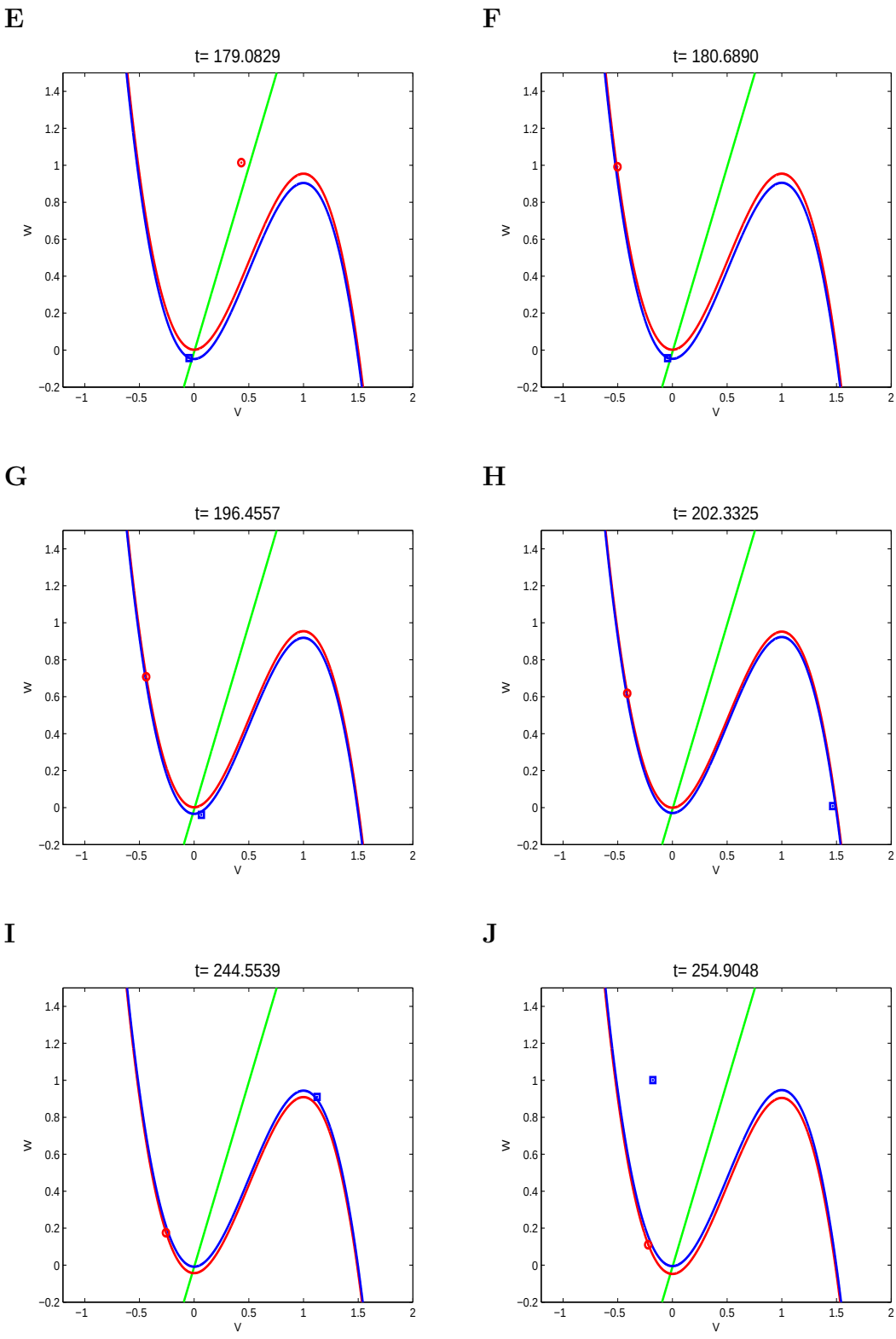

Figure 3.19 Two globally coupled oscillators moving with equation (3.11) in cubic case, and two anti-phase clusters for the following parameters: $\alpha = 2, \gamma = 0.1, \alpha_1 = 0.5, \alpha_2 = 0.5$

A

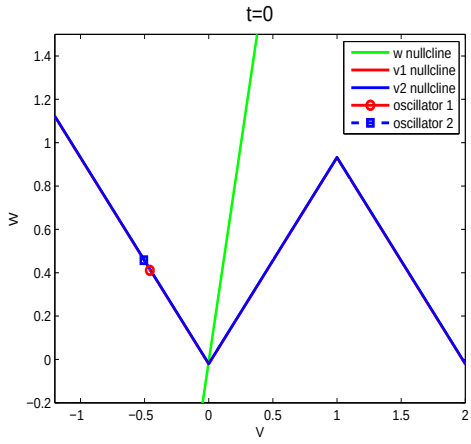
t=0
w nullcline
v1 nullcline
v2 nullcline
oscillator 1
oscillator 2
w
V

B

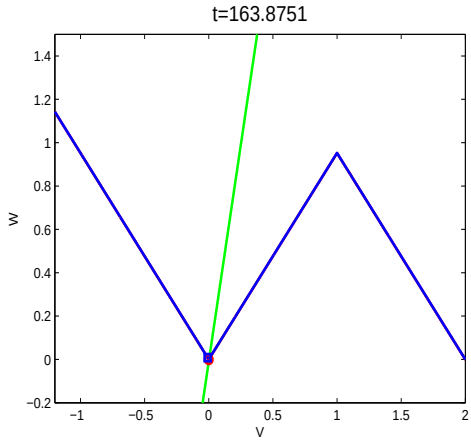
t=163.8751
w
V

Bz

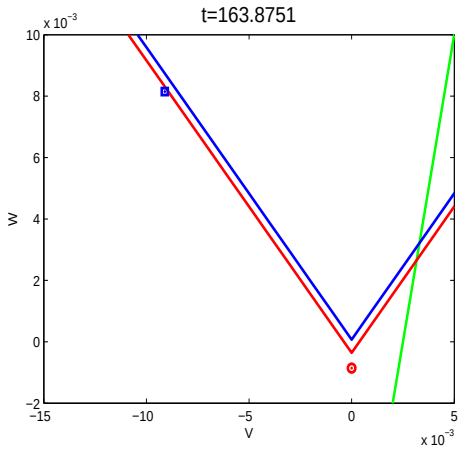
t=163.8751
x 10^-3
w
V
x 10^-3

C

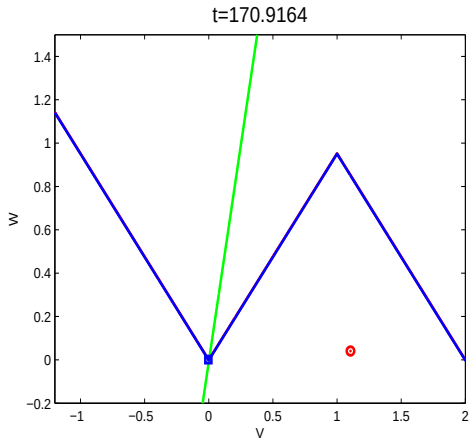
t=170.9164
w
V

Cz

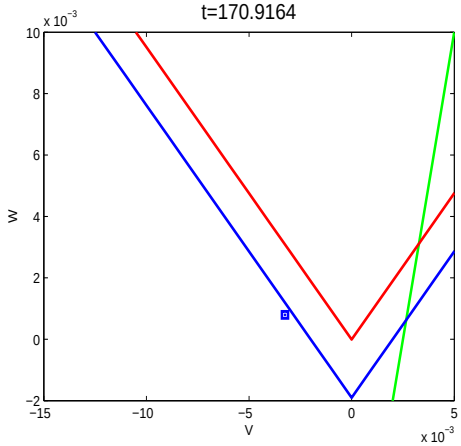
t=170.9164
x 10^-3
w
V
x 10^-3

D

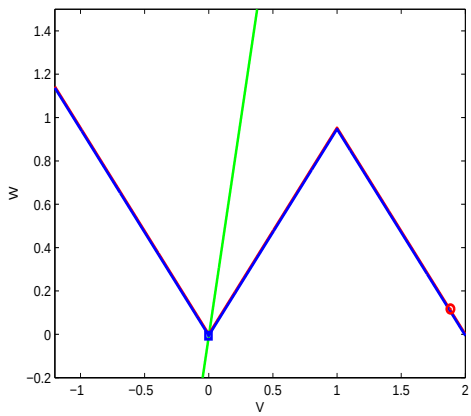
t=178.3717
w
V

Dz

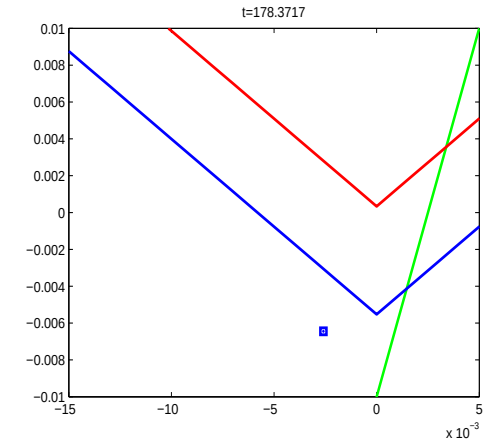
t=178.3717
x 10^-3

E

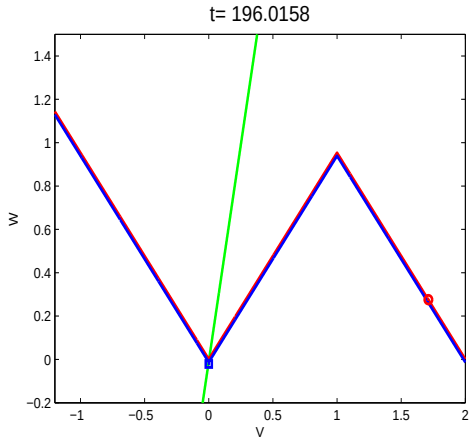
t= 196.0158
w
V

Ez

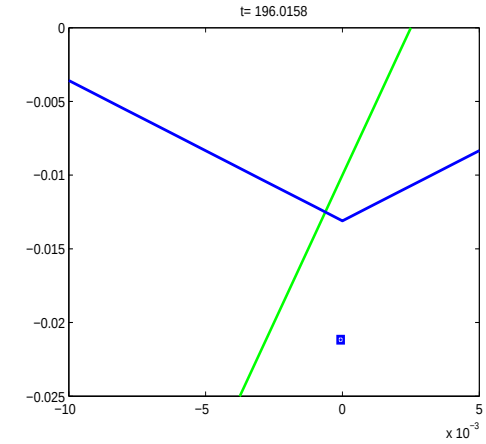
t= 196.0158
x 10^-3

F

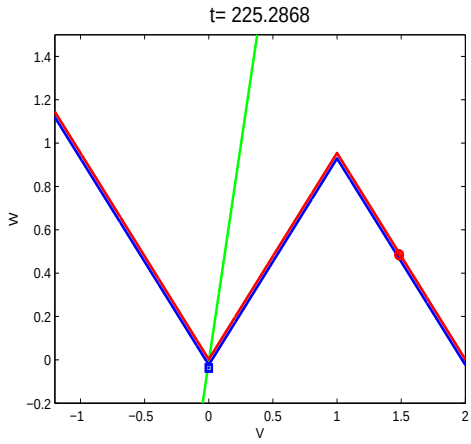
t= 225.2868
w
V

G

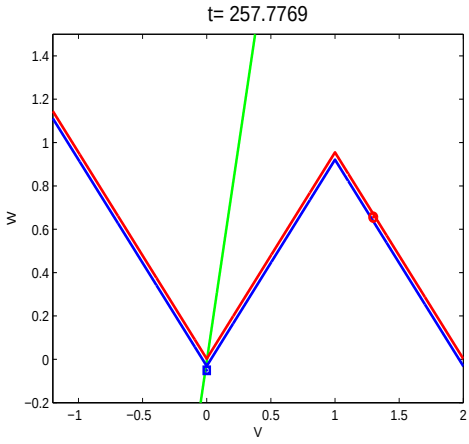
t= 257.7769
w
V

H

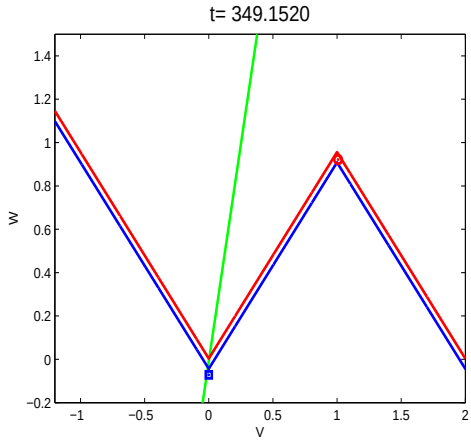
t= 349.1520
w
V

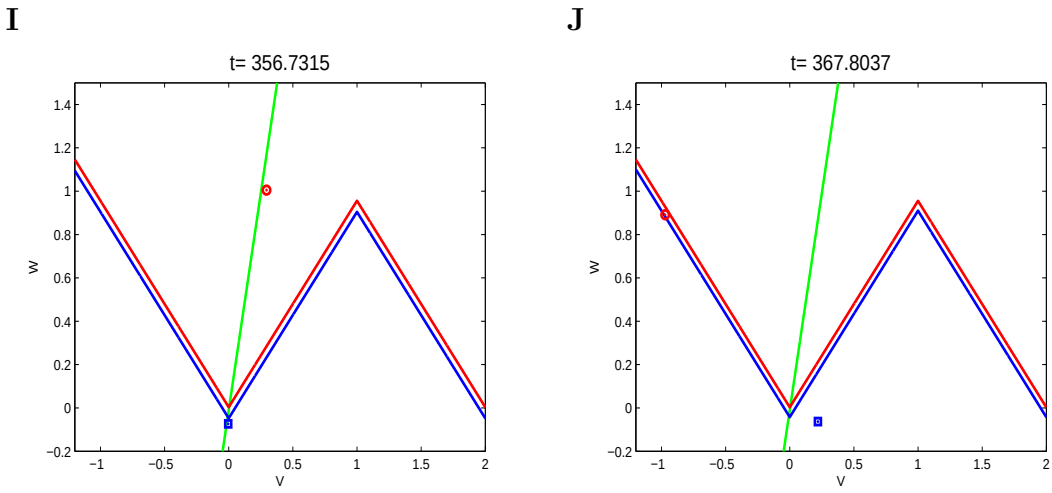

Figure 3.20 Two globally coupled oscillators moving with equation (3.11) in piecewise-linear case, and two out of phase clusters for the following parameters: $\alpha = 4, \gamma = 0.1, \alpha_1 = 0.8, \alpha_2 = 0.2$

3.4 Solution of Piecewise Linear Oscillators

The equations of two globally coupled piecewise oscillators can be expand as:

$$\begin{cases} v_1' = a(v_1 - v_0) - \omega_1 - \gamma(\alpha_1\omega_1 + \alpha_2\omega_2 - \bar{\omega}) \\ v_2' = b(v_2 - \bar{v_0}) - \omega_2 - \gamma(\alpha_1\omega_1 + \alpha_2\omega_2 - \bar{\omega}) \\ \omega_1' = \epsilon(\alpha v_1 - \lambda - \omega_1) \\ \omega_2' = \epsilon(\alpha v_2 - \lambda - \omega_2) \end{cases} \tag{3.13}$$

Where parameter a, v_0 are determined by the position or the branch of the first oscillator, $b, \bar{v_0}$ are determined by the position or the branch of the second oscillator.

The above equation (3.13) can be written to a matrix form:

$$\begin{pmatrix} {v_1}' \\ {v_2}' \\ {\omega_1}' \\ {\omega_2}' \end{pmatrix} = \begin{pmatrix} a & 0 & -(1+\gamma\alpha_1) & -\gamma\alpha_2 \\ 0 & b & -\gamma\alpha_1 & -(1+\gamma\alpha_2) \\ \varepsilon\alpha & 0 & -\varepsilon & 0 \\ 0 & \varepsilon\alpha & 0 & -\varepsilon \end{pmatrix} \begin{pmatrix} v_1 \\ v_2 \\ \omega_1 \\ \omega_2 \end{pmatrix} + \begin{pmatrix} -av_0 + \gamma\omega \\ -bv_0 + \gamma\omega \\ -\epsilon\lambda \\ -\epsilon\lambda \end{pmatrix}$$

A

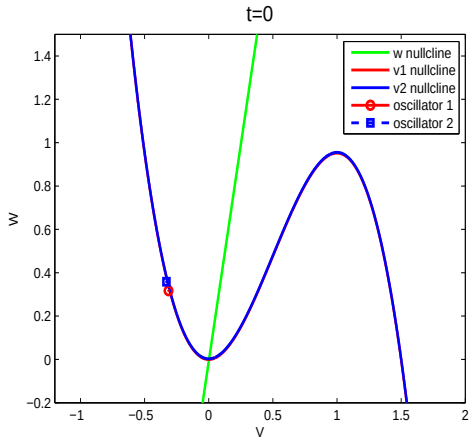
t=0
w nullcline
v1 nullcline
v2 nullcline
oscillator 1
oscillator 2
w
V

B

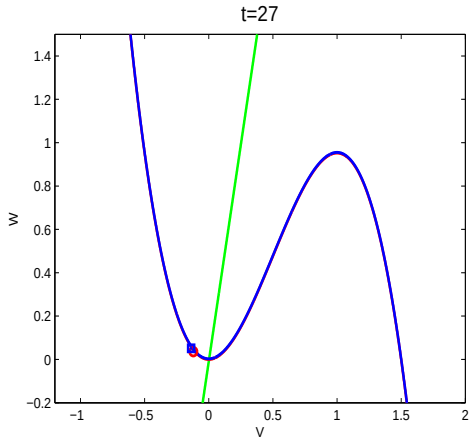
t=27
w
V

Bz

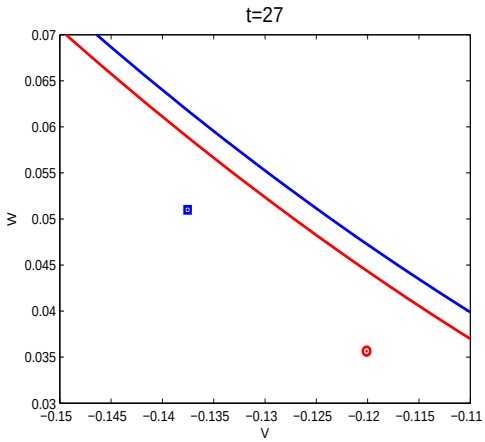
t=27
w
V

C

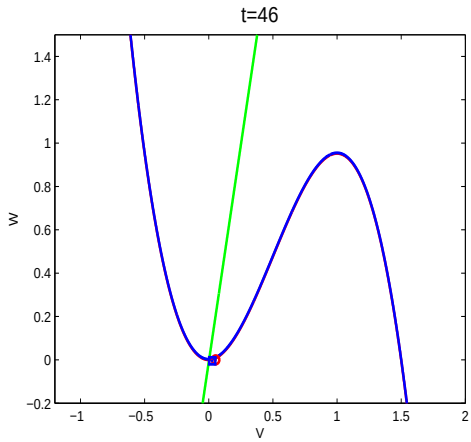
t=46
w
V

Cz

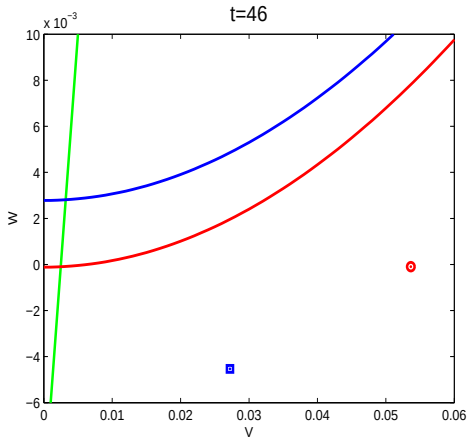
t=46
x 10^-3
w
V

D

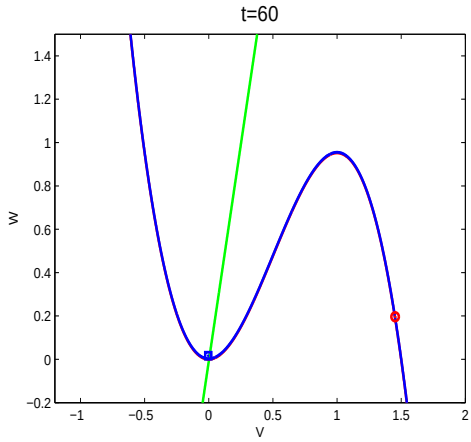
t=60
w
V

Dz

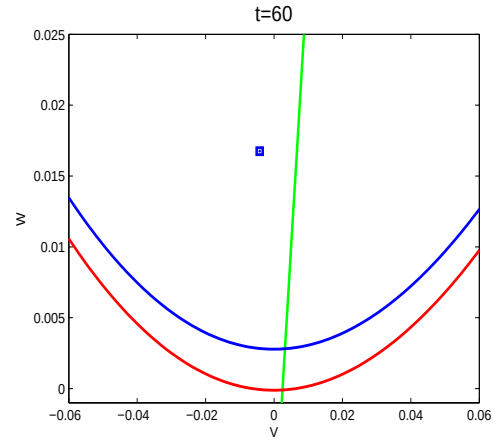

E

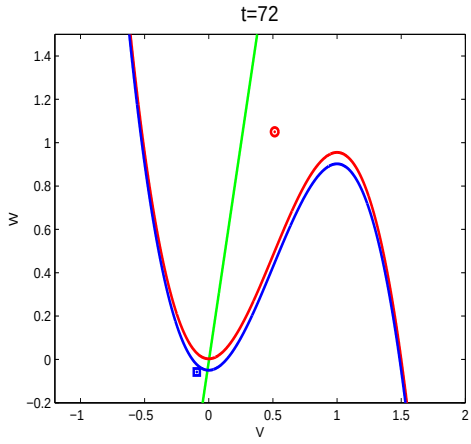

F

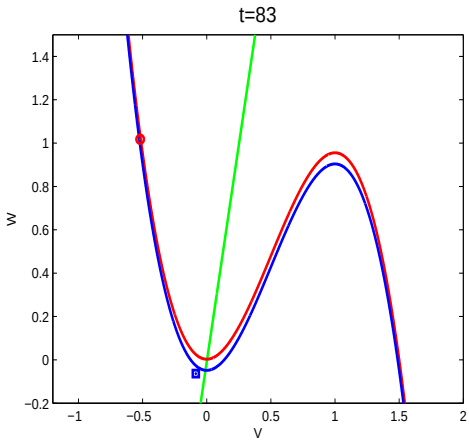

G

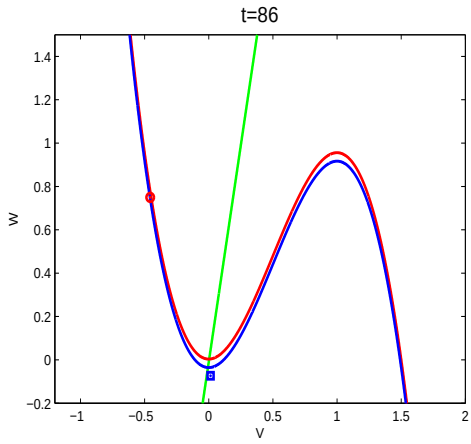

H

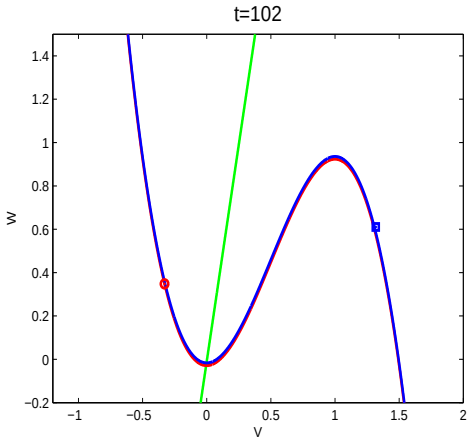

I

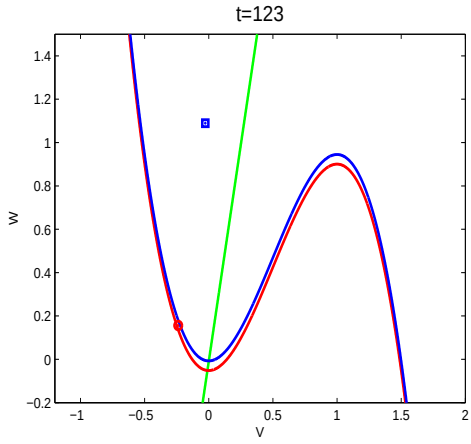

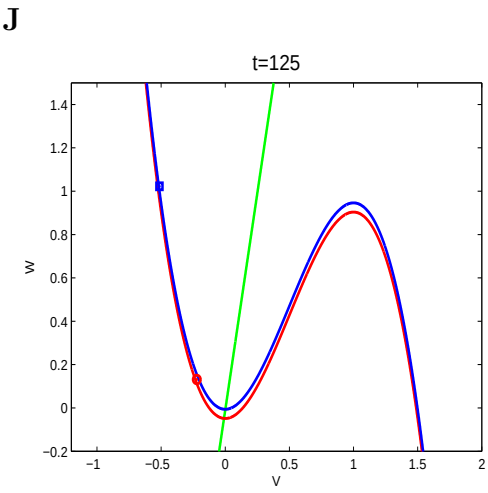

Figure 3.21 Two globally coupled oscillators moving with equation (3.11), and two out of phase clusters for the following parameters:$\alpha = 4, \gamma = 0.1, \alpha_1 = 0.8, \alpha_2 = 0.2$

Theorem 1 *Consider a four variable ODE system given as follows:*

$$\begin{pmatrix} {v_1}' \\ {v_2}' \\ {\omega_1}' \\ {\omega_2}' \end{pmatrix} = D \begin{pmatrix} v_1 \\ v_2 \\ \omega_1 \\ \omega_2 \end{pmatrix} + L$$

The matrix D can be diagonalized:

$$D = \begin{pmatrix} a & 0 & -(1+\gamma\alpha_1) & -\gamma\alpha_2 \\ 0 & b & -\gamma\alpha_1 & -(1+\gamma\alpha_2) \\ \varepsilon\alpha & 0 & -\varepsilon & 0 \\ 0 & \varepsilon\alpha & 0 & -\varepsilon \end{pmatrix} = A \begin{pmatrix} \lambda_1 & 0 & 0 & 0 \\ 0 & \lambda_2 & 0 & 0 \\ 0 & 0 & \lambda_3 & 0 \\ 0 & 0 & 0 & \lambda_4 \end{pmatrix} A^{-1}$$

where A is a matrix whose columns are eigenvectors of D.

The solution of this ODE system is:

A

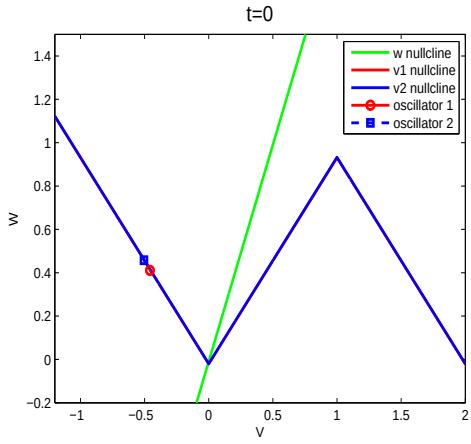
t=0
w nullcline
v1 nullcline
v2 nullcline
oscillator 1
oscillator 2
w
V

B

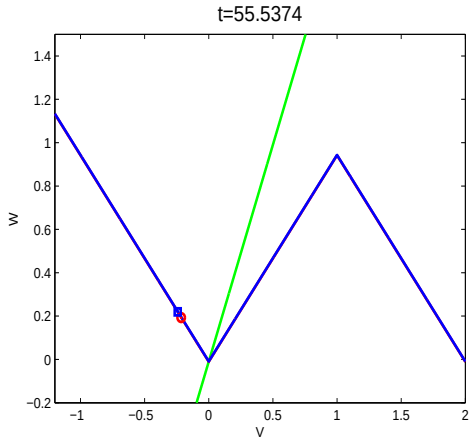
t=55.5374
w
V

C

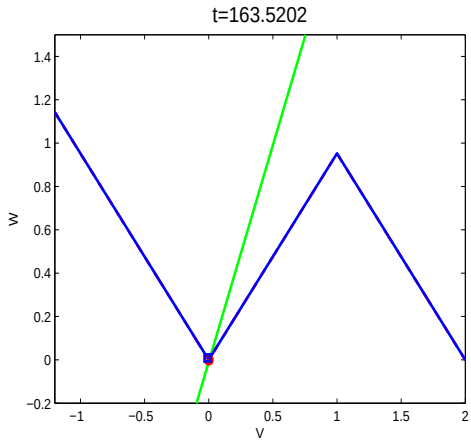
t=163.5202
w
V

Cz

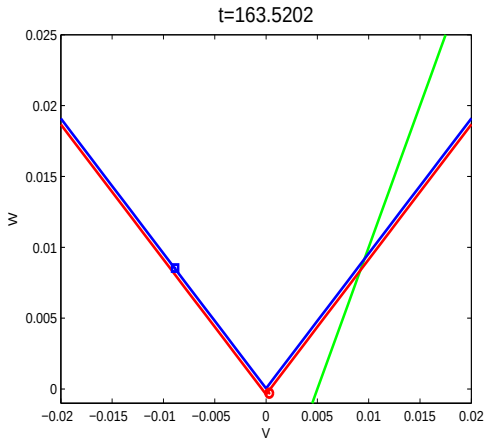
t=163.5202
w
V

D

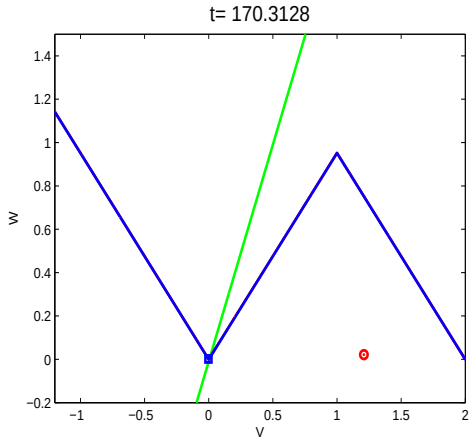
t= 170.3128
w
V

Dz

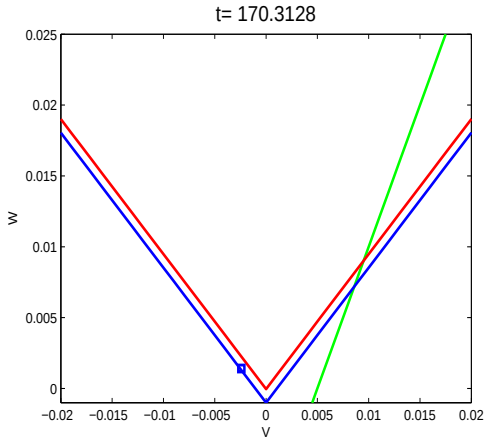
t= 170.3128
w
V

E

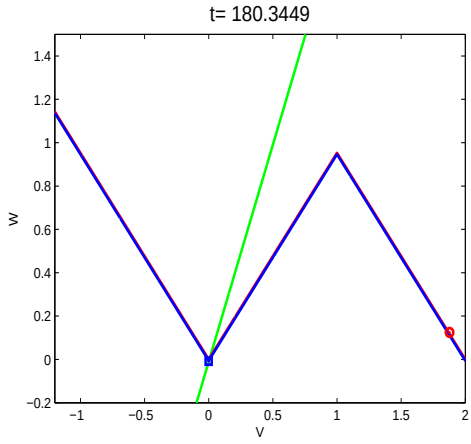
t= 180.3449
w
V

Ez

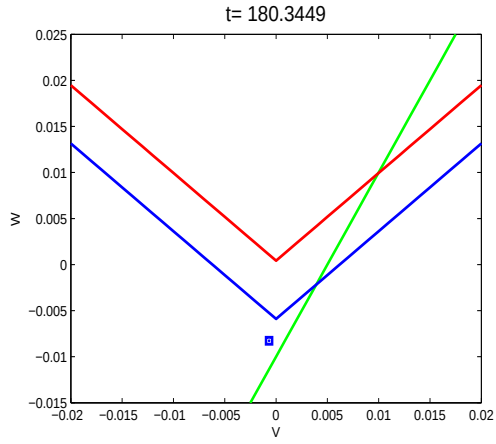
t= 180.3449
w
V

F

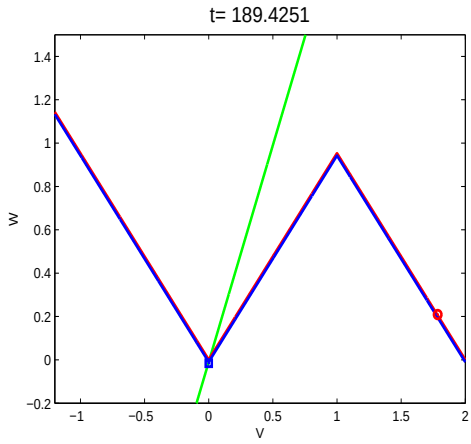
t= 189.4251
w
V

Fz

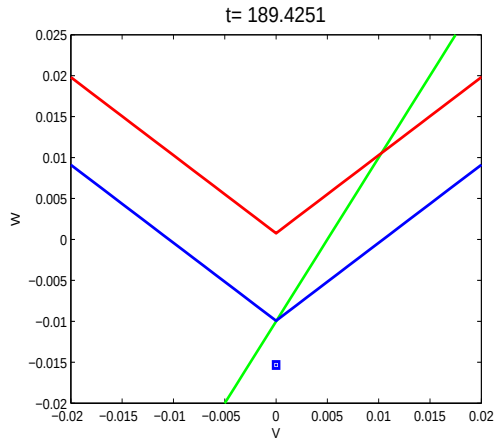
t= 189.4251
w
V

G

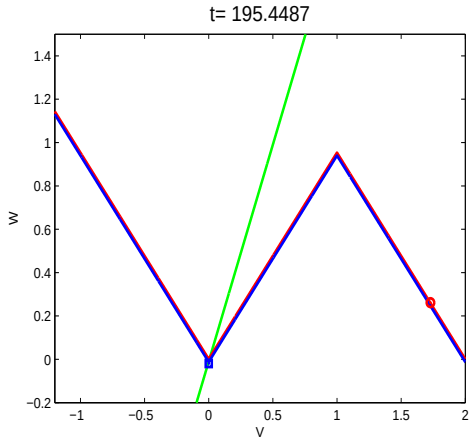
t= 195.4487
w
V

Gz

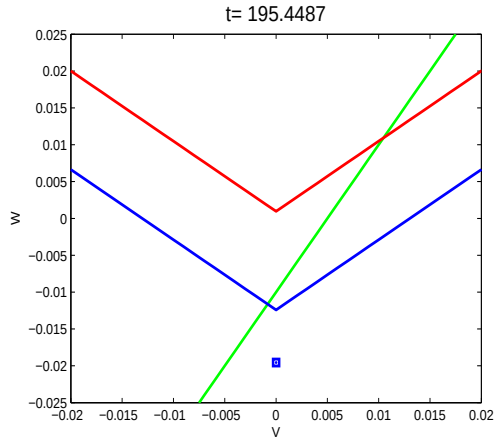
t= 195.4487
w
V

H

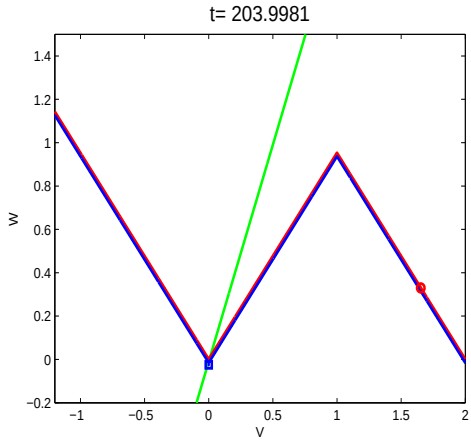
t= 203.9981
w
V

Hz

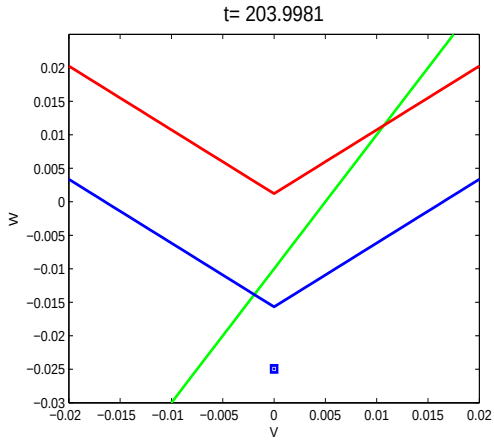
t= 203.9981
w
V

I

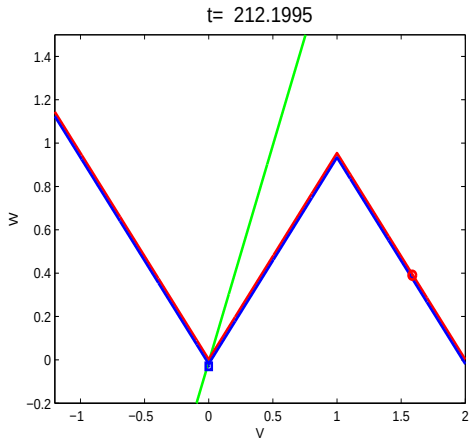
t= 212.1995
w
V

Iz

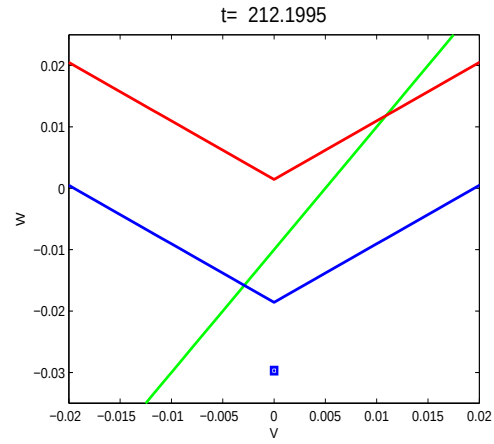
t= 212.1995
w
V

J

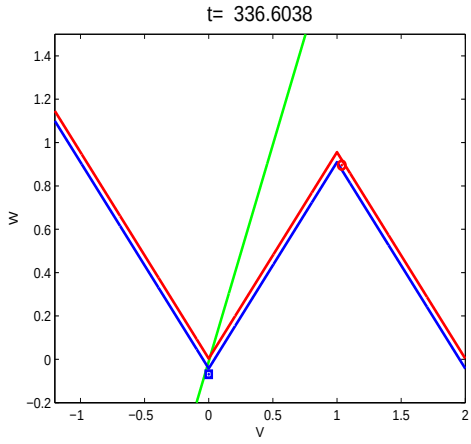
t= 336.6038
w
V

Jz

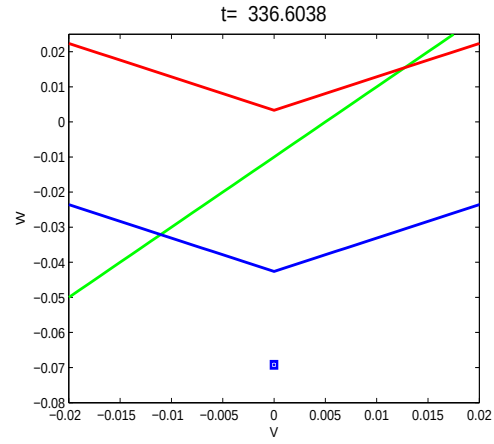
t= 336.6038
w
V

K

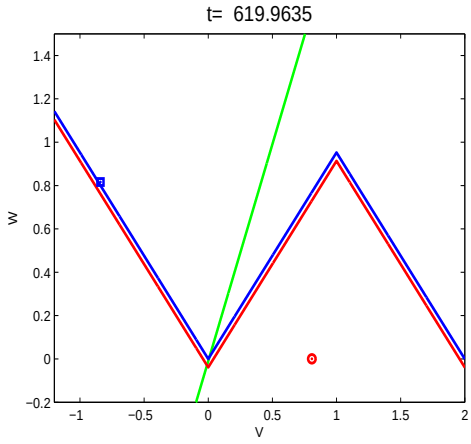

Figure 3.22 Two globally coupled oscillators moving with equation (3.11) in piecewise-linear case, and two out of phase clusters for the following parameters: $\alpha = 2, \gamma = 0.1, \alpha_1 = 0.8, \alpha_2 = 0.2$

$$\begin{pmatrix} v_1 \\ v_2 \\ \omega_1 \\ \omega_2 \end{pmatrix} = A \begin{pmatrix} \frac{1}{\lambda_1} & 0 & 0 & 0 \\ 0 & \frac{1}{\lambda_2} & 0 & 0 \\ 0 & 0 & \frac{1}{\lambda_3} & 0 \\ 0 & 0 & 0 & \frac{1}{\lambda_4} \end{pmatrix}.$$

$$\left\{ \begin{pmatrix} e^{\lambda_1 t} & 0 & 0 & 0 \\ 0 & e^{\lambda_2 t} & 0 & 0 \\ 0 & 0 & e^{\lambda_3 t} & 0 \\ 0 & 0 & 0 & e^{\lambda_4 t} \end{pmatrix} \left[\begin{pmatrix} \lambda_1 & 0 & 0 & 0 \\ 0 & \lambda_2 & 0 & 0 \\ 0 & 0 & \lambda_3 & 0 \\ 0 & 0 & 0 & \lambda_4 \end{pmatrix} A^{-1} \begin{pmatrix} v_1(0) \\ v_2(0) \\ \omega_1(0) \\ \omega_2(0) \end{pmatrix} + A^{-1}L \right] - A^{-1}L \right\} \quad (3.14)$$

The sketch of the proof is given in Appendix (A.1).

The value of matrix D and vector L is determined by the position of the oscillators, so we consider nine cases:

A

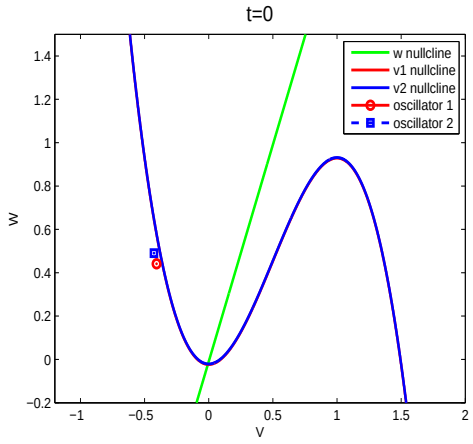
t=0
w nullcline
v1 nullcline
v2 nullcline
oscillator 1
oscillator 2
w
V

B

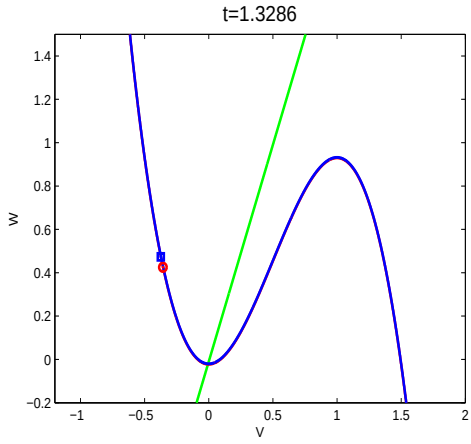
t=1.3286
w
V

C

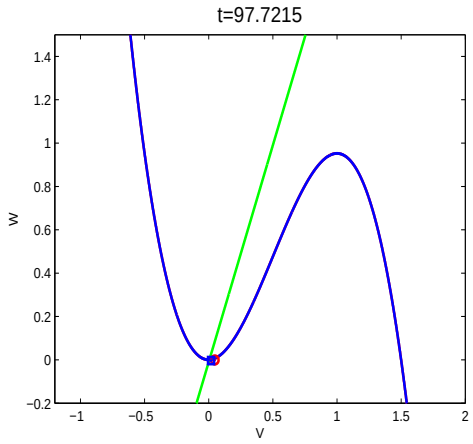
t=97.7215
w
V

Cz

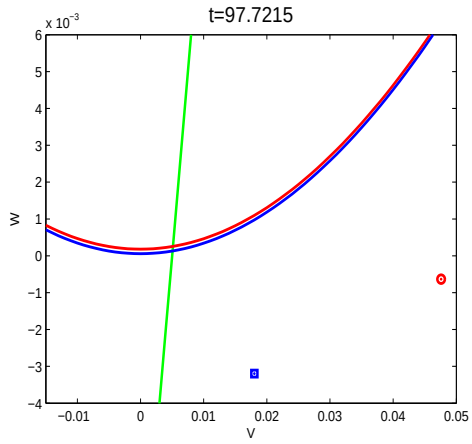
t=97.7215
x 10^-3
w
V

D

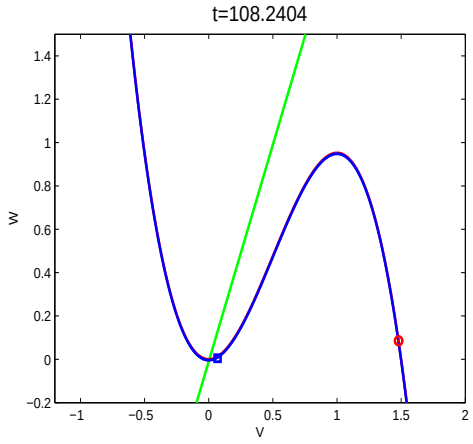
t=108.2404
w
V

Dz

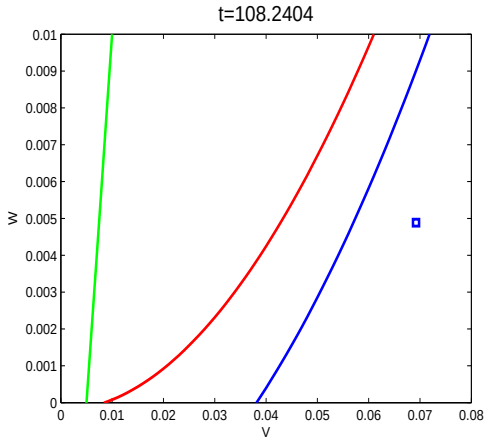
t=108.2404
w
V

E

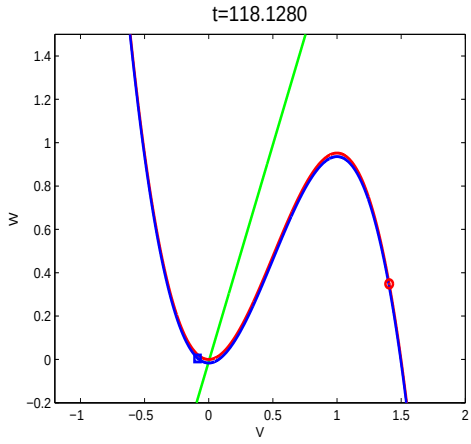
t=118.1280
w
V

Ez

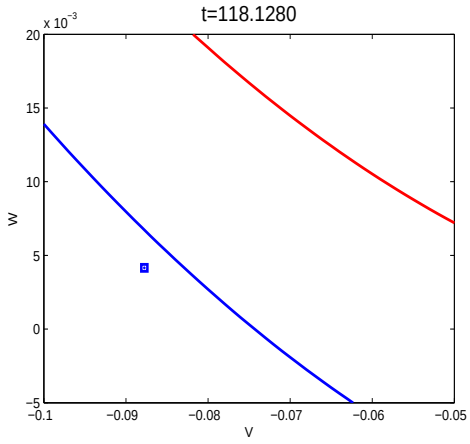
x 10^-3
t=118.1280
w
V

F

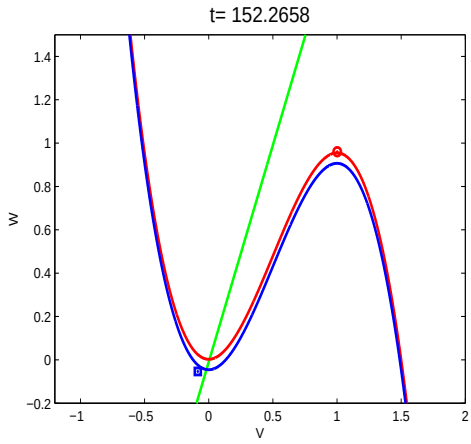
t= 152.2658
w
V

G

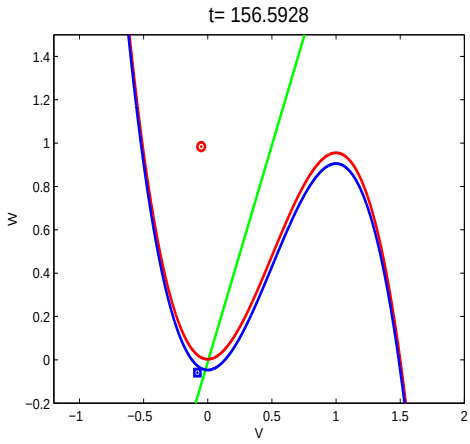
t= 156.5928
w
V

H

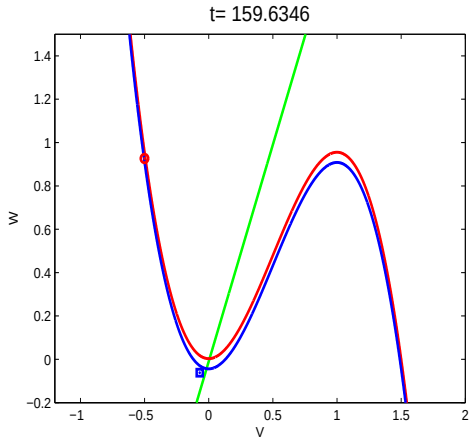
t= 159.6346
w
V

I

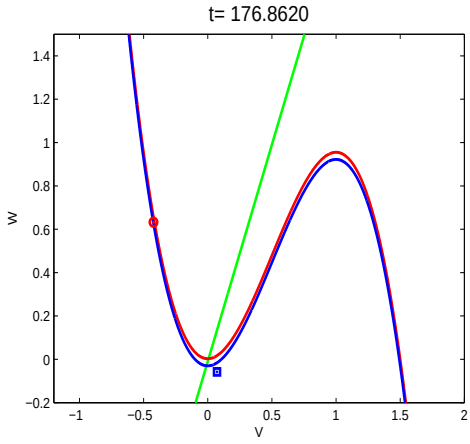
t= 176.8620
w
V

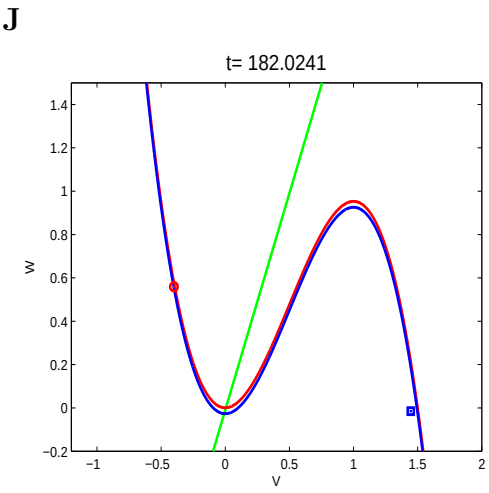

Figure 3.23 Two globally coupled oscillators moving with equation (3.11), and two out of phase clusters for the following parameters:$\alpha = 2, \gamma = 0.1, \alpha_1 = 0.8, \alpha_2 = 0.2$

(i) If both of v_1, v_2 are moving on the left branch, $a = b = -\beta_1$,

$$D = \begin{pmatrix} -\beta_1 & 0 & -(1+\gamma\alpha_1) & -\gamma\alpha_2 \\ 0 & -\beta_1 & -\gamma\alpha_1 & -(1+\gamma\alpha_2) \\ \varepsilon\alpha & 0 & -\varepsilon & 0 \\ 0 & \varepsilon\alpha & 0 & -\varepsilon \end{pmatrix}$$

$$L = \begin{pmatrix} \gamma\bar{\omega} \\ \gamma\bar{\omega} \\ -\varepsilon\lambda \\ -\varepsilon\lambda \end{pmatrix}$$

(ii) v_1 is moving on the left branch, v_2 is moving on the middle branch: $a = -\beta_1, b = 1$,

$$D = \begin{pmatrix} -\beta_1 & 0 & -(1+\gamma\alpha_1) & -\gamma\alpha_2 \\ 0 & 1 & -\gamma\alpha_1 & -(1+\gamma\alpha_2) \\ \varepsilon\alpha & 0 & -\varepsilon & 0 \\ 0 & \varepsilon\alpha & 0 & -\varepsilon \end{pmatrix}$$

$$L = \begin{pmatrix} \gamma\bar{\omega} \\ \gamma\bar{\omega} \\ -\varepsilon\lambda \\ -\varepsilon\lambda \end{pmatrix}$$

(**iii**) **Both of** v_1 **and** v_2 **are moving on the middle branch,** $a = b = 1$

$$D = \begin{pmatrix} 1 & 0 & -(1+\gamma\alpha_1) & -\gamma\alpha_2 \\ 0 & 1 & -\gamma\alpha_1 & -(1+\gamma\alpha_2) \\ \varepsilon\alpha & 0 & -\varepsilon & 0 \\ 0 & \varepsilon\alpha & 0 & -\varepsilon \end{pmatrix}$$

$$L = \begin{pmatrix} \gamma\bar{\omega} \\ \gamma\bar{\omega} \\ -\varepsilon\lambda \\ -\varepsilon\lambda \end{pmatrix}$$

(**iv**) v_1 **is moving on the middle branch,** v_2 **is moving on the right branch,** $a = 1$**,**$b = -\beta_2$

$$D = \begin{pmatrix} 1 & 0 & -(1+\gamma\alpha_1) & -\gamma\alpha_2 \\ 0 & -\beta_2 & -\gamma\alpha_1 & -(1+\gamma\alpha_2) \\ \varepsilon\alpha & 0 & -\varepsilon & 0 \\ 0 & \varepsilon\alpha & 0 & -\varepsilon \end{pmatrix}$$

$$L = \begin{pmatrix} \gamma\bar{\omega} \\ \gamma\bar{\omega} + 1 + \beta_2 \\ -\varepsilon\lambda \\ -\varepsilon\lambda \end{pmatrix}$$

(**v**) **Both of** v_1 **and** v_2 **are moving on the right branch,** $a = b = -\beta_2$

$$D = \begin{pmatrix} -\beta_2 & 0 & -(1+\gamma\alpha_1) & -\gamma\alpha_2 \\ 0 & -\beta_2 & -\gamma\alpha_1 & -(1+\gamma\alpha_2) \\ \varepsilon\alpha & 0 & -\varepsilon & 0 \\ 0 & \varepsilon\alpha & 0 & -\varepsilon \end{pmatrix}$$

$$L = \begin{pmatrix} \gamma\bar{\omega} + 1 + \beta_2 \\ \gamma\bar{\omega} + 1 + \beta_2 \\ -\varepsilon\lambda \\ -\varepsilon\lambda \end{pmatrix}$$

(**vi**) v_2 **is moving on the middle branch,** v_1 **is moving on the right branch,** $a = -\beta_2$**,** $b = 1$

$$D = \begin{pmatrix} -\beta_2 & 0 & -(1+\gamma\alpha_1) & -\gamma\alpha_2 \\ 0 & 1 & -\gamma\alpha_1 & -(1+\gamma\alpha_2) \\ \varepsilon\alpha & 0 & -\varepsilon & 0 \\ 0 & \varepsilon\alpha & 0 & -\varepsilon \end{pmatrix}$$

$$L = \begin{pmatrix} \gamma\bar{\omega} + 1 + \beta_2 \\ \gamma\bar{\omega} \\ -\varepsilon\lambda \\ -\varepsilon\lambda \end{pmatrix}$$

(**vii**) v_2 **is moving on the left branch,** v_1 **is moving on the middle branch,** $a = 1$**,** $b = -\beta_1$

$$D = \begin{pmatrix} 1 & 0 & -(1+\gamma\alpha_1) & -\gamma\alpha_2 \\ 0 & -\beta_1 & -\gamma\alpha_1 & -(1+\gamma\alpha_2) \\ \varepsilon\alpha & 0 & -\varepsilon & 0 \\ 0 & \varepsilon\alpha & 0 & -\varepsilon \end{pmatrix}$$

$$L = \begin{pmatrix} \gamma\bar{\omega} \\ \gamma\bar{\omega} \\ -\varepsilon\lambda \\ -\varepsilon\lambda \end{pmatrix}$$

(**viii**) v_1 **is moving on the left branch,** v_2 **is moving on the right branch,** $a = -\beta_1$**,** $b = -\beta_2$

$$D = \begin{pmatrix} -\beta_1 & 0 & -(1+\gamma\alpha_1) & -\gamma\alpha_2 \\ 0 & -\beta_2 & -\gamma\alpha_1 & -(1+\gamma\alpha_2) \\ \varepsilon\alpha & 0 & -\varepsilon & 0 \\ 0 & \varepsilon\alpha & 0 & -\varepsilon \end{pmatrix}$$

$$L = \begin{pmatrix} \gamma\bar{\omega} \\ \gamma\bar{\omega} + 1 + \beta_2 \\ -\varepsilon\lambda \\ -\varepsilon\lambda \end{pmatrix}$$

(ix) v_2 **is moving on the right branch,** v_1 **is moving on the left branch,** $a = -\beta_1$**,** $b = -\beta_2$

$$D = \begin{pmatrix} -\beta_2 & 0 & -(1+\gamma\alpha_1) & -\gamma\alpha_2 \\ 0 & -\beta_1 & -\gamma\alpha_1 & -(1+\gamma\alpha_2) \\ \varepsilon\alpha & 0 & -\varepsilon & 0 \\ 0 & \varepsilon\alpha & 0 & -\varepsilon \end{pmatrix}$$

$$L = \begin{pmatrix} \gamma\bar{\omega} + 1 + \beta_2 \\ \gamma\bar{\omega} \\ -\varepsilon\lambda \\ -\varepsilon\lambda \end{pmatrix}$$

This is the exact solution of $v_1(t)$, $v_2(t)$, $\omega_1(t)$, $\omega_2(t)$. To see whether two oscillators can synchronize after a long time, we need to see whether $\lim_{t\to\infty} v_1(t) - v_2(t) = 0$.

3.5 Comparison of Analytical Solution and Numerical Solution for Two Piecewise Linear Coupling Oscillators

We use piecewise linear system to approximate cubic system, so we want to check the patterns of piecewise linear coupling oscillators. The analytical solution for two piecewise linear coupling oscillators is given in equation (3.14).

In order to check if numerical simulations accurately predicts the analytical solutions of the oscillators, an important step is to check the error of the numerical simulation.

The equations of dynamical system with global coupling terms are given in (3.10) and (3.11). We fix the coefficients and the initial conditions as follows:

The graph is shown in Fig. 3.24. The analytical solution is given by the (3.14) above. The error of functions $v(t)$ and $\omega(t)$ between the numerical (2-stage-Runge-Kutta(RK2) scheme [5, 6] and the analytical solutions is very small. So the numerical simulation makes accurate prediction for the phase property of the analytical solutions. If the numerical solutions of two oscillators go anti-phase(same phase), the exact solutions will also go anti-phase(same phase).

3.6 The Moving Nullclines Approach

Lemma of moving nullclines

Lemma 3.6.1 *For the two piecewise linear oscillators system (3.10),(3.11), the nullcline of one oscillator (v_k, ω_k) is moving up(moving down) $\Leftrightarrow$ The other oscillator (v_i, ω_i) lies on the left side (right side) of ω nullcline.*

The sketch of the proof is given in the appendix (A.2).

The moving nullclines graphs are shown in Fig 3.25.

The function of global feedback oscillators is:

$$\begin{cases} v_k' &= f(v_k) - \omega_k - 0.2 \cdot (\frac{1}{2}\omega_k + \frac{1}{2}\omega_i - \bar{\omega}) \\ \omega_k' &= 0.01(10v_k - 0.2 - \omega_k) \end{cases} \tag{3.15}$$

where

$$f(v) = \begin{cases} -v, & \text{when} \quad v < 0 \\ v, & \text{when} \quad 0 \le v \le 1 \\ 2 - v, & \text{when} \quad v > 1 \end{cases} \tag{3.16}$$

When both of the initial points are on the left branch, both oscillators lie on the left side of the ω- nullcline, $\omega_j' = \alpha v_j - \lambda - \omega_j < 0$, both v-nullclines move up in the

A

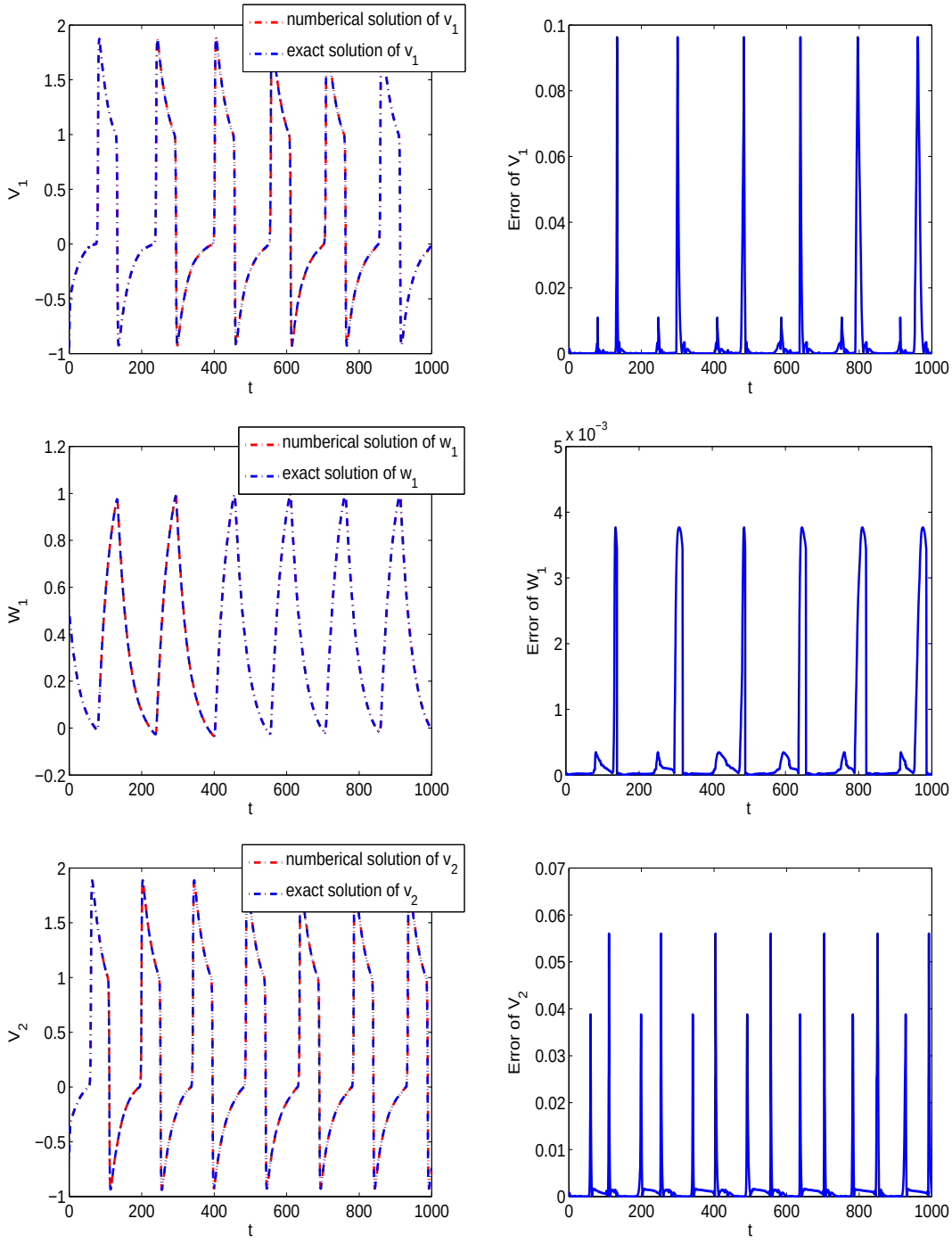
numberical solution of v1
exact solution of v1
V1
t
Error of V1
numberical solution of w1
exact solution of w1
W1
x 10−3
Error of W1
numberical solution of v2
exact solution of v2
V2
Error of V2

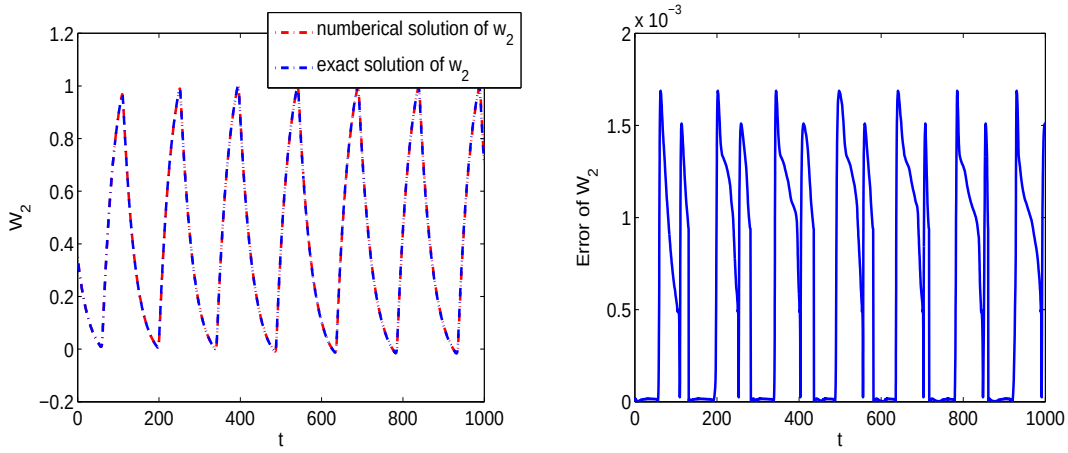
numberical solution of w2
exact solution of w2
w2
t
x 10−3
Error of W2
t

B

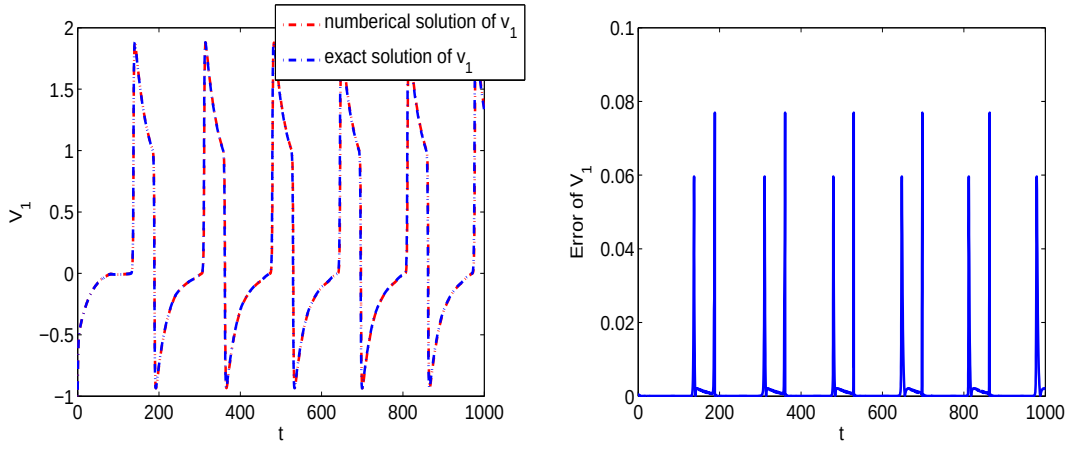
numberical solution of v1
exact solution of v1
V1
t
Error of V1
t

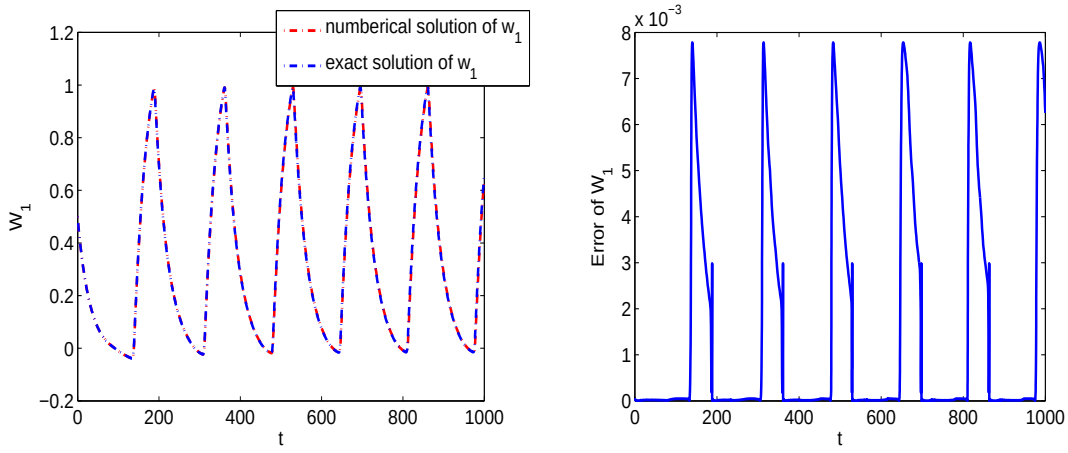
numberical solution of w1
exact solution of w1
W1
t
x 10−3
Error of W1
t

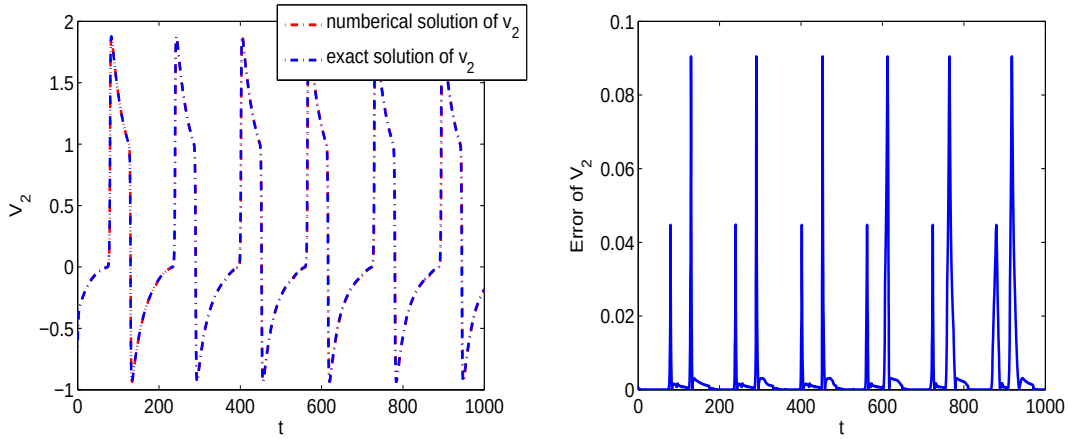
numberical solution of v2
exact solution of v2
v2
t
Error of V2
t

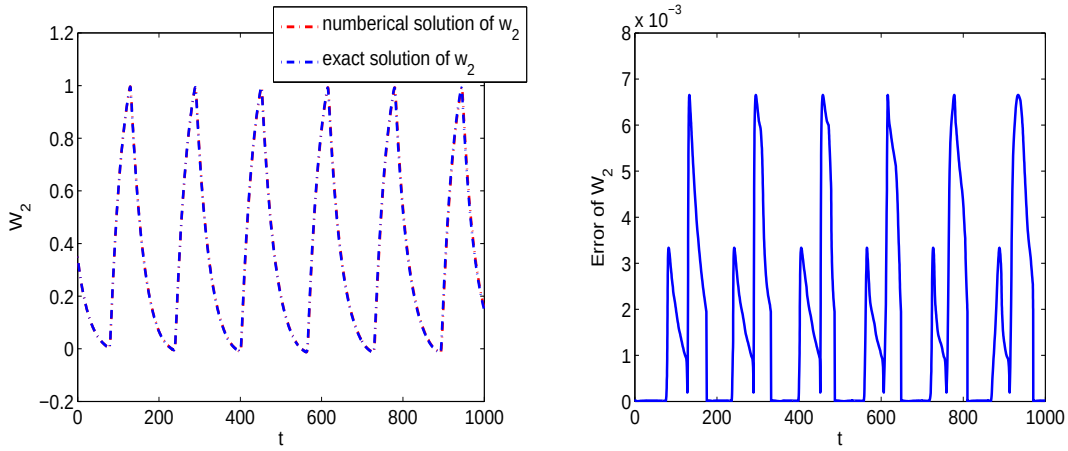
numberical solution of w2
exact solution of w2
w2
t
x 10−3
Error of W2
t

C

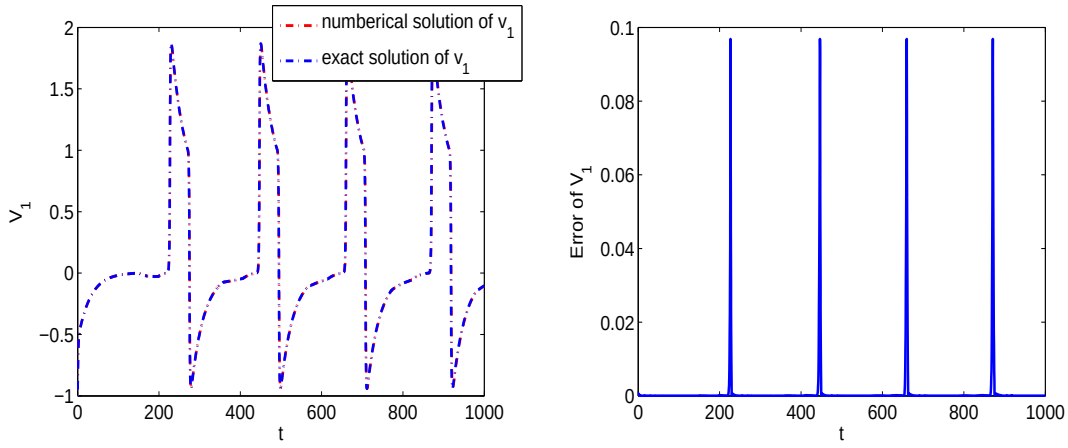
numberical solution of v1
exact solution of v1
v1
t
Error of V1
t

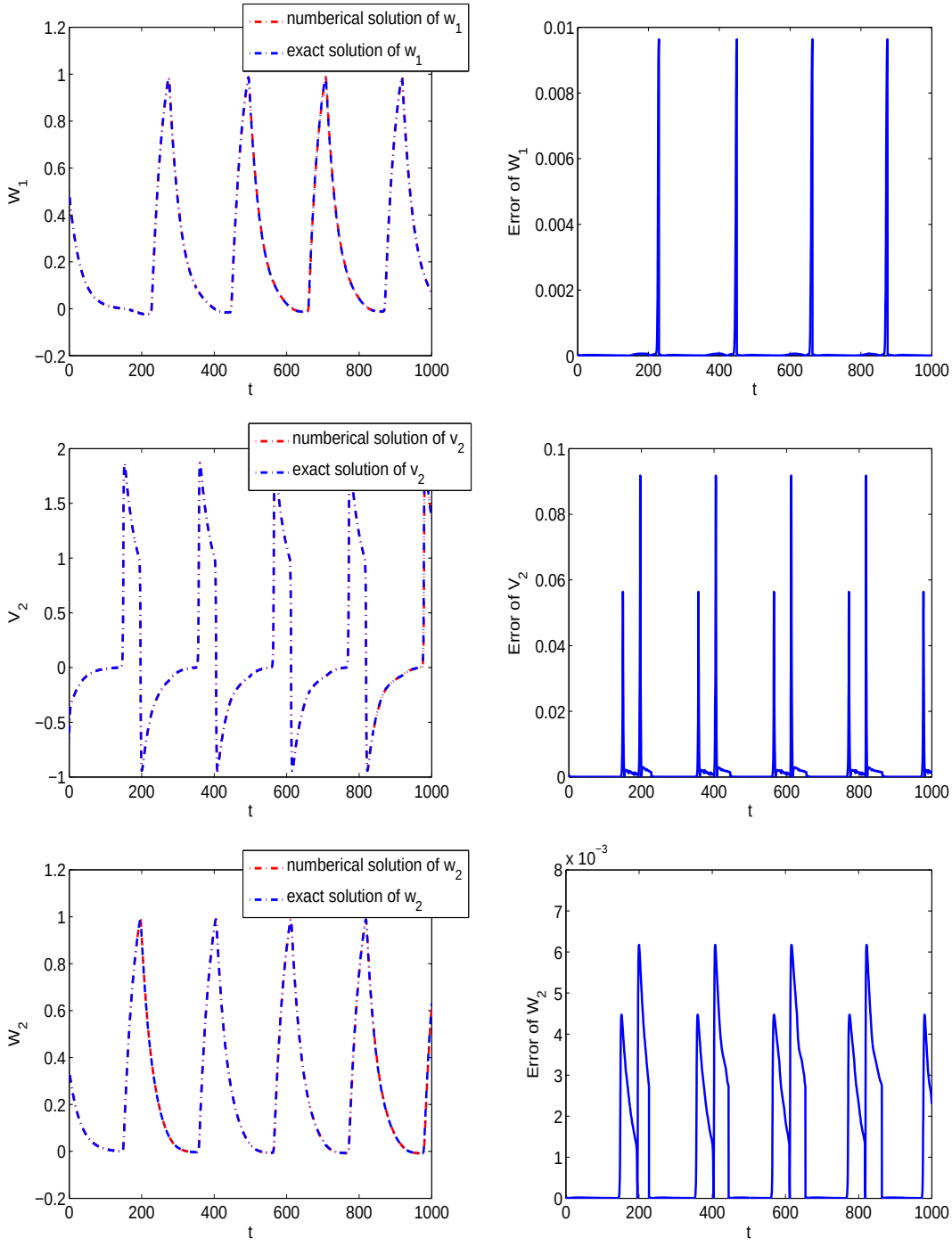

Figure 3.24 Comparison of the numerical solution and exact solution of two oscillators system by initial conditions:$v_1(0) = -1$, $\omega_1(0) = 0.5$, $v_2(0) = -0.65$, $\omega_2(0) = 0.35$ There are three set of parameters: (**A**) $\lambda = 0.2$, (**B**) $\lambda = 0.1$ and (**C**) $\lambda = 0.01$; other parameters $\gamma = 0.1$, $\varepsilon = 0.01$, $\alpha = 2$, $\beta_1 = 1$, $\beta_2 = 1$

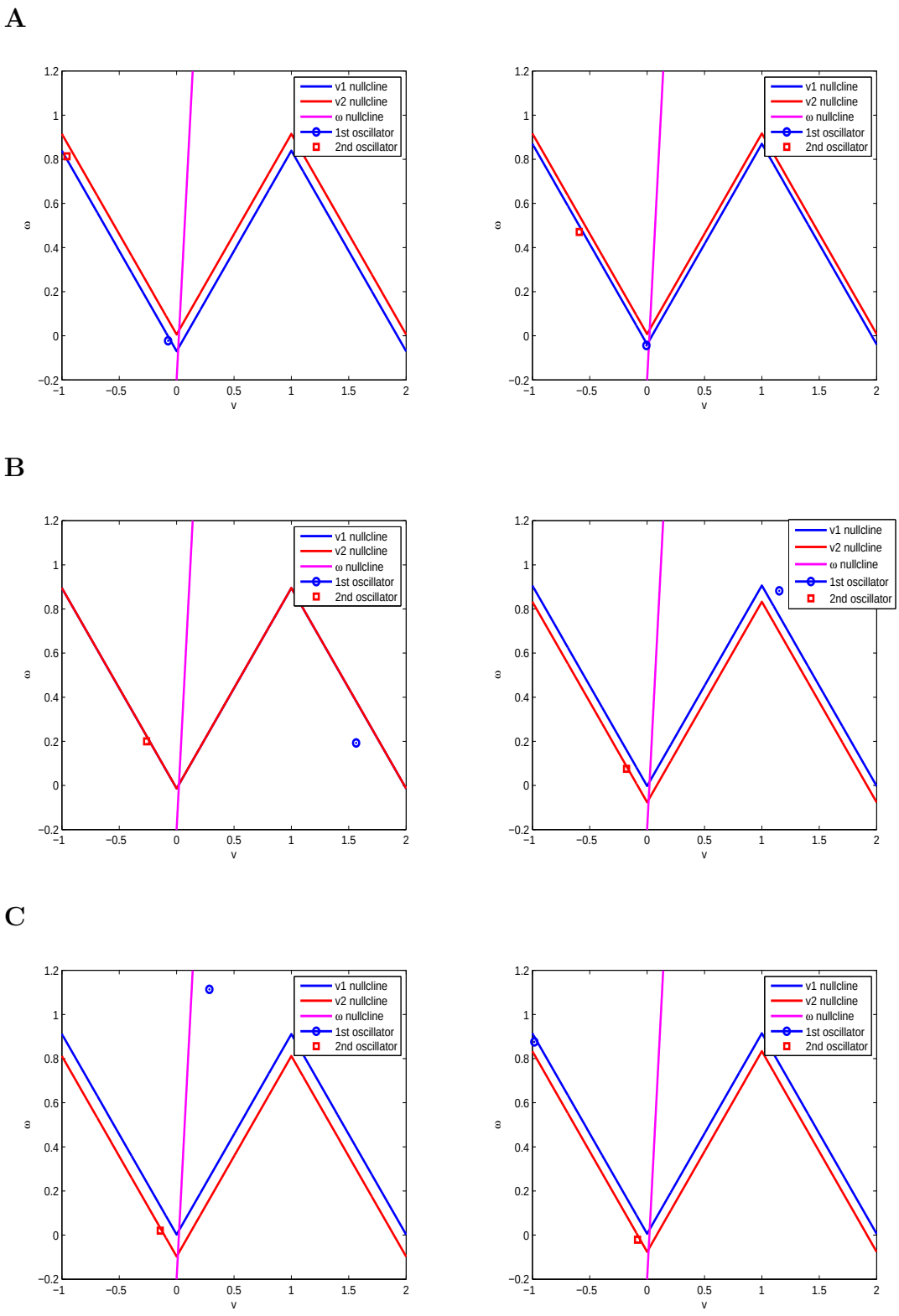

Figure 3.25 The v-nullclines are moving, the equations are (3.15),(3.16)

beginning. The first oscillator cross the ω-nullcline fast, because it has already been away from the left branch of v nullcline and go along the fast direction before it passing through the ω-nullcline. The v-nullcline of the second oscillator begin to move down when the first oscillator has passed ω nullcline above the v-nullcline.

In the piecewise-linear case: Fig A.1, the two oscillator starts on the left branch, the v-nullclines are moving up together. The first oscillator crosses the ω-nullcline fast, however, when the first oscillator is moving on the right side of the ω-nullcline, the v-nullclines of the second oscillator is moving down. The second oscillator is moving down with the v-nullcline, that makes $\omega_2'(t) < 0$. To cross the ω-nullcline from the left side to right side, $\omega'(t)$ should be changed from negative to positive, so the second oscillator takes more time to cross the ω-nullcline, and this makes the two oscillators separate. The same process happens in the cubic case: Fig 3.17, Fig A.2 and Fig 3.21.

In Fig 3.25, two oscillators start far away, they get closer on the first branch before the first oscillator (v_1, ω_1) passing the ω-nullcline, both of the v-nullclines move up. When the first oscillator (v_1, ω_1) has passed the ω-nullcline, the v-nullcline of second oscillator (v_1, ω_1) continue to move up, and the v-nullcline of (v_2, ω_2) begin to move down. and it continue to move down until (v_1, ω_1) passing the ω-nullcline through the top of v-nullcline.

CHAPTER 4

SPIKE-TIME RESPONSE CURVES (STRC) AND SPIKE-TIME DIFFERENCE MAPS (STDM)

Spike time difference curves (STRCs) allow one to predict the dynamical behavior of neuronal networks with mutual synaptic connections from relatively simple measurements in single neurons. In the FHN model, we don't have the synaptic shaped inhibitory term, but our w- term is synaptic shaped. we have used spike-time difference maps method in the FHN model. we extended our work on the phase estimation in the piecewise linear FHN model.

4.1 Introduction for Spike Time Response Method

Phase response curve (PRC) methods have been widely used in various fields of science to investigate the synchronization properties of coupled oscillators. These include [47],[24].

A classical experiment was preformed in 1960 by Patricia DeCoursey. She created an experiment to investigate how flying squirrels respond to light pulses. The flying squirrels were running free in a dark environment which occasionally received light pulses. DeCoursey found that when these nocturnal animals were exposed to light at the beginning of their daily activity, the phase of the onset of activity would be delayed on subsequent days. Conversely, when these animals received light pulses at the end of their daily activity, their phase of activity onset would be advanced on subsequent days. Phase response curve and spike time response curve methods have been used in neuroscience and other fields. In order to get a PRC, we divide the circadian clock into discrete number of points, then administer a perturbation at these points, and measure the phase shift in the circadian clock, i.e., the phase difference between the perturbed and non-perturbed oscillators. Example of perturbation include pulses of light, drugs, chemicals, or temperature. PRC is a standard tool to study biological rhythms, such as synchrony of mutually coupled neurons.

Some people used PRCs to investigate the synchronization properties of neurons [31], [18]. PRCs describe the relationship between the timing and the effect of a perturbation administered to affect periodic rhythms. A variation of the PRC method are the so called spike-time response curves (STRCs) and spike-time difference maps (STDMs). In a Spike Time Response Curve (STRC) one measures time differences between neurons instead of phase-differences. More specifically, if a neuron is perturbed δt units of time after a spike has occurred, then we plot the time difference between the next spike time of the perturbed neuron and the corresponding spike time of the unperturbed neuron as a function of δt. [38], [16], [21], [47].

4.2 Definition of the Spike Time Response Curve and Spike Time Difference Map

If we have two neurons interacting we can construct a STRC for each one of them as a result of the perturbation received from the other one. More specifically, let us call t_1 and t_2 the spike times of the two neurons during a given cycle, $\bar{t_1}$ and $\bar{t_2}$ the spike times of these two oscillators in the next cycle, and T_1 and T_2 the spiking periods of the two oscillators, and we consider them to be equal (and both equal to T). Neuron 1 is perturbed by neuron 2 at a time t_2.

The next spike of neuron 1 will occur at

$$\bar{t_1} = t_1 + T - P(t_2 - t_1) \tag{4.1}$$

Here P is the STRC. Note that in the absence of any perturbation, $\bar{t_1} = t_1 + T$; i.e., P measures spike time advances and delays with respect to the spike times of the unperturbed oscillators. Conversely, assuming the second spike of neuron 2 arrives after the second spike of neuron 1 ($t_2 > \bar{t_1}$), then

$$\bar{t_2} = t_2 + T - P(\bar{t_1} - t_2). \tag{4.2}$$

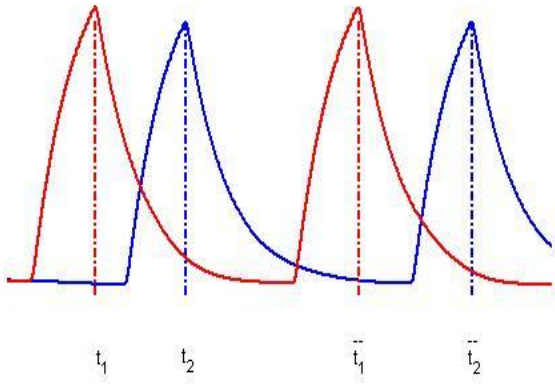

STRCs can be used to construct STDMs in the following way. We follow [1], subtracting (4.2) from (4.1) we obtain

$$\bar{t_2} - \bar{t_1} = t_2 - t_1 + P(t_2 - t_1) - P(\bar{t_1} - t_2) \tag{4.3}$$

Substituting (4.1) into the last term in (4.3) we get:

$$\bar{t_2} - \bar{t_1} = t_2 - t_1 + P(t_2 - t_1) - P(t_1 - t_2 + T - P(t_2 - t_1)). \tag{4.4}$$

Calling $\Delta = t_2 - t_1$ and $\bar{\Delta} = \bar{t_2} - \bar{t_1}$ and substituting in (4.4) we get the STDM

$$\bar{\Delta} = \Delta + P(\Delta) - P(\Delta + T - P(\Delta)). \tag{4.5}$$

For simplicity, let us call

$$F(\Delta) = P(\Delta) - P(\Delta + T - P(\Delta)). \tag{4.6}$$

Thus the STDM (4.5) reads

$$\bar{\Delta} = \Delta + F(\Delta) \tag{4.7}$$

The function F in (4.7) can be computed and the stability properties of the STDM can be analyzed.

We can determine equilibrium solutions Δ^0, which satisfies $F(\Delta^0) = 0$ and describe the time difference between the neurons at steady state.

Stable solutions for STDM satisfy:

$$-2 < \frac{d}{d\Delta}F < 0$$

STRCs and STDM have been used to investigate the synchronization properties of coupled neurons [1], [4], [30], [28], [29].

In our Fitzhugh-Nagumo(FHN) model, because the ω-function has a synaptic-like shape, Here we explore the possibility of using STDM methods to examine the stability of any solutions.

$$\begin{cases} v_k' &= f(v_k) + \gamma\bar{w} - (1+\gamma\alpha_k)w_k - \gamma\alpha_j w_j, \\ w_k' &= \epsilon(\alpha v_k - \lambda - w_k) \quad k, j = 1, 2, j \neq k. \end{cases} \tag{4.8}$$

We refer to the period of an unperturbed oscillator as its natural period, T is the natural period without forcing term:

$$\begin{cases} v_k' &= f(v_k) + \gamma\bar{w} - (1+\gamma\alpha_k)w_k \\ w_k' &= \epsilon(\alpha v_k - \lambda - w_k) \end{cases} \tag{4.9}$$

When $\alpha_1 \neq \alpha_2$, T_1 is the period of first oscillator without the perturbation of the second oscillator:

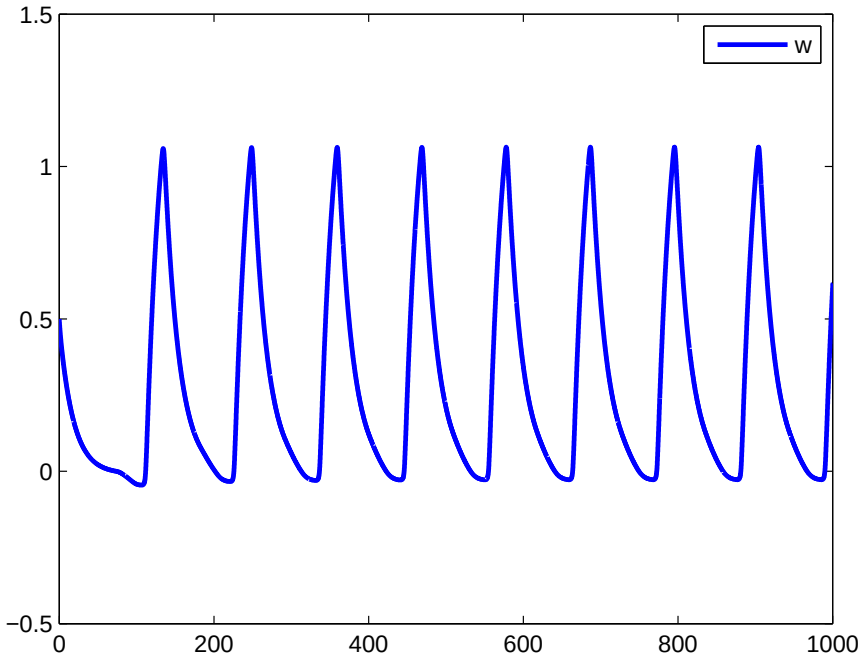

Figure 4.1 The synaptic shaped ω-function

$$\begin{cases} v_1' &= f(v_1) + \gamma\bar{w} - (1+\gamma\alpha_1)w_1 \\ w_1' &= \epsilon(\alpha v_1 - \lambda - w_1) \end{cases} \tag{4.10}$$

T_2 is the period of the second oscillator without the perturbation of the first oscillator:

$$\begin{cases} v_2' &= f(v_2) + \gamma\bar{w} - (1+\gamma\alpha_2)w_2 \\ w_2' &= \epsilon(\alpha v_2 - \lambda - w_2) \end{cases} \tag{4.11}$$

4.3 The Analytical Approach for Three Piecewise Linear Systems

To build the spike time difference map, we first build the spike time response curve. We neglect the time the oscillators spend on the slow trajectory when ϵ is very small. We perturb the second oscillator by the uncoupled first oscillator at different times in the cycle

and measure the change in its next spike time. Let us consider the function of uncoupled first oscillator:

$$\begin{cases} v_1' = f(v_1) - w_1 - r\alpha_1 w_1 + r\bar{w} \\ w_1' = \varepsilon(\alpha v_1 - \lambda - w_1) \end{cases} \tag{4.12}$$

Here $\varepsilon \to 0$, rescale the time value: $\tau = \varepsilon t$,

$$f(v_1) = w_1 + r\alpha_1 w_1 - r\bar{w} = (1 + r\alpha_1)w_1 - r\bar{w}$$

$$(1 + r\alpha_1)\frac{dw_1}{d\tau} = f'(v_1)\frac{dv_1}{d\tau}$$

So

$$(1 + r\alpha_1)(\alpha v_1 - \lambda - w_1) = \eta\frac{dv_1}{d\tau}$$

$\Rightarrow$

$$\begin{cases} \dfrac{dv_1}{d\tau} = \dfrac{1}{\eta}(1 + r\alpha_1)(\alpha v_1 - \lambda - w_1) \\ \dfrac{dw_1}{d\tau} = \dfrac{1}{1 + r\alpha_1} f'(v_1)\dfrac{dv_1}{d\tau} = \dfrac{1}{\eta} f'(v_1)(\alpha v_1 - \lambda - w_1) \end{cases} \tag{4.13}$$

$\Rightarrow$

$$\begin{cases} \dfrac{dv_1}{d\tau} = \dfrac{1}{\eta}(1 + r\alpha_1)\alpha v_1 - \dfrac{1}{\eta}(1 + r\alpha_1)w_1 - \dfrac{\lambda}{\eta}(1 + r\alpha_1) \\ \dfrac{dw_1}{d\tau} = \alpha v_1 - \lambda - w_1 \end{cases} \tag{4.14}$$

$$\frac{d\begin{pmatrix} v_1 \\ w_1 \end{pmatrix}}{d\tau} = \begin{pmatrix} \frac{\alpha}{\eta}(1+r\alpha_1) & -\frac{1}{\eta}(1+r\alpha_1) \\ \alpha & -1 \end{pmatrix} \begin{pmatrix} v_1 \\ w_1 \end{pmatrix} + \begin{pmatrix} -\frac{\lambda}{\eta}(1+r\alpha_1) \\ -\lambda \end{pmatrix}$$

So

$$\frac{d\begin{pmatrix} v_1 \\ w_1 \end{pmatrix}}{d\tau} = T^{-1} \begin{pmatrix} \lambda_1 & 0 \\ 0 & \lambda_2 \end{pmatrix} T \begin{pmatrix} v_1 \\ w_1 \end{pmatrix} + \begin{pmatrix} -\frac{\lambda}{\eta}(1+r\alpha_1) \\ -\lambda \end{pmatrix}$$

$$\frac{dT\begin{pmatrix} v_1 \\ w_1 \end{pmatrix}}{d\tau} = \begin{pmatrix} \lambda_1 & 0 \\ 0 & \lambda_2 \end{pmatrix} T \begin{pmatrix} v_1 \\ w_1 \end{pmatrix} + T \begin{pmatrix} -\frac{\lambda}{\eta}(1+r\alpha_1) \\ -\lambda \end{pmatrix}$$

$$T \begin{pmatrix} v_1 \\ w_1 \end{pmatrix} = \begin{pmatrix} \bar{v_1} \\ \bar{w_1} \end{pmatrix}$$

Which derives:

$$\begin{cases} \frac{d\bar{v_1}}{d\tau} = \lambda_1 \bar{v_1} - \frac{a_1\lambda}{\eta}(1+r\alpha_1) - b_1\lambda \\ \frac{d\bar{w_1}}{d\tau} = \lambda_2 \bar{w_1} - \frac{c_1\lambda}{\eta}(1+r\alpha_1) - d_1\lambda \end{cases} \tag{4.15}$$

In the case $\lambda_2 = 0$,

$$\begin{cases} \frac{d(\lambda_1\bar{v_1} - \frac{a_1\lambda}{\eta}(1+r\alpha_1) - b_1\lambda)}{d\tau} = \lambda_1(\lambda_1\bar{v_1} - \frac{a_1\lambda}{\eta}(1+r\alpha_1) - b_1\lambda) \\ \frac{d\bar{w_1}}{d\tau} = -\frac{c_1\lambda}{\eta}(1+r\alpha_1) - d_1\lambda \end{cases} \tag{4.16}$$

$$\bar{w_1} = -(\frac{c_1\lambda}{\eta}(1+r\alpha_1) + d_1\lambda)\tau + \bar{w_1}(0)$$

So

$$\lambda_1\bar{v_1} - \frac{a_1\lambda}{\eta}(1+r\alpha_1) - b_1\lambda = k_1 e^{\lambda_1\tau}$$

$$k_1 = \lambda_1 \bar{v_1}(0) - \frac{a_1\lambda}{\eta}(1 + r\alpha_1) - b_1\lambda$$

$$\bar{v_1}(\tau) = \frac{1}{\lambda_1}(\frac{a_1\lambda}{\eta}(1 + r\alpha_1) + b_1\lambda + (\lambda_1\bar{v_1}(0) - \frac{a_1\lambda}{\eta}(1 + r\alpha_1) - b_1\lambda)e^{\lambda_1\tau})$$

$$T = \begin{pmatrix} a_1 & b_1 \\ c_1 & d_1 \end{pmatrix}$$

$$\bar{v_1}(0) = a_1 v_1(0) + b_1 w_1(0)$$

$$\bar{w_1}(0) = c_1 v_1(0) + d_1 w_1(0)$$

$$\begin{pmatrix} v_1 \\ w_1 \end{pmatrix} = T^{-1} \begin{pmatrix} \bar{v_1} \\ \bar{w_1} \end{pmatrix}$$

$$\begin{cases} v_2' = f(v_2) - w_2 - r(\alpha_1 w_1 + \alpha_2 w_2 - \bar{w}) \\ w_2' = \varepsilon(\alpha v_2 - \lambda - w_2) \end{cases} \tag{4.17}$$

If we let $\tau = \varepsilon t$,

$$\begin{cases} \varepsilon\dfrac{dv_2}{d\tau} = f(v_2) - w_2 - r(\alpha_1 w_1 + \alpha_2 w_2 - \bar{w}) \\ \dfrac{dw_2}{d\tau} = \alpha v_2 - \lambda - w_2 \end{cases} \tag{4.18}$$

$\varepsilon \to 0 \Rightarrow$

$$f(v_2) = w_2 + r(\alpha_1 w_1 + \alpha_2 w_2 - \bar{w}) = (1 + r\alpha_2)w_2 + r\alpha_1 w_1 - r\bar{w}$$

$$(1 + r\alpha_2)\frac{dw_2}{d\tau} = f'(v_2)\frac{dv_2}{d\tau} - r\alpha_1\frac{dw_1}{d\tau}$$

$$(1 + r\alpha_2)(\alpha v_2 - \lambda - w_2) = \eta\frac{dv_2}{d\tau} - r\alpha_1(\alpha v_1 - \lambda - w_1)$$

$$\begin{cases} \dfrac{dv_2}{d\tau} = \dfrac{1}{\eta}((1 + r\alpha_2)(\alpha v_2 - \lambda - w_2) + r\alpha_1(\alpha v_1 - \lambda - w_1)) \\ \dfrac{dw_2}{d\tau} = \alpha v_2 - \lambda - w_2 \end{cases} \tag{4.19}$$

$$\frac{d\begin{pmatrix} v_2 \\ w_2 \end{pmatrix}}{d\tau} = \begin{pmatrix} \frac{\alpha(1+r\alpha_2)}{\eta} & -\frac{(1+r\alpha_2)}{\eta} \\ \alpha & -1 \end{pmatrix}\begin{pmatrix} v_2 \\ w_2 \end{pmatrix} + \begin{pmatrix} \frac{r\alpha_1}{\eta}(\alpha v_1 - \lambda - w_1) - \frac{\lambda(1+r\alpha_2)}{\eta} \\ -\lambda \end{pmatrix}$$

$$\frac{dT\begin{pmatrix} v_2 \\ w_2 \end{pmatrix}}{d\tau} = \begin{pmatrix} \lambda_1 & 0 \\ 0 & \lambda_2 \end{pmatrix} T\begin{pmatrix} v_2 \\ w_2 \end{pmatrix} + T\begin{pmatrix} \frac{r\alpha_1}{\eta}(\alpha v_1 - \lambda - w_1) - \frac{\lambda(1+r\alpha_2)}{\eta} \\ -\lambda \end{pmatrix}$$

$$\frac{d\begin{pmatrix} \bar{v_2} \\ \bar{w_2} \end{pmatrix}}{d\tau} = \begin{pmatrix} \lambda_1 & 0 \\ 0 & \lambda_2 \end{pmatrix}\begin{pmatrix} \bar{v_2} \\ \bar{w_2} \end{pmatrix} + \begin{pmatrix} s_1 \\ s_2 \end{pmatrix}$$

If $\alpha_1 = \alpha_2 = 0.5$, $\lambda_2 = 0$,

$$\begin{cases} \dfrac{d\bar{v_2}}{d\tau} = \lambda_1\bar{v_2} + s_1, \\ \dfrac{d\bar{w_2}}{d\tau} = s_2 \end{cases} \tag{4.20}$$

Here

$$s_1 = a_1(\frac{r\alpha_1}{\eta}(\alpha v_1 - \lambda - w_1) - \frac{\lambda(1+r\alpha_2)}{\eta}) - \lambda b_1$$

$$s_2 = c_1(\frac{r\alpha_1}{\eta}(\alpha v_1 - \lambda - w_1) - \frac{\lambda(1+r\alpha_2)}{\eta}) - \lambda d_1$$

$$\begin{cases} \bar{v_1}(\tau) = \frac{1}{\lambda_1}(\frac{a_1\lambda}{\eta}(1+r\alpha_1) + b_1\lambda + (\lambda_1\bar{v_1}(0) - \frac{a_1\lambda}{\eta}(1+r\alpha_1) - b_1\lambda)e^{\lambda_1\tau}) \\ \bar{w_1}(\tau) = -(\frac{c_1\lambda}{\eta}(1+r\alpha_1) + d_1\lambda)\tau + \bar{w_1}(0) \end{cases} \tag{4.21}$$

$$T^{-1} = \begin{pmatrix} a_1' & b_1' \\ c_1' & d_1' \end{pmatrix}$$

$$\begin{pmatrix} v_1 \\ w_1 \end{pmatrix} = T^{-1}\begin{pmatrix} \bar{v_1} \\ \bar{w_1} \end{pmatrix} = \begin{pmatrix} a_1' & b_1' \\ c_1' & d_1' \end{pmatrix}\begin{pmatrix} \bar{v_1} \\ \bar{w_1} \end{pmatrix}$$

$\bar{v_1}(\tau)$ is a linear combination of $e^{\lambda_1\tau}$ and 1, $\bar{w_1}(\tau)$ is a linear combination of τ and 1. v_1 and w_1 are linear combination of $\bar{v_1}$ and $\bar{w_1}$, so v_1 and w_1 are linear combination of $e^{\lambda_1\tau}$, τ and 1. s_1 and s_2 are also linear combination of $e^{\lambda_1\tau}$, τ and 1.

$$\frac{dv_2}{d\tau} = \lambda_1 v_2 + ae^{\lambda_1\tau} + b\tau + c$$

If we make $v_2 = e^{\lambda_1\tau}f$,

$$\frac{dv_1}{d\tau} = \lambda_1 e^{\lambda_1\tau}f + e^{\lambda_1\tau}f' = \lambda_1 e^{\lambda_1\tau}f + ae^{\lambda_1\tau} + b\tau + c$$

$$f' = e^{-\lambda_1\tau}(ae^{\lambda_1\tau} + b\tau + c) = a + b\tau e^{-\lambda_1\tau} + ce^{-\lambda_1\tau}$$

$$f = a\tau - \frac{b\tau}{\lambda_1}e^{-\lambda_1\tau} - \frac{b}{\lambda_1^2}e^{-\lambda_1\tau} - \frac{c}{\lambda_1}e^{-\lambda_1\tau} + s$$

$$s = v_1(0) + \frac{b}{\lambda_1^2} + \frac{c}{\lambda_1}$$

so

$$v_1 = a\tau e^{\lambda_1\tau} - \frac{b\tau}{\lambda_1} + v_1(0)$$

$$\frac{d\bar{w}_2}{d\tau} = \bar{a}e^{\lambda_1\tau} + \bar{b}\tau + \bar{c}$$

$$\bar{w_2} = \frac{\bar{a}}{\lambda_1}e^{\lambda_1\tau} + \frac{\bar{b}\tau^2}{2} + \bar{c}\tau + \bar{w_2}(0) - \frac{\bar{a}}{\lambda_1}$$

4.4 Comparison of Numerical and Analytical Results

We can numerically and analytically compute the effect of perturbation of the second oscillator with respect to the first oscillator and build the spike time response curve and spike time response map and compare these results. The error between the two curves is close to 0.

Consider the piecewise-linear systems, here are two examples:

When $\alpha_1 = 0.3$, $\alpha_2 = 0.7$, if $\lambda \geq 1.4$, we can get in phase pattern, however, if $\lambda \leq 1.3$, we get out of phase-pattern. In the Spike time difference map, when $\lambda = 1.4$, the slope of STDM at the two endpoints are negative, and if $\lambda = 1.3$, the slope of STDM at the endpoints are non-negative.

When $\alpha_1 = 0.2$, $\alpha_2 = 0.8$, if $\lambda \geq 1$, we can get in phase pattern, however, if $\lambda \leq 0.9$, we get out of phase-pattern. In the Spike time difference map, when $\lambda = 1$, the slope of STDM at the two endpoints are negative, and if $\lambda = 0.9$, the slope of STDM at the endpoints are non-negative.

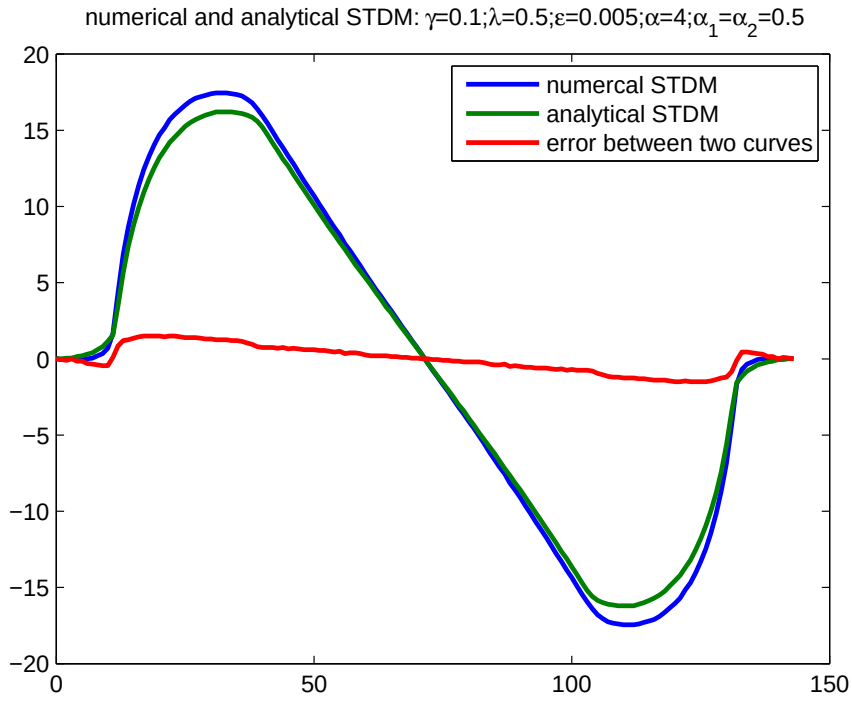

If the slope of the STDM between -2 and 0 , the two oscillators are stable. When the slope of STDM is negative, the pattern is stable. When $\alpha_1 = 0.3$, $\alpha_2 = 0.7$, if $\lambda \geq 1.4$, we get in phase pattern. When $\alpha_1 = 0.2$, $\alpha_2 = 0.8$, if $\lambda \geq 1$, we get in phase pattern. So the result using STDM method is consistent in the phase figures Fig. 4.3 and Fig. 4.4.

For cubic systems, here are also two examples:

When $\alpha_1 = 0.5$, $\alpha_2 = 0.5$, if $\lambda > 0.45$, we can get in phase pattern, however, if $\lambda \leq 0.45$, we get out of phase-pattern. In Fig. 4.6, the Spike time difference map shows that when $\lambda = 0.5$, the slope of STDM at the two endpoints are negative, and if $\lambda = 0.45$, the slope of STDM at the endpoints are non-negative.

For $\alpha_1 = 0.3$, $\alpha_2 = 0.7$, if $\lambda > 0.25$, we can get in phase pattern, however, if $\lambda \leq 0.25$, we get out of phase-pattern. In Fig. 4.8, the Spike time difference map shows that when $\lambda = 0.3$, the slope of STDM at the two endpoints are negative, and if $\lambda = 0.25$, the slope of STDM at the endpoints are non-negative.

These examples shows that the result of phases by using STDM method is consistent with the result in the phase picture. So we can use the STDM method to estimate the

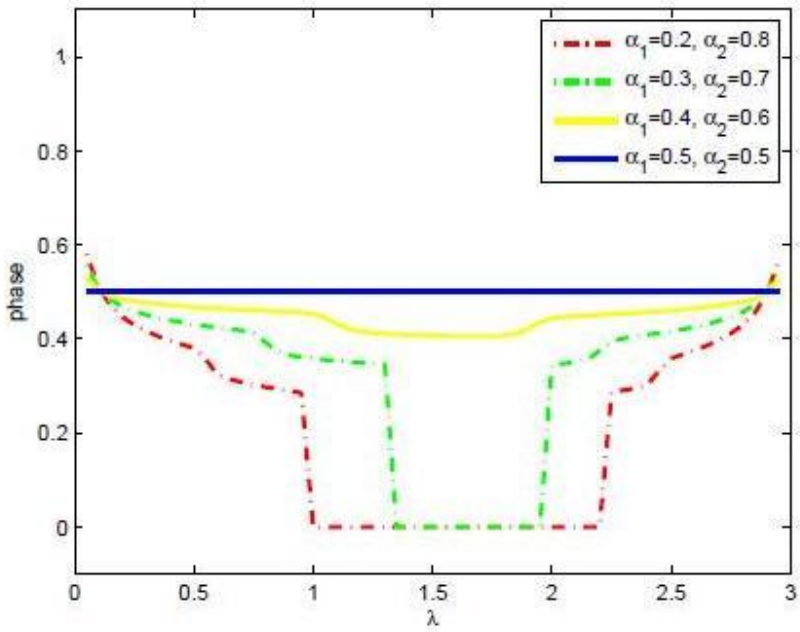

Figure 4.2 The phase of two piecewise-linear oscillators system with parameters: $\gamma = 0.1$,$\epsilon = 0.005$,$\alpha = 4$

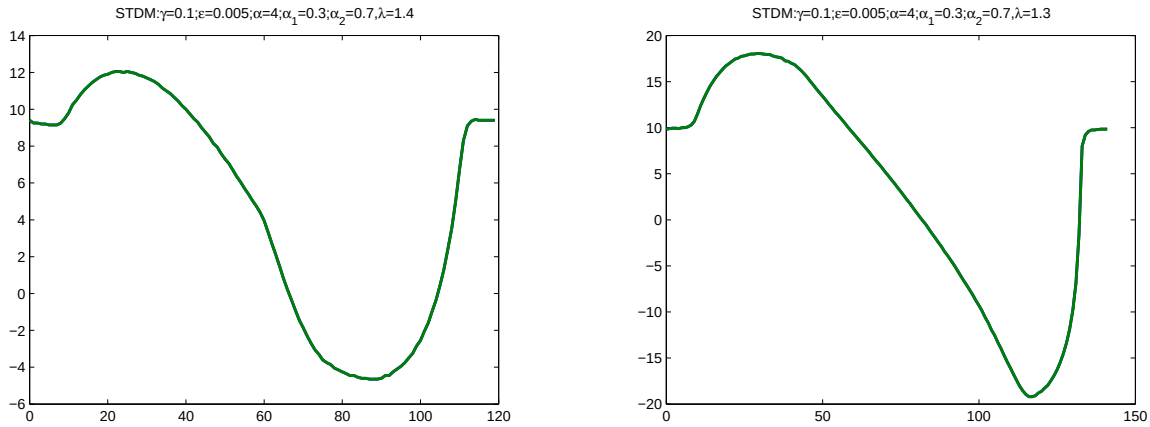

Figure 4.3 The spike time difference map of two piecewise-linear oscillators with parameters: $\gamma = 0.1$,$\epsilon = 0.005$,$\alpha = 4$,$\alpha_1 = 0.3$,$\alpha_2 = 0.7$, $\lambda = 1.4$ and $\lambda = 1.3$

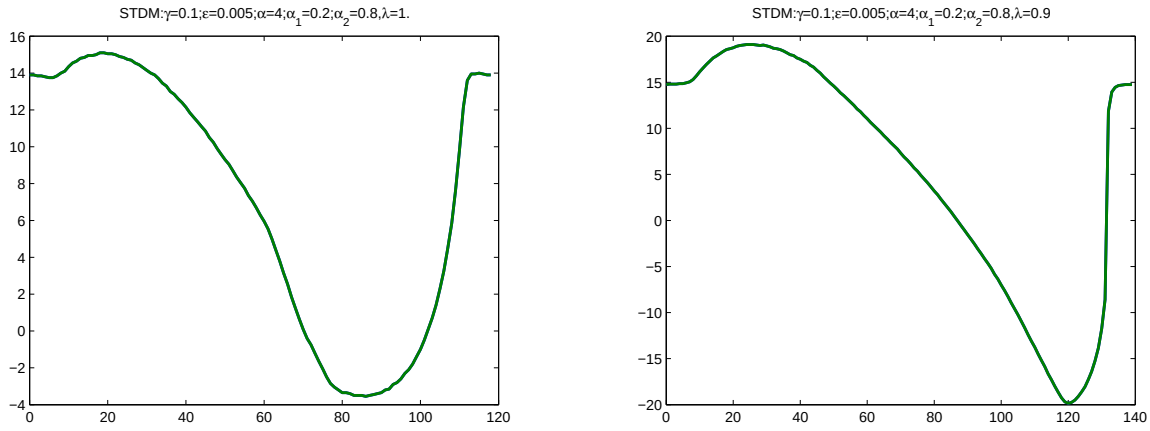

Figure 4.4 The spike time difference map of two piecewise-linear oscillators with parameters: $\gamma = 0.1$,$\epsilon = 0.005$,$\alpha = 4$,$\alpha_1 = 0.2$,$\alpha_2 = 0.8$, $\lambda = 1$ and $\lambda = 0.9$

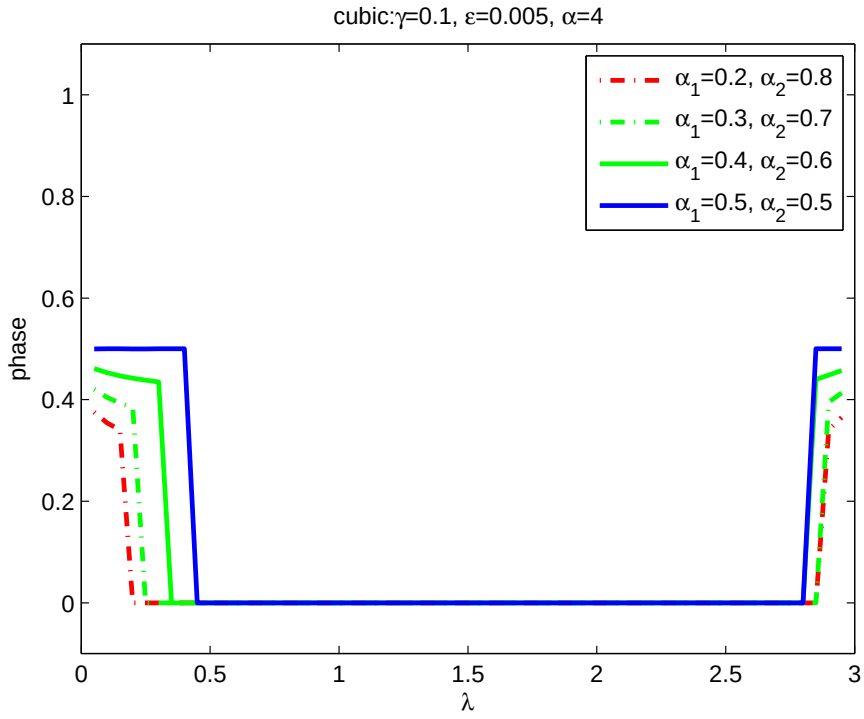

Figure 4.5 The phase of two cubic oscillators system with parameters: $\gamma = 0.1$,$\epsilon = 0.005$,$\alpha = 4$

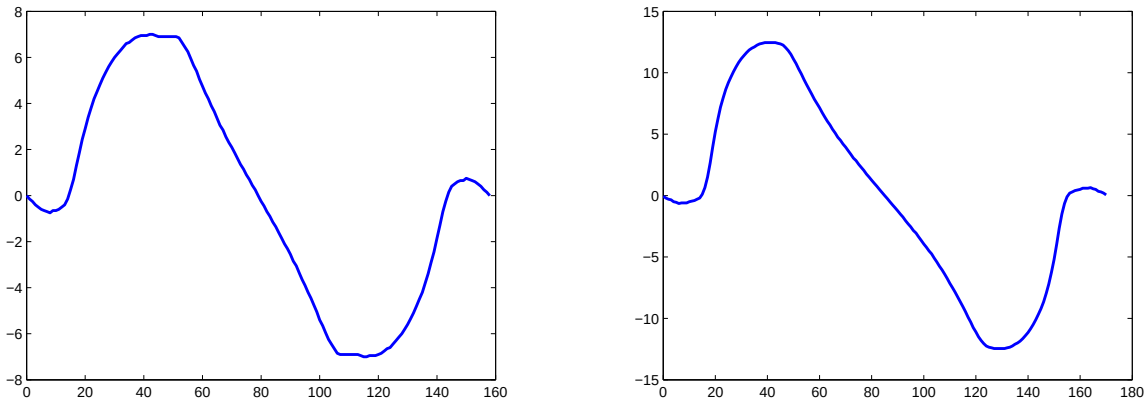

Figure 4.6 The spike time difference map of two cubic oscillators with parameters:$\gamma = 0.1$, $\epsilon = 0.005$, $\alpha = 4$, $\alpha_1 = 0.5$, $\alpha_2 = 0.5$, $\lambda = 0.5$ and $\lambda = 0.45$

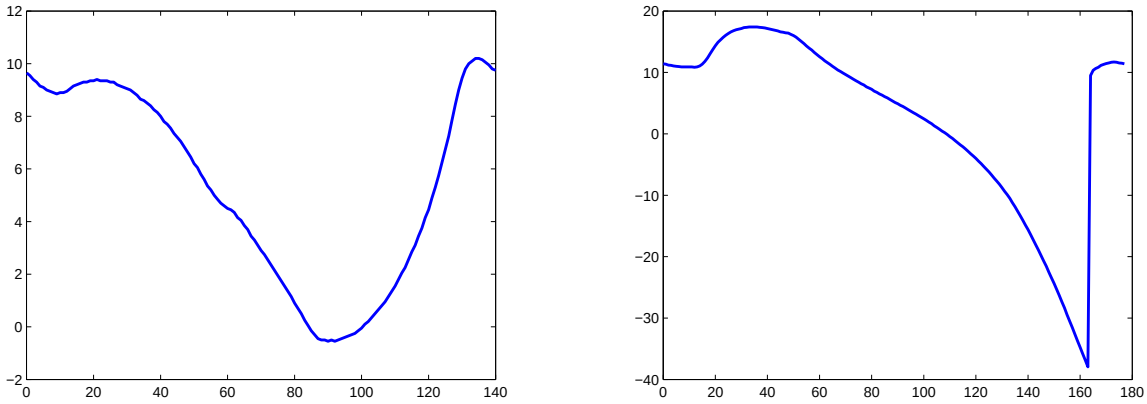

Figure 4.7 The spike time difference map of two cubic oscillators with parameters:$\gamma = 0.1$,$\epsilon = 0.005$,$\alpha = 4$,$\alpha_1 = 0.3$,$\alpha_2 = 0.7$, $\lambda = 0.3$ and $\lambda = 0.25$

critical value of λ_c: When $\lambda < \lambda_c$, We can get an out of phase pattern; when $\lambda \geq \lambda_c$, We could only get the in phase pattern.

The STDM method can also be used to estimate the phase, Here α goes from 0.15 to 0.5. We estimate the phases using STDM method and the result is consistent with the numerical phases.

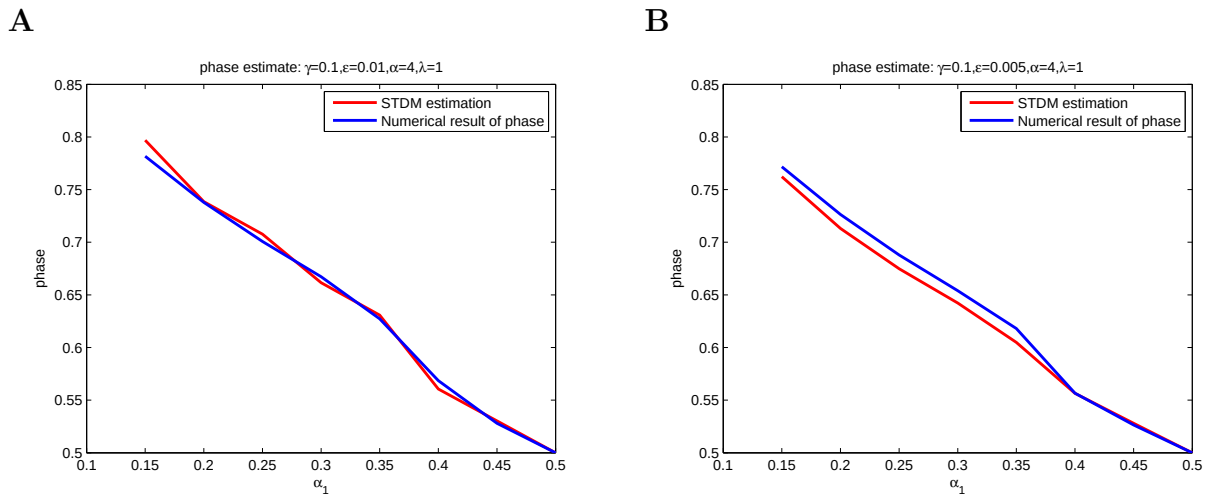

Figure 4.8 Comparison of the phase estimation of piecewise-linear systems by using the spike time difference map and the numerical result with parameters:$\gamma = 0.1$,$\alpha = 4$,$\lambda = 1$,$\epsilon = 0.01$ and $\epsilon = 0.005$

Table 4.1 Phase values of STDM estimation and numerical result of phase in Fig. 4.8-A

The value of α_1	0.15	0.2	0.25	0.3	0.35	0.4	0.45	0.5
Phase values in STDM estimation	0.7969	0.7385	0.7077	0.6615	0.6308	0.5606	0.5303	0.5000
Phase values in numerical result	0.7817	0.7379	0.7007	0.6672	0.6273	0.5685	0.5280	0.5000

In our FHN model, when the coupling is strong enough, in other words, if γ is large enough, the two oscillators will separate and we could get anti-phase pattern. The more the nullclines are moving up and down, the more quickly the oscillators will separate.

Table 4.2 Phase values of STDM estimation and numerical result of phase in Fig. 4.8-B

The value of α_1	0.15	0.2	0.25	0.3	0.35	0.4	0.45	0.5
Phase values in STDM estimation	0.7623	0.7131	0.6748	0.6423	0.6048	0.5564	0.5280	0.5000
Phase values in numerical result	0.7718	0.7264	0.6879	0.6539	0.6181	0.5567	0.5264	0.5000

We know that in STDM, the more the slope of the middle point of the STDM is close to value -1, the more quickly two oscillators will separate. In Fig. 4.9, the slope of the middle point of the curve in the STDM approaching to -1 by increasing the value of γ, so two oscillators separate more quickly by increasing the value of γ. That's because that the extend the V-nullclines moving up and down is increasing by increasing the value of γ. That makes the "moving nullclines" strong enough to make the second oscillator stay around the point $v = 0$ for more time while the first oscillator moves on to the right branch, which makes the two oscillators separate more quickly.

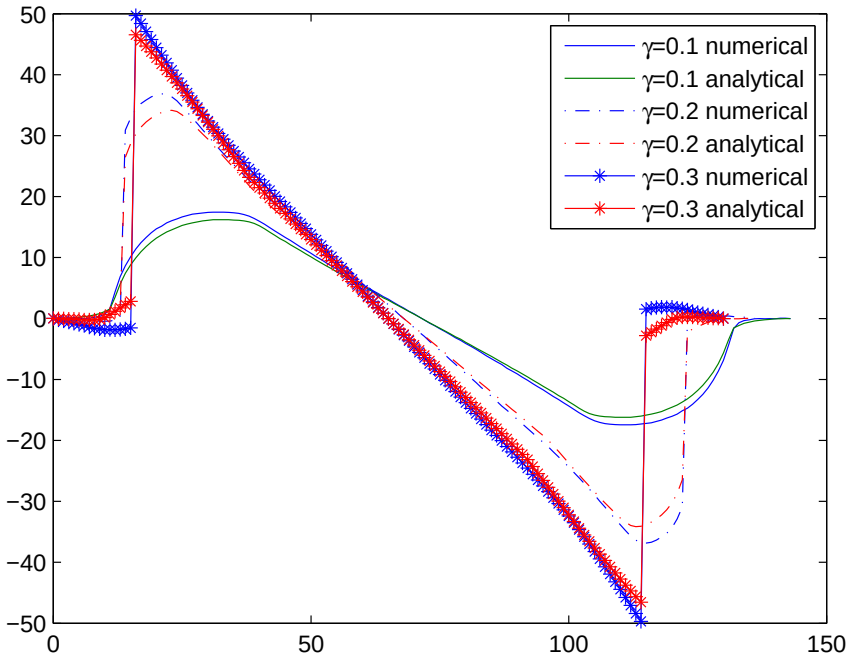

Figure 4.9 STDM for different values of γ: $\lambda = 0.5; \epsilon = 0.005;\ \alpha = 4$

CHAPTER 5
CONCLUSION

5.1 Summary of Results and Discussion

The Kuramoto model describes the synchronization behavior of a large population of coupled limit-cycle oscillators whose natural frequencies satisfy some certain distribution. The Kuramoto model predicts that, if the oscillators have strong coupling, they will become phase-locked. Kuramoto gave an estimate for the distribution for the order parameter, but the order parameter has an error from Kuramoto's estimation. My research involved studying the basics of Kuramoto's analysis and then investigating how the order parameter is distributed around Kuramoto's estimation by given different initial conditions.

The Belousov-Zhabotinsky reaction is a laboratory example of pattern formation in a chemical system that involves nothing more than chemical reaction and molecular diffusion. The FitzHugh-Nagumo (FHN) model is a generic model for excitable media and can be applied to a variety of systems, most notably chemistry, biology and neuroscience. My research focuses on the synchronization of FHN model. I use piecewise linear systems to approximate the cubic systems in FHN model. In both cases, the 'motion' of the nullclines cause the two oscillators to separate. Especially, when the value of γ is large enough, the 'moving nullcline' is strong enough to make the second oscillator stay around the origin for a while and the two oscillators separate.

The nervous system is a very efficient and massively parallel computational device. Models may capture this property to solve a certain class of problems. The system contains only 302 neurons, and it forms about 7000 chemical synapses. The synapses are the connections made by an axon to another neuron. When an action potential arrives at a synapse from the postsynaptic cell, neurotransmitter is released into the synaptic cleft. The neurotransmitter will interact with ion channels on the membrane of the postsynaptic cell causing them to open letting some ions into the cell while letting other ions escape. In [1] and [32], they use a synaptic perturbation on the timing of subsequent spikes to predict the behavior of synchronization of neurons. Changes in firing times depend nonlinearly

on synaptic strength. They apply "spike time response methods" on the model. In our model, there are two oscillators coupled with each other. We don't have the synaptic input. However, the coupling term includes the w-function, which has a synaptic-like shape, so we can also use the spike time response method. The spike time response method can predict oscillatory patterns and the values of phases.

5.2 Future Work

There are several open questions in these problems which are very interesting and useful to consider.

In the present work of Kuramoto model, we explored the distribution of the order parameter of the Kuramoto model without noise terms. We still need to see how the order parameter changes with the noise term. We only numerically verified the locked terms and the unlocked terms, which are independent. Works have to be continued on seeing whether analytical proof is possible.

In the project of Belousov-Zhabotinsky (BZ) reaction, we focused on a system of two oscillators, systems of three and more oscillators should be explored in the future. We only tried three piecewise linear approximations, In the future, it is possible to increase the number of linear pieces to produce a better approximation.

APPENDIX A
PROOFS AND EXAMPLES

A.1 Proof of Lemma 1

Proof

$$\begin{pmatrix} {v_1}' \\ {v_2}' \\ {\omega_1}' \\ {\omega_2}' \end{pmatrix} = D \begin{pmatrix} v_1 \\ v_2 \\ \omega_1 \\ \omega_2 \end{pmatrix} + L$$

Because the matrix D can be diagonalized:

$$D = \begin{pmatrix} a & 0 & -(1+\gamma\alpha_1) & -\gamma\alpha_2 \\ 0 & b & -\gamma\alpha_1 & -(1+\gamma\alpha_2) \\ \varepsilon\alpha & 0 & -\varepsilon & 0 \\ 0 & \varepsilon\alpha & 0 & -\varepsilon \end{pmatrix} = A \begin{pmatrix} \lambda_1 & 0 & 0 & 0 \\ 0 & \lambda_2 & 0 & 0 \\ 0 & 0 & \lambda_3 & 0 \\ 0 & 0 & 0 & \lambda_4 \end{pmatrix} A^{-1}$$

Plug D into the above equation and multiply both sides by A^{-1}:

$$A^{-1} \begin{pmatrix} {v_1}' \\ {v_2}' \\ {\omega_1}' \\ {\omega_2}' \end{pmatrix} = \begin{pmatrix} \lambda_1 & 0 & 0 & 0 \\ 0 & \lambda_2 & 0 & 0 \\ 0 & 0 & \lambda_3 & 0 \\ 0 & 0 & 0 & \lambda_4 \end{pmatrix} A^{-1} \begin{pmatrix} v_1 \\ v_2 \\ \omega_1 \\ \omega_2 \end{pmatrix} + A^{-1}L$$

If we let

$$A^{-1} \begin{pmatrix} v_1 \\ v_2 \\ \omega_1 \\ \omega_2 \end{pmatrix} = \begin{pmatrix} \bar{v_1} \\ \bar{v_2} \\ \bar{\omega_1} \\ \bar{\omega_2} \end{pmatrix}$$

Then

$$\begin{pmatrix} \bar{v_1}' \\ \bar{v_2}' \\ \bar{\omega_1}' \\ \bar{\omega_2}' \end{pmatrix} = \begin{pmatrix} \lambda_1 & 0 & 0 & 0 \\ 0 & \lambda_2 & 0 & 0 \\ 0 & 0 & \lambda_3 & 0 \\ 0 & 0 & 0 & \lambda_4 \end{pmatrix} \begin{pmatrix} \bar{v_1} \\ \bar{v_2} \\ \bar{\omega_1} \\ \bar{\omega_2} \end{pmatrix} + A^{-1}L$$

$\Rightarrow$

$$\left[\begin{pmatrix} \lambda_1 & 0 & 0 & 0 \\ 0 & \lambda_2 & 0 & 0 \\ 0 & 0 & \lambda_3 & 0 \\ 0 & 0 & 0 & \lambda_4 \end{pmatrix} \begin{pmatrix} \bar{v_1} \\ \bar{v_2} \\ \bar{\omega_1} \\ \bar{\omega_2} \end{pmatrix} + A^{-1}L \right]' = \begin{pmatrix} \lambda_1 & 0 & 0 & 0 \\ 0 & \lambda_2 & 0 & 0 \\ 0 & 0 & \lambda_3 & 0 \\ 0 & 0 & 0 & \lambda_4 \end{pmatrix} \begin{pmatrix} \bar{v_1}' \\ \bar{v_2}' \\ \bar{\omega_1}' \\ \bar{\omega_2}' \end{pmatrix}$$

$$= \begin{pmatrix} \lambda_1 & 0 & 0 & 0 \\ 0 & \lambda_2 & 0 & 0 \\ 0 & 0 & \lambda_3 & 0 \\ 0 & 0 & 0 & \lambda_4 \end{pmatrix} \left[\begin{pmatrix} \lambda_1 & 0 & 0 & 0 \\ 0 & \lambda_2 & 0 & 0 \\ 0 & 0 & \lambda_3 & 0 \\ 0 & 0 & 0 & \lambda_4 \end{pmatrix} \begin{pmatrix} \bar{v_1} \\ \bar{v_2} \\ \bar{\omega_1} \\ \bar{\omega_2} \end{pmatrix} + A^{-1}L \right]$$

$\Rightarrow$

$$\begin{pmatrix} \lambda_1 & 0 & 0 & 0 \\ 0 & \lambda_2 & 0 & 0 \\ 0 & 0 & \lambda_3 & 0 \\ 0 & 0 & 0 & \lambda_4 \end{pmatrix} \begin{pmatrix} \bar{v_1} \\ \bar{v_2} \\ \bar{\omega_1} \\ \bar{\omega_2} \end{pmatrix} + A^{-1}L$$

$$= \begin{pmatrix} e^{\lambda_1 t} & 0 & 0 & 0 \\ 0 & e^{\lambda_2 t} & 0 & 0 \\ 0 & 0 & e^{\lambda_3 t} & 0 \\ 0 & 0 & 0 & e^{\lambda_4 t} \end{pmatrix} \left[\begin{pmatrix} \lambda_1 & 0 & 0 & 0 \\ 0 & \lambda_2 & 0 & 0 \\ 0 & 0 & \lambda_3 & 0 \\ 0 & 0 & 0 & \lambda_4 \end{pmatrix} \begin{pmatrix} \bar{v_1}(0) \\ \bar{v_2}(0) \\ \bar{\omega_1}(0) \\ \bar{\omega_2}(0) \end{pmatrix} + A^{-1}L \right]$$

$$= \begin{pmatrix} e^{\lambda_1 t} & 0 & 0 & 0 \\ 0 & e^{\lambda_2 t} & 0 & 0 \\ 0 & 0 & e^{\lambda_3 t} & 0 \\ 0 & 0 & 0 & e^{\lambda_4 t} \end{pmatrix} \left[\begin{pmatrix} \lambda_1 & 0 & 0 & 0 \\ 0 & \lambda_2 & 0 & 0 \\ 0 & 0 & \lambda_3 & 0 \\ 0 & 0 & 0 & \lambda_4 \end{pmatrix} A^{-1} \begin{pmatrix} v_1(0) \\ v_2(0) \\ \omega_1(0) \\ \omega_2(0) \end{pmatrix} + A^{-1}L \right]$$

$\Rightarrow$

$$A^{-1} \begin{pmatrix} v_1 \\ v_2 \\ \omega_1 \\ \omega_2 \end{pmatrix} = \begin{pmatrix} \bar{v_1} \\ \bar{v_2} \\ \bar{\omega_1} \\ \bar{\omega_2} \end{pmatrix} = \begin{pmatrix} \frac{1}{\lambda_1} & 0 & 0 & 0 \\ 0 & \frac{1}{\lambda_2} & 0 & 0 \\ 0 & 0 & \frac{1}{\lambda_3} & 0 \\ 0 & 0 & 0 & \frac{1}{\lambda_4} \end{pmatrix}.$$

$$\left\{ \begin{pmatrix} e^{\lambda_1 t} & 0 & 0 & 0 \\ 0 & e^{\lambda_2 t} & 0 & 0 \\ 0 & 0 & e^{\lambda_3 t} & 0 \\ 0 & 0 & 0 & e^{\lambda_4 t} \end{pmatrix} \left[\begin{pmatrix} \lambda_1 & 0 & 0 & 0 \\ 0 & \lambda_2 & 0 & 0 \\ 0 & 0 & \lambda_3 & 0 \\ 0 & 0 & 0 & \lambda_4 \end{pmatrix} A^{-1} \begin{pmatrix} v_1(0) \\ v_2(0) \\ \omega_1(0) \\ \omega_2(0) \end{pmatrix} + A^{-1}L \right] - A^{-1}L \right\}$$

$\Rightarrow$

$$\begin{pmatrix} v_1 \\ v_2 \\ \omega_1 \\ \omega_2 \end{pmatrix} = A \begin{pmatrix} \frac{1}{\lambda_1} & 0 & 0 & 0 \\ 0 & \frac{1}{\lambda_2} & 0 & 0 \\ 0 & 0 & \frac{1}{\lambda_3} & 0 \\ 0 & 0 & 0 & \frac{1}{\lambda_4} \end{pmatrix}.$$

$$\left\{ \begin{pmatrix} e^{\lambda_1 t} & 0 & 0 & 0 \\ 0 & e^{\lambda_2 t} & 0 & 0 \\ 0 & 0 & e^{\lambda_3 t} & 0 \\ 0 & 0 & 0 & e^{\lambda_4 t} \end{pmatrix} \left[\begin{pmatrix} \lambda_1 & 0 & 0 & 0 \\ 0 & \lambda_2 & 0 & 0 \\ 0 & 0 & \lambda_3 & 0 \\ 0 & 0 & 0 & \lambda_4 \end{pmatrix} A^{-1} \begin{pmatrix} v_1(0) \\ v_2(0) \\ \omega_1(0) \\ \omega_2(0) \end{pmatrix} + A^{-1}L \right] - A^{-1}L \right\}$$

A.2 Proof of Lemma 3.6.1

Proof Consider the moving v-nullclines function (3.8):

$$w_k = \frac{f(v_k) + \gamma\,\bar{w}}{1 + \alpha_k \gamma} - \frac{\gamma\,\alpha_j w_j}{1 + \alpha_k \gamma}$$

The above function $f(v)$, parameters $\bar{\omega}$, α_k,γ are all fixed, it is the term $-\gamma\alpha_j\omega_j$ that makes the v-nullcline moving. The v-nullcline of (v_k, ω_k) is moving up(down) is equivalent to ω_k' positive(ω_k' negative) for any value of v_k fixed. It is also equivalent to $-\gamma\alpha_j\omega_j$ increasing(decreasing), it is equivalent to ${\omega_j}' = \alpha v_j - \lambda - \omega_j$ positive (negative).

The position of the point(v_j, ω_j) determines whether it is positive, zero, or negative:

(**i**) When the point (v_j, ω_j) lies on the left side of ω nullcline, $\omega_j' = \alpha_j v - \lambda_j - \omega_j < 0$,

(**ii**) When the point (v_j, ω_j) lies on the ω nullcline, $\omega_j' = \alpha_j v - \lambda_j - \omega_j = 0$,

(**iii**) When the point (v_j, ω_j) lies on the right side of ω nullcline, $\omega_j' = \alpha_j v - \lambda_j - \omega_j > 0$.

So whether the nullcline of one oscillator (v_k, ω_k) is moving up (moving down) is determined by the position of the other oscillator (v_j, ω_j), if the other oscillator lies on

the left side of ω-nullcline, the v-nullcline of the oscillator (v_k, ω_k) move up; if the other oscillator lies on the right side of ω-nullcline, the v-nullcline of this oscillator (v_k, ω_k) move down.

A.3 Example of Piecewise-linear Oscillators

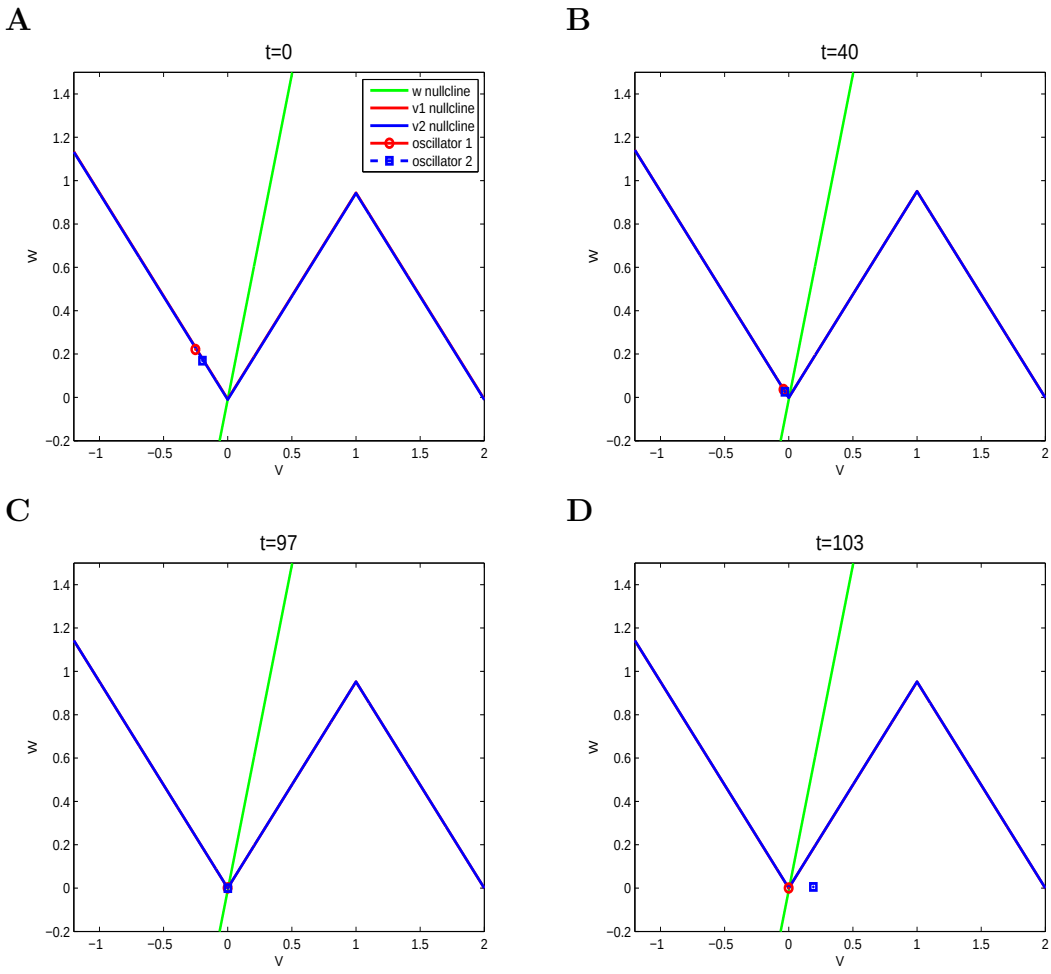

E

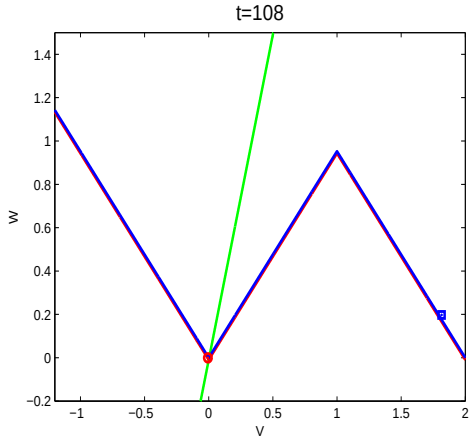

F

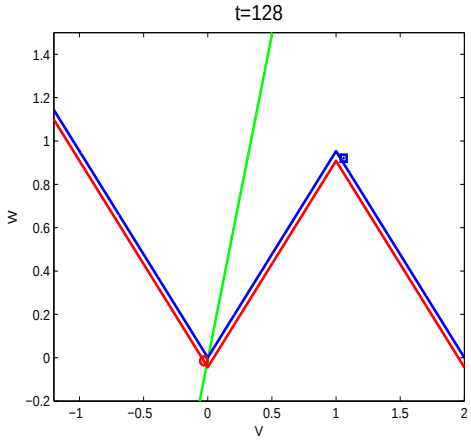

G

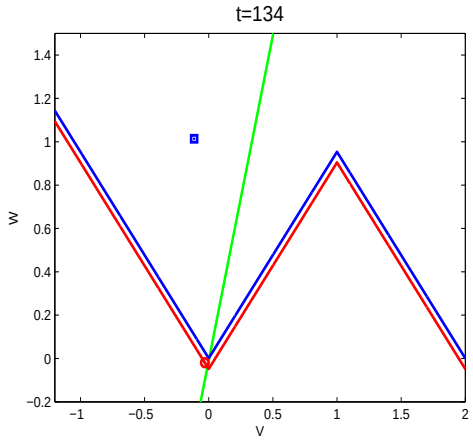

H

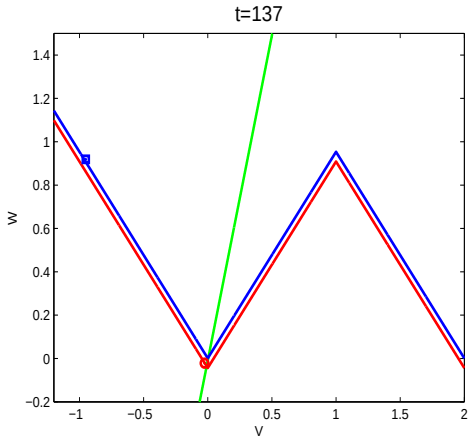

I

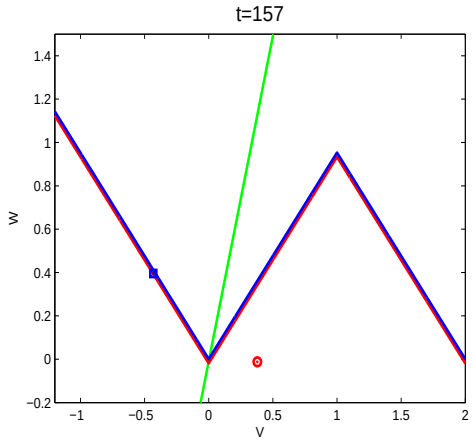

J

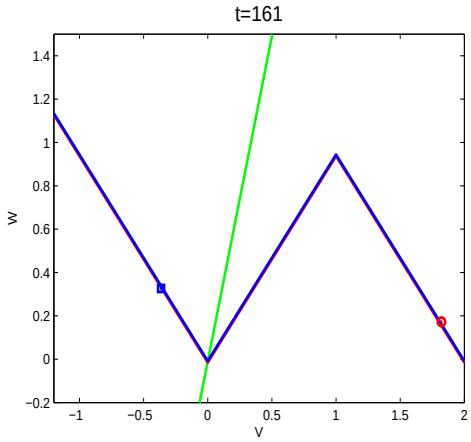

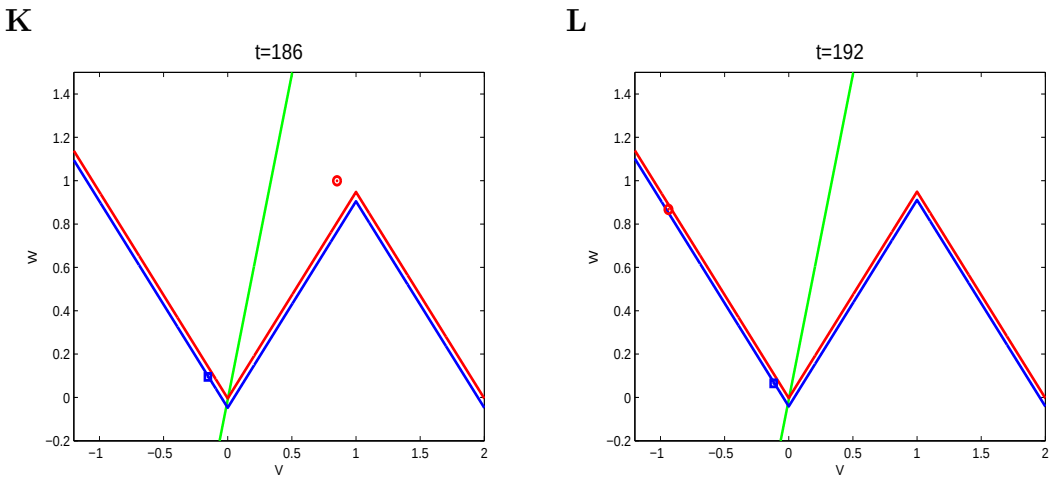

Figure A.1 Two globally coupled oscillators moving with equation (3.11)in piecewise-linear case, and two out of phase clusters for the following parameters: $\alpha = 3, \gamma = 0.1, \alpha_1 = 0.5, \alpha_2 = 0.5$

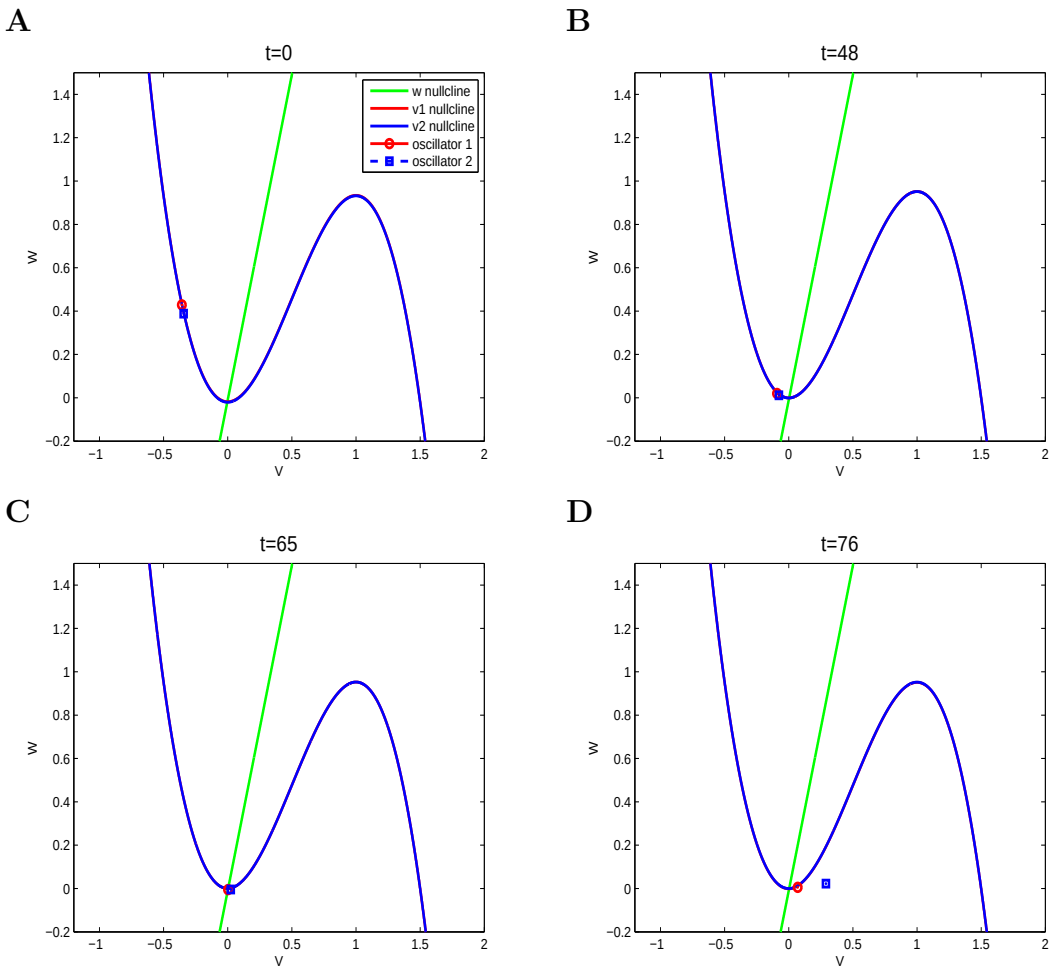

E

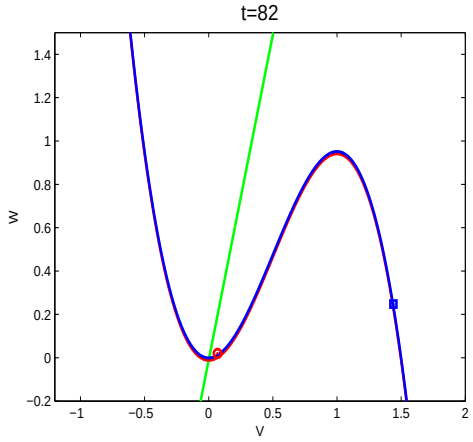

F

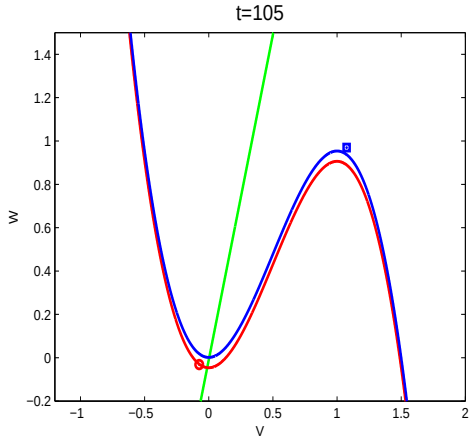

G

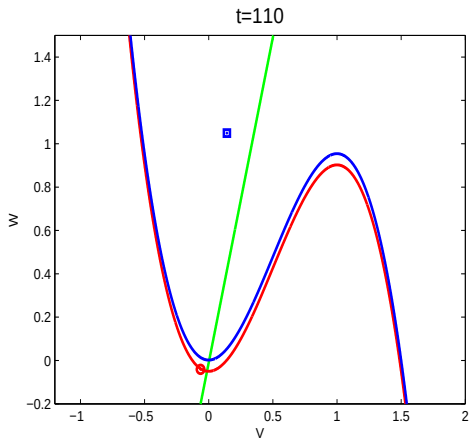

H

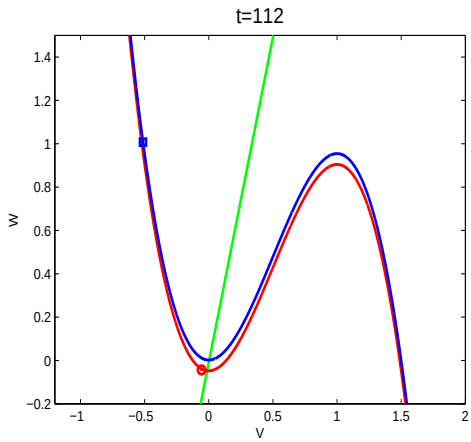

I

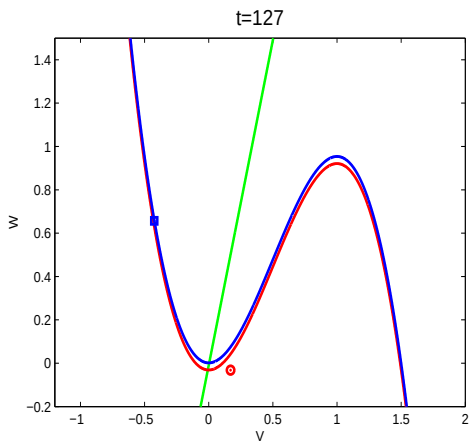

J

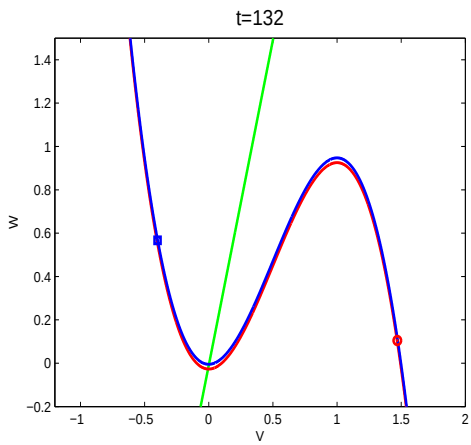

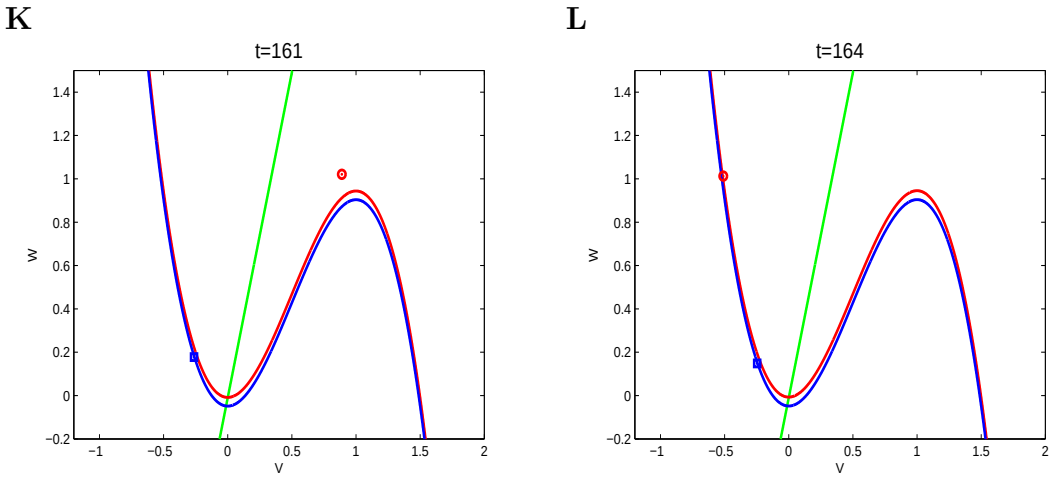

Figure A.2 Two globally coupled oscillators moving with equation (3.11), and two out of phase clusters for the following parameters: $\alpha = 3, \gamma = 0.1, \alpha_1 = 0.5, \alpha_2 = 0.5$

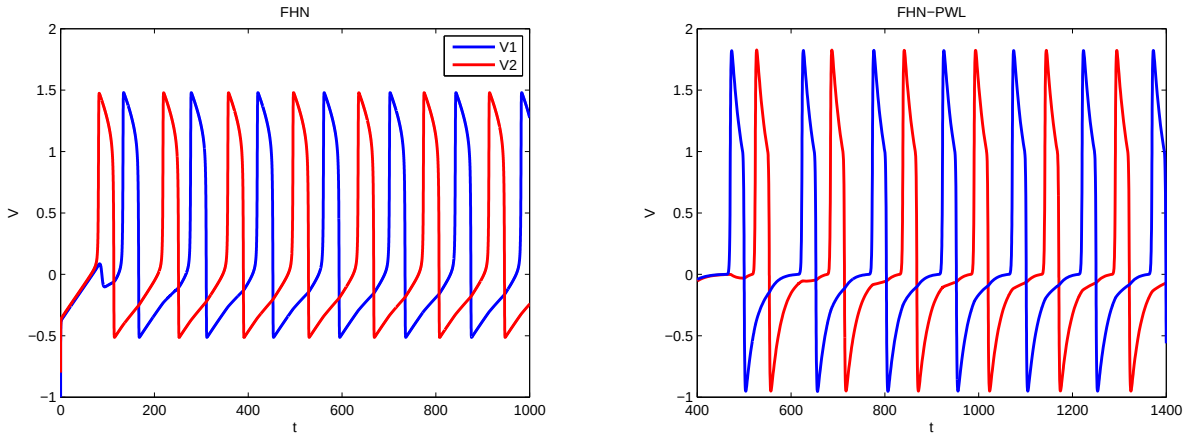

Figure A.3 Two globally coupled oscillators moving with equation (3.11), and two anti-phase clusters for the following parameters: $\alpha = 3, \gamma = 0.1, \alpha_1 = 0.5, \alpha_2 = 0.5$

REFERENCES

[1] C. D. Acker, N. Kopell, and J. A. White. Synchronization of strongly coupled excitatory neurons: relating network behavior to biophysics. *J Comput Neurosci*, 15(1):71–90, 2003.

[2] B. P. Belousov. A periodic reaction and its mechanism. *Compilation of Abstracts on Radiation Medicine (Med. Publ., Moscow)*, 147:145, 1959.

[3] R. J. Belousov, B. P.& in Field and Burger. *A periodic reaction and its mechanism; Oscillations and traveling waves in chemical systems.* Wiley, New York, 1985.

[4] Yassine Boubendir, Vicenç Méndez, and Horacio G. Rotstein. Dynamics of one- and two-dimensional fronts in a bistable equation with time-delayed global feedback: Propagation failure and control mechanisms. *Physical Review E*, 82(3):036601+, Sep 2010.

[5] J.C. Butcher. *The Numerical Analysis of Ordinary Differential Equations:Runge-Kutta and General Linear Methods.* Wiley, 1987.

[6] John Charles Butcher. *Numerical methods for ordinary differential equations.* Wiley, 2008.

[7] D. T. W. Chick, S. Coombes, and Z. D. Wang. Clustering through post inhibitory rebound in synaptically coupled neurons. *Phys. Rev. E 70, 011908*, 70:Issue 1, 2004.

[8] S. Coombes. Phase locking in networks of synaptically-coupled mckean relaxation oscillators. *Physicad*, 160:173–188, 2008.

[9] Christopher M. Dobson. Protein folding and disease: a view from the first horizon symposium. *Nat Rev Drug Discov*, 2(2):154–160, February 2003.

[10] J. A. Epstein, I. R.; Pojman. An introduction to nonlinear chemical dynamics: Oscillations, waves, patterns, and chaos. *J. Chem. Educ.*, 77 (4):450, 2000.

[11] R. J. Fields, E. Koros, and R. M. Noyes. Oscillations in chemical systems. 2. thorough analysis of temporal oscillation in bromate-cerium-malonic acid system. *Jamchemsoc*, 94:8649–8664, 1972.

[12] R. Fitzhugh. Impulses and physiological states in theoretical models of nerve membrane. *Biophysical Journal*, 1(6):445–466, July 1961.

[13] Richard FitzHugh. Mathematical models of threshold phenomena in the nerve membrane. *Bulletin of Mathematical Biology*, 17(4):257–278, December 1955.

[14] D. Golomb, D. Hansel, B. Shraiman, and H. Sompolinksy. Clustering in globally coupled phase oscillators. *pra*, 45:3516–3530, 1992.

[15] A. Zhabotinsky H. G. Rotstein, N. Kopell and I. R. Epstein. A canard mechanism for localization in systems of globally coupled oscillators. *SIAM J. Appl. Math.*, 63:1998C 2019, 2003.

[16] D. Hansel, G. Mato, and C. Meunier. Synchrony in Excitatory Neural Networks. *Neural Computation*, 7(2):307–337, March 1995.

[17] Eugene M. Izhikevich. *Dynamical systems in neuroscience: the geometry of excitability and bursting*. Computational neuroscience. MIT Press, 2007.

[18] O. Jensen, P. Goel, N. Kopell, M. Pohja, R. Hari, and B. Ermentrout. On the human sensorimotor-cortex beta rhythm: sources and modeling. *Neuroimage*, 26(2):347–355, June 2005.

[19] Conrad J Perez Vicente Felix Ritort Renato Spigler Juan A.Acebron, L.L.Bonilla. The kuramoto model: A simple parpadigm for synchronization phenomena. *Reviews of Modern Physics*, 77(1):137C185, January 2005.

[20] J. Keener and J. Sneyd. *Mathematical Physiology*. Springer-Verlag, 1998.

[21] N. Kopell and G. Ermentrout. Mechanisms of phase-locking and frequency control in pairs of coupled neural oscillators, 2000.

[22] Yoshiki Kuramoto. *Chemical oscillations, waves, and turbulence*. Springer-Verlag, New York, 1984.

[23] H. P. McKean. Nagumo's equation. *Advances in Mathematics*, 4:209–223, 1970.

[24] Renato E. Mirollo and Steven H. Strogatz. Synchronization of pulse-coupled biological oscillators. *SIAM Journal on Applied Mathematics*, 50(6):1645–1662, 1990.

[25] JD Murray. *Mathematical Biology: an Introduction*. Springer, 2002.

[26] J. D. Murry. *Mathematical Biology: I. An Introduction (Interdisciplinary Applied Mathematics)*. Springer; 3rd edition, December 8, 2007.

[27] J. Nagumo, S. Arimoto, and S. Yoshizawa. An active pulse transmission line simulating nerve axon. *Proceedings of the IRE*, 50(10):2061–2070, October 1962.

[28] Theoden Netoff, Corey Acker, Jonathan Bettencourt, and John White. Beyond Two-Cell Networks: Experimental Measurement of Neuronal Responses to Multiple Synaptic Inputs. *Journal of Computational Neuroscience*, 18(3):287–295, June 2005.

[29] Theoden I. Netoff, Robert Clewley, Scott Arno, Tara Keck, and John A. White. Epilepsy in Small-World Networks. *J. Neurosci.*, 24(37):8075–8083, September 2004.

[30] Myongkeun Oh and Victor Matveev. Loss of phase-locking in non-weakly coupled inhibitory networks of type-I model neurons. *Journal of Computational Neuroscience*.

[31] S. A. Oprisan, A. A. Prinz, and C. C. Canavier. Phase resetting and phase locking in hybrid circuits of one model and one biological neuron. *Biophys J*, 87(4):2283–2298, October 2004.

[32] D. D. Pervouchine, T. I. Netoff, H. G. Rotstein, J. A. White, M. O. Cunningham, M. A. Whittington, and N. J. Kopell. Low-dimensional maps encoding dynamics in entorhinal cortex and hippocampus. *Neural Comput*, 18(11):2617–2650, November 2006.

[33] J. Rinzel and J. B. Keller. Traveling wave solutions of a nerve conduction equation. *Physicad*, 13:1313–1337, 1973.

[34] H. G. Rotstein, N. Kopell, A. Zhabotinsky, and I. R. Epstein. A canard mechanism for localization in systems of globally coupled oscillators. *Siamap*, 63:1998–2019, 2003.

[35] H. G. Rotstein, N. Kopell, A. Zhabotinsky, and I. R. Epstein. Canard phenomenon and localization of oscillations in the belousov-zhabotinsky reaction with global feedback. *JCHP*, 119 (17):8824–8832, 2003.

[36] F. Sagues and I. R Epstein. Nonlinear chemical dynamics. *Dalton Trans*, 1:1201–1217, 2003.

[37] RM Schoen. The existence of weak solutions with prescribed singular behavior for a conformally invariant scalar equation. *Communications on pure and applied mathematics*, 41, no. 3:317–392, 1988.

[38] Roy M. Smeal, G. Bard Ermentrout, and John A. White. Phase-response curves and synchronized neural networks. *Philosophical Transactions of the Royal Society B: Biological Sciences*, 365(1551):2407–2422, August 2010.

[39] S. H. Strogatz. *Sync: the emerging science of spontaneous order*. Hyperion, New York, 2003.

[40] Steven H. Strogatz. From kuramoto to crawford: exploring the onset of synchronization in populations of coupled oscillators. *Physica D*, 143:1–20, September 2000.

[41] Steven Henry Strogatz. *Nonlinear Dynamics and Chaos with Applications to Physics, Biology, Chemistry, and Engineering*. Addison-Wesley, Reading, MA, 1994.

[42] A. Tonnelier. The mckean's caricature of the fitzhugh-nagumo model. the space-clamped system. *Siap*, 63:459–484, 2002.

[43] V. K. Vanag, L. Yang, M. Dolnik, and Epstein I. R. Zhabotinsky, A. M. Oscillatory cluster patterns in a homogeneous chemical system with global feedback. *Nature*, 406:(6794):389–391, 2000.

[44] V. K. Vanag, A. M. Zhabotinsky, and I. R. Epstein. Pattern formation in the belusov-zhabotinsky reaction with photochemical global feedback. *JCHP*, 104A:11566–11577, 2000.

[45] V. K. Vanag, A. M. Zhabotinsky, and I. R. Epstein. Oscillatory clusters in the periodically illuminated, spatially extended belousov-zhabotinsky reaction. *PRL*, 86:3, 2001.

[46] W. P. Wang. Multiple impulse solutions to mckean's caricature of the nerve equation. 2. stability. *Communications on pure and applied mathematics*, 41:997–1025, 1988.

[47] Arthur T. Winfree. *The Geometry of Biological Time*. Springer, 2nd edition, June 2001.

[48] N. Zaikin and Zhabotinsky. Concentration wave propagation in two-dimensional liquid-phase self-oscillating system. *Nature*, 225:535–537, 1970.

[49] Daniel E. Zak, Haiping Hao, Rajanikanth Vadigepalli, Gregory M. Miller, Babatunde A. Ogunnaike, and James S. Schwaber. Systems analysis of circadian time-dependent neuronal epidermal growth factor receptor signaling. *Genome Biology*, 7:R48+, June 2006.

[50] A. M. Zhabotinksy. Periodic processes of malonic acid oxidation in a liquid phase. *Biofizika*, 9:306–311, 1964.

[51] A. M. Zhabotinksy. Belousov-zhabotinsky reaction. *Scholarpedia*, 2:1435, 2007.

[52] A. M. Zhabotinsky, F. Buchholtz, A. B. Kiyatkin, and I. R. Epstein. Oscillations and waves in metal-ion-catalyzed bromate oscillating reactions in highly oxidized states. *JCHP*, 97:7578–7584, 1993.